

---


Electronic Theses and Dissertations, 2004-2019

---

2008

## Development Of Hydraulic And Soil Properties For Soil Amendments And Native Soils For Retention Ponds In Marion County, Florida

Lisa Naujock  
*University of Central Florida*

 Part of the [Civil Engineering Commons](#)  
Find similar works at: <https://stars.library.ucf.edu/etd>  
University of Central Florida Libraries <http://library.ucf.edu>

This Masters Thesis (Open Access) is brought to you for free and open access by STARS. It has been accepted for inclusion in Electronic Theses and Dissertations, 2004-2019 by an authorized administrator of STARS. For more information, please contact [STARS@ucf.edu](mailto:STARS@ucf.edu).

---

### STARS Citation

Naujock, Lisa, "Development Of Hydraulic And Soil Properties For Soil Amendments And Native Soils For Retention Ponds In Marion County, Florida" (2008). *Electronic Theses and Dissertations, 2004-2019*. 3479. <https://stars.library.ucf.edu/etd/3479>

DEVELOPMENT OF HYDRAULIC AND SOIL PROPERTIES FOR SOIL  
AMENDMENTS AND NATIVE SOILS FOR RETENTION PONDS IN  
MARION COUNTY, FLORIDA

by

LISA J. NAUJOCK  
B.S. Colorado State University, 1999

A thesis submitted in partial fulfillment of the requirements  
for the degree of Master of Science  
in the Department of Civil, Environmental, and Construction Engineering  
in the College of Engineering and Computer Science  
at the University of Central Florida  
Orlando, Florida

Fall Term  
2008

© 2008 Lisa J. Naujock

## **ABSTRACT**

The vadose zone plays an important role in managing stormwater. Predicting the water balance and water movement is crucial in ground water remediation to keep water suitable for use. To aid in understanding soils ability to transmit and store water, soil and hydraulic properties were analyzed for soils in Marion County, Florida, and potential soil amendments.

Soil and hydraulic properties were examined for two soil amendments and for the soils in Marion County, Florida, at the South Oak and the Hunter's Trace locations. The hydraulic properties measured were the soil moisture retention curve (SMRC) and saturated hydraulic conductivity ( $K_s$ ). The soil properties measured were the particle-size distribution (PSD) and the specific gravity. From these, the bulk density and porosity were calculated. The SMRC corresponds to the water holding capacities, while the  $K_s$  corresponds to the soils ability to transmit water. Both are dependent on the soil properties.

The SMRC for the soil amendments and native soils were developed in the laboratory using a Tempe cell apparatus. In addition, the SMRC was measured in the field at the Hunter's Trace location with time domain reflectometry (TDR) and tensiometer equipment at three depths of 1-ft, 2-ft, and 3-ft over approximate a two month period. The SMRC obtained in the laboratory was compared to two analytical models, Brooks and Corey and van Genuchten, and to the field data. There is a strong correlation between the laboratory, analytical, and field SMRC for both South Oak and Hunter's Trace. In addition, there is a strong correlation between the laboratory SMRC and analytical models for the soil amendments.

The Arya and Paris (AP) model, a pedotransfer function, was examined for its accuracy in predicting the SMRC for the soils at South Oak and Hunter's Trace, in addition to the soil amendments. Measuring the SMRC in the lab is a time consuming process; therefore, inferring the SMRC from textural and structural soil properties which are easier measured characteristics would be advantageous.

## **ACKNOWLEDGMENTS**

I would like to thank Dr. Manoj Chopra, Dr. Martin Wanielista, and Dr. Lakshmi Reddi for providing their valuable time and support in helping me achieve my graduate degree as well as sitting on my committee. As my major advisor, Dr. Chopra provided guidance, knowledge, and advice that were invaluable throughout my research. Dr. Wanielista provided support, encouragement, and great insight. Dr. Reddi was patient and helpful whenever a question was posed to him.

A very special thanks goes to Andrew O'Reilly for his guidance and encouragement in the laboratory, as well as his knowledge and expertise in ground water. Special regards for the support I received from USGS as it was greatly appreciated. I would also like to thank Brian Rivera and Zhemin Xuan for help obtaining the samples from the field. In addition, I would like to thank Dr. David Sumner, Dr. Gour Tsyh Yeh, Dr. Erica Stone, Cheng Wang, Elizabeth Landowski, Devan Henderson, and Dr. Sai Kakuturu for answering specific questions that would always present themselves throughout my research.

I would especially like to thank my family and friends for their love, encouragement, and patience during my research and graduate studies, especially my husband, Tyson Naujock, and my parents, Gerald and Audrey Dummer.

## TABLE OF CONTENTS

LIST OF FIGURES .....	x
LIST OF TABLES .....	xiv
LIST OF ACRONYMS AND SYMBOLS.....	xvii
CHAPTER 1: INTRODUCTION.....	1
Introduction.....	1
Objectives .....	2
Limitations .....	2
CHAPTER 2: BACKGROUND.....	3
Theoretical .....	3
Sieve Analysis.....	3
Bulk Density .....	4
Porosity .....	4
Specific Gravity .....	4
Hydraulic Conductivity.....	5
Soil Moisture Retention Curves.....	8
Double-Ring Infiltrometer .....	12
SMRC Case Studies.....	14
Pedotransfer Functions.....	17

CHAPTER 3: EXPERIMENTAL DESIGN AND APPROACH.....	20
Introduction.....	20
Samples and Field Measurements.....	20
Sieve Analysis.....	24
Specific Gravity .....	24
Hydraulic Conductivity.....	24
Soil Moisture Retention Curve .....	26
Double-Ring Infiltrometer .....	27
CHAPTER 4: RESULTS AND DISCUSSION.....	29
Soil Properties.....	29
Sieve Analysis.....	29
Specific Gravity, Bulk Density, and Porosity.....	37
Hydraulic Properties .....	38
Hydraulic Conductivity.....	38
Soil Moisture Retention Curve .....	40
Laboratory Measurement.....	40
South Oak.....	40
Hunter’s Trace .....	43
Soil Amendments.....	46
Brooks and Corey and van Genuchten Models.....	47
Field Measurements .....	54



Double-Ring Infiltrometer .....	58
Pedotransfer Function (Arya and Paris Model) .....	59
South Oak.....	59
Hunter’s Trace .....	62
Soil Amendments.....	64
Comparing Different Scaling Factors for South Oak .....	66
CHAPTER 5: SUMMARY.....	69
Summary .....	69
Conclusions.....	70
Recommendations.....	73
Future Work .....	74
APPENDIX A: SIEVE ANALYSIS DATA.....	75
South Oak.....	76
Hunter’s Trace .....	78
Soil Amendments.....	80
APPENDIX B: SPECIFIC GRAVITY DATA.....	82
South Oak.....	83
Hunter’s Trace .....	84
Soil Amendments.....	84
APPENDIX C: HYDRAULIC CONDUCTIVITY DATA .....	85

South Oak.....	86
Hunter’s Trace .....	89
Soil Amendments.....	91
APPENDIX D: SOIL MOISTURE RETENTION CURVES .....	93
South Oak.....	94
Hunter’s Trace .....	99
Soil Amendments.....	102
APPENDIX E: ARYA AND PARIS MODEL.....	103
South Oak.....	104
Hunter’s Trace .....	109
Soil Amendments.....	112
REFERENCES .....	114

## LIST OF FIGURES

Figure 1: Sorption and desorption curves, illustrating hysteresis (adapted from Tindall et al, 1999) .....	10
Figure 2: SMRC showing textural differences and air-entry head (adapted from Tindall et al, 1999) .....	11
Figure 3: Outer and Inner Cylinders for the Hammer-Drive Core Sampler .....	21
Figure 4: Hammer-Driven Core Sampler .....	21
Figure 5: TDR equipment at 1-ft, 2-ft, and 3-ft depths.....	23
Figure 6: Above ground configuration of the tensiometer (pressure-sensing device).....	23
Figure 7: Tensiometer at the 3-ft depth with TDRs (porous element).....	23
Figure 8: Equipment set up for determining the permeability for the native soil using the falling head permeameter .....	25
Figure 9: Equipment set up for determining the permeability for the soil amendments using the falling head permeameter .....	25
Figure 10: Tempe Pressure Cell.....	26
Figure 11: Double-ring infiltrometer at South Oak .....	27
Figure 12: Double-ring infiltrometer at Hunter's Trace .....	27
Figure 13: Plugged leaks around the buffer cylinder with Bentonite .....	28
Figure 14: South Oak Particle-Size Distribution (1-ft depth).....	30
Figure 15: South Oak Particle-Size Distribution (1.5-ft depth).....	30
Figure 16: South Oak Particle-Size Distribution (2-ft depth).....	31

Figure 17: South Oak Particle-Size Distribution (3-ft depth).....	31
Figure 18: South Oak Particle-Size Distribution (4.5-ft depth).....	32
Figure 19: Hunter's Trace Particle-Size Distribution (1-ft depth) .....	33
Figure 20: Hunter's Trace Particle-Size Distribution (2-ft depth).....	33
Figure 21: Hunter's Trace Particle-Size Distribution (3-ft depth) .....	34
Figure 22: Combined PSD for South Oak and Hunter's Trace .....	35
Figure 23: Media 1 Particle-Size Distribution .....	36
Figure 24: Media 2 Particle-Size Distribution .....	36
Figure 25: Laboratory SMRC for South Oak soils at a depth of 1-ft .....	41
Figure 26: Laboratory SMRC for South Oak soils at a depth of 1.5-ft .....	41
Figure 27: Laboratory SMRC for South Oak soils at a depth of 2-ft .....	42
Figure 28: Laboratory SMRC for South Oak soils at a depth of 3-ft .....	42
Figure 29: Laboratory SMRC for South Oak soils at a depth of 4.5-ft .....	43
Figure 30: Laboratory SMRC for Hunter's Trace soils at a depth of 1-ft .....	44
Figure 31: Laboratory SMRC for Hunter's Trace soils at a depth of 2-ft .....	45
Figure 32: Laboratory SMRC for Hunter's Trace soils at a depth of 3-ft .....	45
Figure 33: Laboratory SMRC for media 1 .....	46
Figure 34: Laboratory SMRC for media 2.....	47
Figure 35: Comparison of measured SMRC to analytical models for South Oak (1-ft depth) ....	49
Figure 36: Comparison of measured SMRC to analytical models for South Oak (1.5-ft depth) .	50
Figure 37: Comparison of measured SMRC to analytical models for South Oak (2-ft depth) ....	50
Figure 38: Comparison of measured SMRC to analytical models for South Oak (3-ft depth) ....	51

Figure 39: Comparison of measured SMRC to analytical models for South Oak (4.5-ft depth) .	51
Figure 40: Comparison of measured SMRC to analytical models for Hunter’s Trace (1-ft depth)	
.....	52
Figure 41: Comparison of measured SMRC to analytical models for Hunter’s Trace (2-ft depth)	
.....	52
Figure 42: Comparison of measured SMRC to analytical models for Hunter’s Trace (3-ft depth)	
.....	53
Figure 43: Comparison of measured SMRC to analytical models for media 1 .....	53
Figure 44: Comparison of measured SMRC to analytical models for media 2 .....	54
Figure 45: Hunter's Trace volumetric moisture content over time .....	55
Figure 46: SMRC field measurements (1-ft depth) .....	56
Figure 47: SMRC field measurements (2-ft depth) .....	57
Figure 48: SMRC field measurements (3-ft depth) .....	58
Figure 49: Comparison of AP model to measured SMRC for South Oak at 1-ft depth .....	60
Figure 50: Comparison of AP model to measured SMRC for South Oak at 1.5-ft depth .....	60
Figure 51: Comparison of AP model to measured SMRC for South Oak at 2-ft depth .....	61
Figure 52: Comparison of AP model to measured SMRC for South Oak at 3-ft depth .....	61
Figure 53: Comparison of AP model to measured SMRC for South Oak at 4.5-ft depth .....	62
Figure 54: Comparison of AP model to measured SMRC for Hunter's Trace at 1-ft depth.....	63
Figure 55: Comparison of AP model to measured SMRC for Hunter's Trace at 2-ft depth.....	63
Figure 56: Comparison of AP model to measured SMRC for Hunter's Trace at 3-ft depth.....	64
Figure 57: Comparison of AP model to measured SMRC for the Media 1.....	65

Figure 58: Comparison of AP model to measured SMRC for the Media 2.....	65
Figure 59: Comparing SMRC with different AP scaling factors for South Oak at 1-ft depth .....	66
Figure 60: Comparing SMRC with different AP scaling factors for South Oak at 1.5-ft depth ..	67
Figure 61: Comparing SMRC with different AP scaling factors for South Oak at 2-ft depth .....	67
Figure 62: Comparing SMRC with different AP scaling factors for South Oak at 3-ft depth .....	68
Figure 63: Comparing SMRC with different AP scaling factors for South Oak at 4.5-ft depth ..	68
Figure 64: Limestone screening particle-size distribution.....	81

## LIST OF TABLES

Table 1: Specific gravity, bulk density, and porosity for the soil amendments and native soils..	38
Table 2: Hydraulic conductivity for the native soils.....	39
Table 3: Hydraulic conductivity for soil amendments.....	39
Table 4: Brooks and Corey Model Fitted Parameters.....	48
Table 5: van Genuchten Model Fitted Parameters.....	49
Table 6: Summary of AP scaling factor for soils at South Oak.....	59
Table 7: South Oak sieve analysis (1-ft depth).....	76
Table 8: South Oak sieve analysis (1.5-ft depth).....	76
Table 9: South Oak sieve analysis (2-ft depth).....	77
Table 10: South Oak sieve analysis (3-ft depth).....	77
Table 11: South Oak sieve analysis (4.5-ft depth).....	78
Table 12: Hunter's Trace sieve analysis (1-ft depth) .....	78
Table 13: Hunter's Trace sieve analysis (2-ft depth).....	79
Table 14: Hunter's Trace sieve analysis (3-ft depth) .....	79
Table 15: Media 1 sieve analysis .....	80
Table 16: Media 2 sieve analysis .....	80
Table 17: Limestone screening sieve analysis .....	81
Table 18: Specific gravity for South Oak soil samples.....	83
Table 19: Specific gravity for Hunter's Trace soil samples .....	84
Table 20: Specific gravity for Medias .....	84

Table 21: Hydraulic conductivity at South Oak (1-ft depth) .....	86
Table 22: Hydraulic conductivity at South Oak (1.5-ft depth) .....	87
Table 23: Hydraulic conductivity at South Oak (2-ft depth) .....	87
Table 24: Hydraulic conductivity at South Oak (depth 3 ft) .....	88
Table 25: Hydraulic conductivity at South Oak (4.5-ft depth) .....	88
Table 26: Hydraulic conductivity at Hunter's Trace (1-ft depth).....	89
Table 27: Hydraulic conductivity at Hunter's Trace (2-ft depth).....	90
Table 28: Hydraulic conductivity at Hunter's Trace (3-ft depth).....	90
Table 29: Hydraulic conductivity of Media 1 .....	91
Table 30: Hydraulic conductivity of Media 2 .....	92
Table 31: SMRC for South Oak (1-ft depth) .....	94
Table 32: SMRC for South Oak (1.5-ft depth) .....	95
Table 33: SMRC for South Oak (2-ft depth) .....	96
Table 34: SMRC for South Oak (3-ft depth) .....	97
Table 35: SMRC for South Oak (4.5-ft depth) .....	98
Table 36: SMRC for Hunter's Trace (1-ft depth) .....	99
Table 37: SMRC for Hunter's Trace (2-ft depth) .....	100
Table 38: SMRC for Hunter's Trace (3-ft depth) .....	101
Table 39: SMRC for Media 1 .....	102
Table 40: SMRC for Media 2 .....	102
Table 41: AP model for South Oak 1-ft depth.....	104
Table 42: AP model for South Oak 1.5-ft depth.....	105



Table 43: AP model for South Oak 2-ft depth.....	106
Table 44: AP model for South Oak 3-ft depth.....	107
Table 45: AP model for South Oak 4.5-ft depth.....	108
Table 46: AP model for Hunter's Trace 1-ft depth .....	109
Table 47: AP model for Hunter's Trace 2-ft depth .....	110
Table 48: AP model for Hunter's Trace 3-ft depth .....	111
Table 49: AP model for Media 1 .....	112
Table 50: AP model for Media 2 .....	113

## LIST OF ACRONYMS AND SYMBOLS

$\Psi_b$	Air-entry pressure head (Bubbling pressure head)
AP	Arya and Paris
$\alpha$	Arya and Paris tortuosity correcting parameter (scaling factor)
BMP	Best management practices
$\lambda$	Brooks and Corey's pore size distribution index
$\rho_b$	Bulk density
$\theta_g$	Gravimetric water content
$g_w$	Gravimetric water content
HT	Hunter's Trace
$\Psi$	Matric Head
$\Theta$	Normalized water content or reduced saturation
MSE	Mean square error
$n_i$	Number of particles for the Arya and Paris Model
$\rho_p$	Particle density
PSD	Particle-size distribution
PTF	Pedotransfer function
$n$	Porosity
$\Phi$	Porosity for Arya and Paris Model
$k_r$	Relative permeability
$\theta_r$	Residual volumetric water content

RMSE	Root mean square error
$K_s$	Saturated hydraulic conductivity
$G_s$	Specific Gravity
SMRC	Soil moisture retention curves
$w_i$	Soil mass of the $i^{\text{th}}$ fraction
SO	South Oak
TDR	Time domain reflectometry
$K$	Unsaturated hydraulic conductivity
$\beta$	van Genuchten's pore size distribution parameter
$\alpha$	van Genuchten's reciprocal of the inflection point of SMRC
$e$	Void ratio
$\theta_w$	Volumetric water content

# CHAPTER 1: INTRODUCTION

## Introduction

Water flowing in the unsaturated zone plays an important role for agronomists, soil scientists, engineers, and hydrologists. Ground water is susceptible to contamination from nitrogen species due to the impacts of land-use activities. Stormwater runoff, septic tank leakage, fertilizer, and land-based applications of reclaimed water seep into the ground water. If soil-borne nitrogen migrates to water bodies or accumulates in the ground water, the water may be rendered as an unsuitable source of fresh water. Ground water is an important area to study because management of stormwater can be accomplished (Wanielista et al, 1997). Furthermore, predicting the water balance and water movement of ground water is crucial in ground water remediation to keep water suitable for use.

The analysis of water movement within the vadose zone to reduce contaminant transport begins with the understanding of water movement and accurately predicting the water balance or rates and patterns of contaminant transport. The ability of the soil to transmit water is measured by hydraulic conductivity, whereas the ability to store water is expressed in the soil moisture retention curve (SMRC) (Klute et al, 1986). The SMRC and the relationship between hydraulic conductivity, pressure head, and water content must be understood to increase the accuracy in modeling the unsaturated zone (Charbeneau, 2000). The SMRC is dependent on the soil structure and soil texture. Therefore, soil type is characterized by this information from which the pore-size distribution and water holding capacities can be derived.

## Objectives

The effects on the Upper Floridan aquifer of stormwater retention ponds best management practices (BMP) needs to be quantified. This research will provide data to assist in modeling of ground water in the vadose zone with the addition of a soil amendment to retention ponds. Specifically, the objectives of this study are to:

- Develop the SMRC for the soil amendments and native soils in Marion County, Florida;
- Evaluate the relationship between the SMRC developed with the Tempe cell apparatus in the laboratory against the time domain reflectometry (TDR), and tensiometers which obtained the field data;
- Compare the SMRC obtained with the Tempe cell apparatus to the Brooks and Corey model and van Genuchten model;
- Examine the relationship between the hydraulic properties and the soil properties of the soil amendments and native soils; and
- Test the accuracy of the Arya and Paris (AP) model to predict the SMRC for the soil amendments and native soils in Marion County, Florida.

## Limitations

The results of this research are limited by:

- The wet climate in Central Florida between the months of May through September;
- The soil morphology found in Marion County, Florida;
- The air-entry value of the porous plate used in the Tempe cell apparatus; and
- The effects hysteresis has on the SMRC in the laboratory and in the field measurements.

## CHAPTER 2: BACKGROUND

### Theoretical

#### *Sieve Analysis*

Particle size has a large effect on the behavior of the soil; for example, how it interacts with fluids, along with the soils compressibility, strength, and thermal regime (Hillel, 1980). Sieve analysis is a process used to establish the particle-size distribution (PSD) in a given soil. Sieve analysis is ideal for soils that are mostly granular, larger than 0.075 millimeter in diameter, with some fines whereas hydrometer analysis is for determining soil size for soil fines smaller than 0.075mm. The process consists of shaking the dried soil through a set of sieves such that the openings get progressively smaller. The data from the sieve analysis is displayed in a particle-size distribution curve. The ordinate of the graph indicates the percent finer with the diameter of the soil particle on the abscissa. This graph indicates a cumulative representation of the percent finer compared to the grain size. The effective size or the particle-size distribution curve corresponding to 10% finer of the soil is a good indicator to estimate the drainage or hydraulic conductivity of the soil. The information obtained from the particle size distribution curve includes not only the range of particle sizes, but the uniformity of the particle size or grading pattern. Soils with a smooth and flattened graph are evenly distributed and consist of a continuous display of particle sizes. These are called well graded soils. Soils which indicate several distinct size groups, graphing a step like distribution curve, are called gap graded. Soils with most of the same size grains are called uniformly graded.

### *Bulk Density*

Bulk density is the ratio of mass to the total volume of media. Values of bulk density range from 1220 kg/m<sup>3</sup> for clay soil to 1850 kg/m<sup>3</sup> for sandy soil (Tindall et al, 1999). Like porosity, the bulk density is affected by the structure of the soil, more specifically, the degree of compaction, size distribution, and shrink/swell characteristics. However, bulk density will be moderately lower than particle density because the particles will never interlock perfectly. If pores comprise half the sample volume, then the bulk density will be half of the particle density (Hillel, 1980).

### *Porosity*

Porosity is the volume of voids per the total volume. One method of calculation is seen in Equation 1.

$$n = 1 - \frac{\rho_b}{\rho_p} \qquad \text{Equation 1}$$

Fine textured soil tend to be more porous than coarse textured soil, however the mean size of the pores is greater in coarse textured soil. For an ideal soil, one that has sufficient aeration, permeability, and water-holding capacities, the pore space should be approximately equally divided between small and large pores (Baver et al, 1972). The porosity reveals nothing about pore size distribution within the soil (Hillel, 1980).

### *Specific Gravity*

Specific gravity of soil solids is an important parameter in groundwater flow and soil mechanics. Specific gravity is defined as the ratio of the unit weight of soil solids to the unit

weight of water at a given temperature. It is useful for calculation of weight-volume relationships. Specific gravity is also referred to in reference to particle density, as it is the ratio of particle density to the density of water at a given temperature (Flint, 2002). Most common minerals have a specific gravity ranging between 2.6 to 2.9 (Das, 2006). The greater the organic matter within the soil, the lower the specific gravity.

### *Hydraulic Conductivity*

Reynolds et al (2002) state the degree of saturated hydraulic conductivity,  $K_s$ , and unsaturated hydraulic conductivity,  $K$ , varies on particle size distribution, roughness, shape, structure, and pore inter-connectedness. Saturated hydraulic conductivity will range from  $10^{-2}$  m/s to  $10^{-4}$  m/s for coarse textured soil to as low as  $10^{-8}$  m/s to  $10^{-10}$  m/s for fine textured, clayey soils. Unsaturated hydraulic conductivity is measured when infiltration occurs into initially unsaturated soils to account for entrapped air in the porous media. As a result, saturated hydraulic conductivity is greater than unsaturated hydraulic conductivity, often on the order of two times.

Determination of  $K_s$  in the laboratory falls under two categories based on the hydraulic control to simulate flow and the type of permeameter used to contain the soil sample. Three tests are available to create the hydraulic gradient, constant head, falling head, and constant flow rate. The constant head test method is for coarse sands whereas the falling head test method is for fine sands. The cells or permeameters used are the rigid-wall and the flexible-wall permeameters. Rigid-wall permeameters have the disadvantage of sidewall leakage between the soil sample and the rigid wall. Flexible-wall permeameters do not have this disadvantage because the sample is



in a latex membrane. However, flexible-wall permeameters are more expensive and require more time to use. The sample is confined at the top and bottom to minimize swelling in the soil. Hydraulic conductivity is reported at a temperature of 20°C. (Reddi, 2003)

Reynolds et al (2002) also stated laboratory measurements of  $K_s$  are best accomplished with in-situ soil samples or undisturbed samples. Texture and structure play vital roles in the measurement of  $K_s$ , along with the temperature of the water, ionic salt speciation, and any air bubbles that may be present in the soil column.  $K_s$  are always corrected to a reference water temperature to compare different soil samples. To decrease the flocculation or dispersion of clay by ionic salt speciation, the use of the most “native” water should be used for the measurement. Tap water is an adequate approximation to the native water. Clay dispersion is promoted by distilled or deionized water and should never be used. Air entrapment is minimized by “bottom up” wetting of the soil column with de-aired water that is the same temperature as the porous media. The texture and structure of the soil can be altered by biological soil activity, such as earthworms burrowing or alga growth. Earthworms can create “pipe flow” from the increase in macropores. Alga growth can plug pores. To inhibit biological activity, it is suggested to keep the samples at approximately -5°C for a period of 5 to 7 days.

Hydraulic conductivity and matric potential in the unsaturated zone is directly affected by moisture content. When soil moisture changes,  $K$  and matric head,  $\Psi$ , varies which complicates modeling the vadose zone (Fetter, 1988). The matric potential is the result of adsorptive and capillary forces within the soil (Tindall et al, 1999). Dane and Hopmans (2002) states the energy state of soil water may be expressed in units of energy per unit mass ( $J\ kg^{-1}$ ), energy per unit volume (Pa), or energy per unit weight (m). Expressing the units in length is most convenient, so

energy per unit weight is used. It is also referred to as head. The matric head is negative for unsaturated soils as it represents the thermodynamic pressure of water within the vadose zone (Charbeneau, 2000).

Van Genuchten (1980) indicates that the most limiting factor in successfully modeling unsaturated flow is the lack of information regarding the parameters entering the governing equations. Rawls and Brakensiek (1985) also indicate the difficulty of obtaining the relationship between matric potential and hydraulic conductivity as a function of water content. Unsaturated hydraulic conductivity is costly to measure and widely variable in the field (van Genuchten, 1980). Therefore, scientists and engineers used models to calculate the unsaturated hydraulic conductivity from the SMRC which is easier to measure. For example, Mualem (1976) derived a model to predict the unsaturated hydraulic conductivity from the SMRC and the saturated hydraulic conductivity.

Relative permeability,  $k_r$ , is the relationship between hydraulic conductivity at specified water content to conductivity at saturation as seen in Equation 2 (Charbeneau, 2000).

$$k_r(\theta_w) = \frac{K(\theta_w)}{K_s} \quad \text{Equation 2}$$

Therefore, the unsaturated hydraulic conductivity can be determined from  $k_r$  and  $K_s$ . The relative hydraulic conductivity can be predicted by either Mulaem's model or Burdine's model in conjunction with the Brooks and Corey (Equation 4) or van Genuchten (Equation 5) models. For example, Mulaem's theory with the van Genuchten model can be seen in Equation 3,

$$k_r = \sqrt{\Theta} \left( 1 - \left( 1 - \Theta^{\frac{1}{\beta}} \right)^\gamma \right)^2 \quad \text{Equation 3}$$

where  $\gamma = 1 - \frac{1}{\beta}$ , and  $\Theta$  is the normalized water content or reduced saturation, where

$$\Theta = \frac{\theta_w - \theta_r}{n - \theta_r}, \text{ from the van Genuchten model (Charbeneau, 2000; van Genuchten, 1980).}$$

### *Soil Moisture Retention Curves*

The SMRC is a graphical representation of the relationship between matric potential and the moisture content of the soil. The hydraulic properties of the soil are determined from the SMRC. The soil water retention curve is dependent on the soil structure and soil texture. The soil is characterized from this information from which the pore-size distribution and water holding capacities can be derived. The SMRC relationship is imperative for solving the Richards equation for flow in the vadose zone (Dane, 2002).

Dane and Hopmans (2002) states the soil holding capacity can be expressed as a gravimetric water content ( $\text{kg kg}^{-1}$ ), volumetric water content ( $\text{m}^3 \text{m}^{-3}$ ), or degree of saturation. Typically the volumetric water content is used as it is more convenient. Water at ambient temperature is the common fluid characterized in these curves.

The SMRC is affected by the saturation history of the soil. In other words, the change in soil moisture and any changes to the soil volume or structure affect the SMRC; therefore, the relationship is not distinctive (Hillel, 1982). The fraction of total porosity filled with water corresponds to the water content. Water content within the soil is a function of the pore size distribution and therefore a function of the matric potential.

Primarily, water moves through the larger soil pores. As the water drains out from gravitational forces, the rate slows down or ceases. The remaining water content is referred to as the field capacity which corresponds to the capillary suction of 1/3 bar. If no rainfall event occurs, the soil moisture will reduce even further from evapotranspiration. This moisture content is known as the wilting point and corresponds to a capillary suction of 15 bars. At the wilting point, plants can no longer use the water because it is bound by adhesive forces and creates a thin film around the soil particles.

The SMRC has two primary curves or main branches due to hysteresis (Figure 1). The primary curves are for the drainage and wetting conditions. The drainage curve is obtained by desorption (drying) of an initially saturated soil sample. The wetting curve can be obtained by sorption (wetting) of an initially dry soil sample. Both methods create a continuous curve, but will not be identical. The drainage curve will correspond to the upper curve in the SMRC whereas the wetting curve will correspond to the lower curve on the SMRC for the same matric potential. This is due to the soil wetness at equilibrium being greater in desorption than sorption. Scanning curves connect the two primary curves if the wetting or drainage stops between the endpoint limits and reverses. In the field, if the wetting or drainage happens for an extended period of time, then the primary curve will be reached. However if rain events are frequent, then the soil moisture curves for the soil will switch between the primary curves along the scanning curves forming loops (Figure 1).

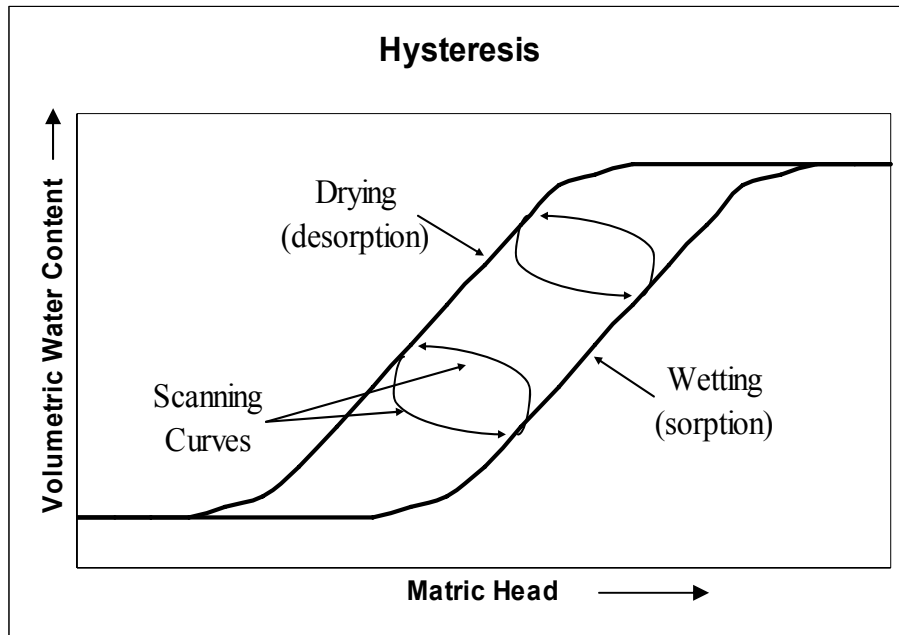


Figure 1: Sorption and desorption curves, illustrating hysteresis (adapted from Tindall et al, 1999)

Hysteresis can affect the hydraulic conductivity and flow phenomena of the soil, however when developing the SMRC, it is ignored for simplifying the analysis for monotonic wetting or drying. On the other hand, this phenomenon is important for cases where wetting and drying occur concurrently or consecutively within the soil profile. Hysteresis can be attributed to the non-uniformity of individual pores, the contact angle between the solid surfaces and liquids, entrapped air, and shrinking or swelling of the soils over time. (Hillel, 1980)

The main branch of the drainage curve begins when the largest pores of entry begin to empty. This critical point is called the air-entry head or bubbling pressure head and is generally small in coarse-textured soils or well-aggregated soils (Figure 2). In addition, the coarse-textured soils exhibit this phenomenon more readily in a sharp or distinctive drop in the SMRC than do fine-textured soils that would exhibit a gradual decrease in the curve. As the suction is

increased, the water content will empty out of progressively smaller pores until only very narrow pores retain water. The water retained at low suctions (0 to 1 bar) depends primarily on capillarity, pore-size distribution, and soil structure. Whereas, at greater suctions the soil moisture depends more on texture and surface area of the particles. The soil texture strongly affects the shape and slope of the SMRC (Figure 2). When the clay content is greater, there is a more uniform pore-size distribution. As a result, the water is absorbed to the particles, so that an increase in the matric suction causes a gradual decrease in water content versus a sharp decrease. (Hillel, 1980)

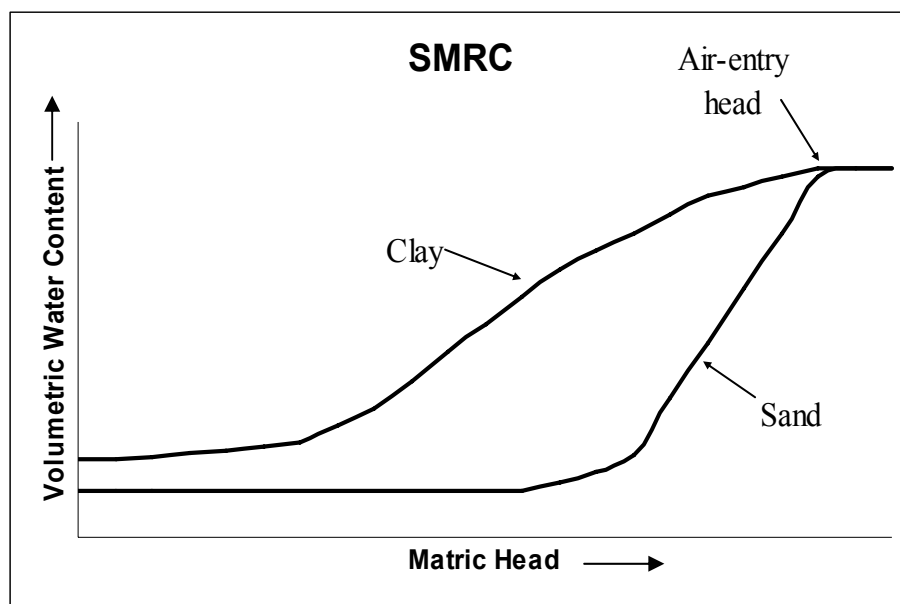


Figure 2: SMRC showing textural differences and air-entry head (adapted from Tindall et al, 1999)

There are three methods to determine the SMRC. The approaches are:

1. To estimate the curve based off of published data for similar soils (Carsel and Parrish, 1988),
2. Use an analytical function, or

3. Measure it directly.

There are two widely used analytical models, the Brooks and Corey model (Equation 4),

$$\theta_w = \left( \frac{\Psi_b}{\Psi} \right)^\lambda (n - \theta_r) + \theta_r \quad \text{Equation 4}$$

or the van Genuchten model (Equation 5),

$$\theta_w = \left[ \left( \frac{1}{1 + (\alpha\Psi)^\beta} \right)^{1 - \frac{1}{\beta}} \right] (n - \theta_r) + \theta_r \quad \text{Equation 5}$$

The curve can be measured directly using incremental equilibrium methods or dynamic methods. (Charbeneau, 2000)

The two most widely used models to represent the SMRC are the Brooks and Corey model and the van Genuchten model. Both are power-law models that relate the reduced saturation to the matric potential. The Brooks and Corey model involves several parameters which are  $n$ , porosity;  $\theta_r$ , residual volumetric moisture content;  $\Psi_b$ , air entry pressure head (bubbling pressure or pressure head at which air phase first becomes continuous); and  $\lambda$ , pore size distribution index that characterizes the slope of the SMRC (Brooks and Corey, 1964). The parameters in the van Genuchten model are  $n$ , porosity;  $\alpha$ , the reciprocal of which approximately equals the pressure head at the inflection point in the SMRC; and  $\beta$ , a pore size distribution parameter characterizing the slope of the SMRC (van Genuchten, 1980).

#### *Double-Ring Infiltrometer*

There are various methods for measuring the  $K_s$  in the field, but most explain testing the soils below the water table. However, for measuring the  $K_s$  above the water table, unsaturated

soils, there are two methods, infiltration testing and borehole testing (Charbeneau, 2000). Reynolds et al (2002) states single-ring, double-ring, or concentric-ring infiltrometers are used to measure cumulative infiltration, infiltration rate, and field-saturated hydraulic conductivity. The single-ring infiltrometer is an open-ended solitary measuring cylinder whereas the double-ring infiltrometer has another open-ended buffer cylinder that is placed outside the measuring cylinder. The double ring is to prevent flow divergence by leaving only vertical flow under the inner ring or measuring ring. In general, infiltrometers range from 10 to 50 cm in diameter and from 5 to 20 cm in length. They are thin-wall high density plastic or metal cylinders with a sharp base end that is beveled for cutting to minimize soil resistance or soil disturbance. Some appropriate techniques for insertion into the soil to a depth of 3 to 10 cm include drop-hammer or hydraulic ram. The cylinders need to be inserted as straight as possible to promote one dimensional flow. If the cylinders are tilted upon insertion, a new location needs to be selected. To maintain a constant head in the measuring cylinder, a Mariotte reservoir or float valve arrangement is used. Infiltration is measured when a constant discharge is achieved in the measuring cylinder.

Bouwer (1986) specifies the cylinders are pushed into the ground about 5 cm and flooded with water that is similar in temperature and quality to the system so the measurement is realistic and reduces error. The rate at which the water flows into the ground is measured until the rate has become essentially a constant value. Cylinder infiltrometers are best used for inundated soils whereas sprinkler-type infiltrometers are better used for simulating rainfall or sprinkler irrigation. Double-cylinder infiltrometers are effective only to eliminate leakage along the inner edge of the inside cylinder wall. The outside cylinder's water level is kept at the same height as the



measuring infiltrometer to minimize the leakage. When lateral capillary gradients create lateral divergence, the outside buffer cylinder does not ensure vertical flow. True vertical flow can be measured when a very large diameter infiltrometer is used, so that the ratio of critical pressure head for wetting (unsaturated-flow capability) and the cylinder's diameter is essential zero. Another way to minimize lateral divergence is to use a smaller pressure head of water at the soil surface.

In addition, Reynolds et al (2002) indicates sources of error include disturbance of the soil when the equipment is installed, short circuit flow along the walls of the cylinders, siltation, changes in soil with depth, and evaporation from the measuring cylinder. The disturbance can be minimized with appropriate insertion of the sharp beveled base on the cylinders. The soil in contact with the inside of the cylinders should be lightly tamped to prevent short circuit flow whereas larger gaps should be backfilled with bentonite or fine clay. Siltation or deflocculated clay or silt can be minimized by reducing the force of incoming water with a diffuser device and by ensuring the water has major cation concentrations. For this reason, distilled water or deionized water should never be used.

### SMRC Case Studies

In addition to being used to model flow in the vadose zone, Li et al (2005) indicated the SMRC is a good prediction of permeability and shear strength in unsaturated soil. This information can then be used to analyze the effects of rainfall in unsaturated slopes to predict landslides. When the matric potential partially or completely disappears, the consequence could be slope failure.

In the study by Li et al (2005), measurements of SMRC were made in the field using TRD and tensiometer equipment whereas the laboratory measurements were made with a pressure-plate extractor. The field measurements show the matric suction decreases after a rain event and increased due to evaporation with little hysteresis. The laboratory measurement shows considerable hysteresis where the wetting front matched the field data. However, the drying portion showed considerable difference to the field measurement. The hysteretic effect in the field or the laboratory SMRC may be a result of the different measurement methods.

Pachepsky et al (2001) indicate that several reasons have been documented for the discrepancies between field and laboratory measurements on the SMRC, such as inadequate representation of the pores, small spatial scale, possible soil disturbance, overburden pressure, hysteresis, and the tensiometers could have overestimated the matric potential. The study concluded that coarse-textured soils, such as sands and loamy sands (sand content > 80%), indicated a significant random difference, but no deterministic bias in the water content, whereas the soils with a higher silt/clay content showed random differences with a definite difference in water content between the field and laboratory measurements.

Cavazza et al (2007) conducted a study on temperature effects on the SMRC. Temperature had an effect on the soil moisture retention curves in areas where the water table oscillates. Two sampling locations were used for this experiment, Cadriano and Baricella, Italy. At both locations, samples were taken from two depths, 10 cm and 65 cm, at three times over the testing period, 1<sup>st</sup> winter, following summer, and 2<sup>nd</sup> winter. The undisturbed samples were taken in 6 inch diameter brass cylinders. A general t-test was used to test the difference between the SMRC by comparing the gravimetric water content ( $\theta_g$ ) values. There were differences

between the two locations and between three seasons. Validity of the soil moisture, thermal correction, and temperature correction were examined as potential source of error. There was a gap between experimental and theoretical outlook on the temperature effects on the water potential in soil; more so in fine textured soil. Any process, microbiological and/or chemical-physical, that altered the soil pore distribution, can play an important role in the SMRC.

Satyavathi (1996) studied the effects of soil disturbance on the shape of the SMRC. Crushing, drying, and sieving the soil samples modifies the structure and hence the porosity which changes the water holding capacity. However, SMRC for soils with high clay content or shrink-swell tendencies are not influenced by the structure or pore size distribution of the soil.

On the other hand, Simms and Yanful (2004) examined the relationship between the SMRC to the pore-size distribution for clayey soils. The pore-size distribution is typically assumed to be constant and monomodal. Therefore, predicting the SMRC from the pore-size distribution should be consistent. The pore-size distribution was examined with a mercury intrusion porosimeter before and after measuring the SMRC. The water content was less than predicted from the pore-size distributions both before and after the SMRC test. Therefore, shrink-swell characteristics need to be taken into account for soils with a high clay content.

Rawls and Pachepsky (2002) stated that the soil structure and consistence parameters reflect the basic soil properties which affect the hydraulic properties of a soil. Therefore, these parameters can be used to predict the SMRC. Including these parameters with textural class in predicting the SMRC leads to better accuracy. Using these parameters alone, however, did not result in better estimation of the SMRC than did using just the soil texture.

## Pedotransfer Functions

Walczak et al (2006) examined statistical-physical model (pedotransfer function) to establish a relationship between soil water content at different soil water potentials to select solid phase parameters. Pedotransfers functions are predictive functions of certain soil properties, such as soil moisture retention curve, from other easily measured properties, such as solid phase properties. The solid phase parameters frequently used are particle size distribution, bulk density, granulometric composition, and organic content. The focus was to involve pedotransfer functions with minimal solid phase parameters and compare its application between two climates, mediterranean and temperate climates. The model was useful for estimation of moisture content from select physical parameters. Two linear multiple regression equations were developed:

$$\theta_p^1 = a_0 + a_1F1 + a_2F2 + a_3P1_{tot} \quad \text{Equation 6}$$

$$\theta_p^2 = b_0 + b_1F1 + b_2F2 + b_3Bd \quad \text{Equation 7}$$

where  $\theta_p^1$  and  $\theta_p^2$  are the predictive water contents; F1 is the percent content of particles 2.0 – 0.2 mm; F2 is the percent content of particles 0.2 – 0.02 mm; F3 is the percent content of particles 0.02 – 0.002 mm;  $P1_{tot}$  is the total porosity determined from the bulk density and particle density; Bd is the bulk density, and  $a_1$ ,  $a_2$ ,  $a_3$ ,  $b_1$ ,  $b_2$ , and  $b_3$  are coefficients. With acceptable accuracy, only three soil physical parameters are needed to predict the water retention curve using pedotransfers. The model for mediterranean climate also worked for temperate climate as the particle size distribution was used in an exchangeable manner even though the particle size fractions between the two locations were different.

Arya and Paris (1981) develop a pedotransfer model that predicts soil water retention curves from taxonomic data such as particle-size distribution. The Arya and Paris (AP) model translates the PSD into pore-size distribution. From there, the pore radii which correspond to the cumulative pore volume are converted into equivalent matric head with the use of the capillarity equation (Equation 8). The cumulative pore volume is divided by the bulk density to get the volumetric water content. This model estimates pore radius from the radius of spherical particles by using a coefficient,  $\alpha$ , to scale pore length to account for the tortuosity within the soil (Haverkamp and Reggiani, 2002). The AP model is sustained by two assumptions (Vaz et al (2005). First, the capillary equation (Equation 8) which relates pore radius,  $r_i$ , and soil matric potential,  $\Psi_i$ ,

$$\psi_i = \frac{2\sigma \cos \Theta}{\rho_w g r_i} \quad \text{Equation 8}$$

where  $\sigma$  is the surface tension (N/m),  $\Theta$  is the contact angle,  $\rho_w$  is the density of water ( $\text{kg/m}^3$ ), and  $g$  is the acceleration due to gravity ( $\text{m/s}^2$ ). The second assumption is the calculation of soil water content for particle-size distribution within each soil size that contributes to soil wetting as seen in Equation 9.

$$\theta_i = \Phi \sum_{i=0}^{i=1} w_i \quad \text{Equation 9}$$

where  $\Phi$  is the soil porosity and  $w_i$  is the soil mass on the  $i^{\text{th}}$  fraction. To calculate the number of particles for each size class  $i$ ,  $n_i$ , equation 10 is used,

$$n_i = \frac{6w_i}{\pi D_i^3 \rho_p} \quad \text{Equation 10}$$

where  $D_i$  is the mean particle diameter (m), and  $\rho_p$  is the particle density ( $\text{kg/m}^3$ ). The pore radius,  $r_i$ , is calculated with Equation 11,

$$r_i = \frac{1}{2} D_i \sqrt{\frac{2en_i^{1-\alpha}}{3}} \quad \text{Equation 11}$$

where  $e$  is the void ratio and  $\alpha$  is a scaling factor. The soil matric potential is then calculated with Equation 8 where the contact angle is assumed to be zero.

Vaz et al (2005) examined the validity of the scaling factor,  $\alpha$ , in the AP model. Brazilian soils were used to validate the AP model by examining  $\alpha$  in this study. Three constant  $\alpha$  values, 1.38, 0.938, and 0.977, were used in addition to an  $\alpha$ -variable approach. The variable approach was to create an expression for  $\alpha$  as a function of the soil water content. Finding  $\alpha$  as a function of the soil water content is the method for obtaining the estimation using the AP model. However, using  $\alpha$  values of 0.977 and 0.938 also provided estimations with similar accuracy.

## **CHAPTER 3: EXPERIMENTAL DESIGN AND APPROACH**

### **Introduction**

To compare the hydraulic and soil properties, various tests were selected to gather information on the soils and the soil amendments. PSD and specific gravity were selected to analyze the physical properties of the soil. For the hydraulic properties, saturated hydraulic conductivity was measured and the SMRC were developed for the native soils and soil amendments. Saturated hydraulic conductivity was measured in the laboratory and in the field. In addition, the SMRC were developed in the field and in the laboratory. The information gathered from these tests, allowed the bulk density and porosity to be determined.

### **Samples and Field Measurements**

Short cores were extracted from the ground using a double-cylinder, hammer-driven core sampler. The outer cylinder which is approximately 10 cm long has an integral beveled cutting edge for insertion into the soil and is attached to a long handle (Figure 3 and Figure 4). The outer cylinder has been manufactured with a lip that sits flush with the inner cylinder. The impact force comes from a sliding hammer that slides into the handle. The inner cylinder is removed and trimmed flush. The brass cylinder that contains the soil is 5 cm in diameter and 3 cm in length. (Grossman, 2002)



**Figure 3: Outer and Inner Cylinders for the Hammer-Drive Core Sampler**



**Figure 4: Hammer-Driven Core Sampler**

A total of 5 soil cores were extracted from the South Oak (SO) retention pond at depths of 1-ft, 1.5-ft, 2-ft, 3-ft, and 4.5-ft. A total of 3 soil cores were obtained from the Hunter's Trace (HT) retention pond at depths of 1-ft, 2-ft, and 3-ft. There were three attempts at obtaining a 4.5-ft sample at HT, but the sample was too saturated to retrieve a solid core upon withdrawal from the ground.

The soil amendments were developed from prior experimentation as the most effective in removal of nitrogen species and phosphorus species for stormwater applications. The amendments were chosen based on various criteria such as removal of nitrogen and phosphorous, permeability, cost, availability in Florida, and additional environmental benefits. (Moberg, 2008; Henderson, 2008)



The soil amendments were composed of 50% fine sand, 30% tire crumb, 20% sawdust by volume for media 1 and 50% fine sand, 25% sawdust, 15% tire crumb, 10% limestone screenings by volume for media 2. The tire crumb aids in phosphorous removal. Sawdust acts as the electron donor or carbon source for denitrification. Limestone is cheaper than tire crumb and aids in pH stabilization. All of the soil amendment components are readily available in Florida.

The soil moisture retention curves were developed in the field with the use of time domain reflectometry (TDR) and tensiometers instrumentation. Tensiometers and TDR's were installed at only the HT location and not at the SO location because the water table was above the ground level at the time of installation. The soil moisture was measured with TDR equipment (Figure 5). The TDR uses the changes in dielectric properties of the soil with water content and is highly accurate. The matric potential was measured with tensiometers (Figure 6 and Figure 7). As the soil sucks the water out of the tensiometers, a negative pressure develops. Both the TDR and tensiometers take reading every 15 minutes.



**Figure 5: TDR equipment at 1-ft, 2-ft, and 3-ft depths**



**Figure 6: Above ground configuration of the tensiometer (pressure-sensing device)**



**Figure 7: Tensiometer at the 3-ft depth with TDRs (porous element)**

## Sieve Analysis

The ASTM D-421-85 Standard Practice for Dry Preparation of Soil Samples for Particle-Size Analysis and Determination of Soil Constants was used. The first step in the sieve analysis was to determine the mass (grams) of dry sample to be tested. The sieves were prepared by stacking the sieves in increasing order using sieve numbers 10, 40, 100, 200, and 270, from top to bottom, respectively. A bottom pan was placed under the stack of sieves to collect material finer than 0.053 mm (Sieve No. 270). The sample was then poured into the stack of sieves and covered with a sieve cover. A sieve shaker was to shake the sieves for approximately 10 minutes. When the sieve shaker stopped, the stack of sieves were removed. The amount of soil retained on each sieve was weighed, starting from the top sieve (No. 10) to the bottom sieve (No. 270), and the bottom pan.

## Specific Gravity

The specific gravity was measured using the ASTM D-854-92 Standard Test Method for Specific Gravity of Soils. The measured volume of the media was approximately 100 g. The pycnometer was a volumetric flask having the capacity of 500 mL.

## Hydraulic Conductivity

The hydraulic conductivity was found using the falling head test method. The soil cores were kept at approximately 4°C to limit biological activity inside the sample. This prevented plugging or boring of soil cores as earthworms create “pipe flow” and algae growth can plug holes (Reynolds et al, 2002). The equipment set up for the native soil samples is seen in Figure 8

while for the soil amendments can be seen in Figure 9. A porous plate was used when testing the soil amendments. However for the soil samples, 160N Mirafi non-woven fabric was used instead of porous plates. The soil specimen was saturated from the bottom using de-aired tap water. Distilled or de-ionized water would have allowed for clay dispersion, so was not used in testing (Reynolds et al, 2002). After the specimen was saturated, any air bubbles within the tubing were removed. The time for the water to flow from the two selected heads,  $h_1$  to  $h_2$ , was measured. Several trials were run and averaged. Then the permeability was converted to a test temperature of water at 20°C.



**Figure 8: Equipment set up for determining the permeability for the native soil using the falling head permeameter**

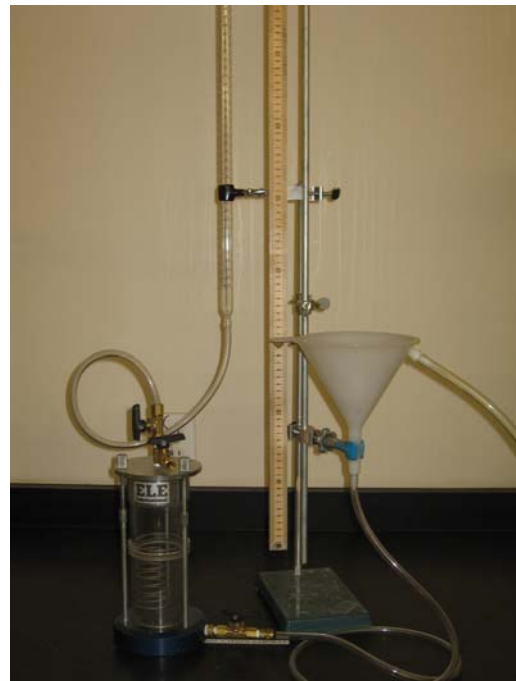


**Figure 9: Equipment set up for determining the permeability for the soil amendments using the falling head permeameter**

## Soil Moisture Retention Curve

The soil moisture retention curves were developed in the laboratory using the 1400 Tempe Pressure Cell obtained from Soilmoisture Equipment Corporation (Figure 10). The Tempe Cell drain outlet was attached to a leveling bulb with deaerated water. The height of the water in the bulb was kept to a level equivalent to the bottom of the Tempe Cell. The porous plate was saturated with deaerated water in a vacuum desiccator before it was placed into the Tempe Cell. Then, the leveling bulb was raised to the same height as the porous plate. The porous plate had an air entry value of 10 m H<sub>2</sub>O (1 bar). Therefore, the testing could not exceed 1 bar if the soil air was to be kept at atmospheric pressure. The soil sample and brass cylinder were placed on top of the porous plate by careful twisting, ensuring good contact between the porous plate and the brass cylinder. The bulb was then raised incrementally to saturate the soil sample. The top half of the Tempe Cell was then attached once the soil sample was saturated.



**Figure 10: Tempe Pressure Cell**

The Tempe Cell was weighed to get the initial mass of the saturated soil. The pump was maintained at a specified suction until the mass of the Tempe Cell had reached equilibrium. After the mass of the Tempe Cell had reached equilibrium or under a 5% change in water content, the suction was increased incrementally until enough points were measured to define the soil moisture retention curve. The sample was then oven dried at 105° to determine the residual moisture content within the soil sample.

### Double-Ring Infiltrometer

A metal double-ring infiltrometer with a sharp base was used (Figure 11 and Figure 12). The measuring cylinder is 30 cm in diameter and 50 cm in length. The buffer cylinder is 50 cm in diameter and 50 cm in length. Infiltration was measured when a constant discharge was achieved in the measuring cylinder.



**Figure 11: Double-ring infiltrometer at South Oak**



**Figure 12: Double-ring infiltrometer at Hunter's Trace**



The measuring cylinder was pushed into the ground about 5 cm at all locations while the buffer cylinder depth varied at each location from 3 to 5 cm. If significant tilting occurred, a new location was used. Bentonite was used to plug any leaks from the buffer cylinder (Figure 13).



**Figure 13: Plugged leaks around the buffer cylinder with Bentonite**

The cylinders were flooded with tap water from surrounding homes to saturate the system. The rate at which the water infiltrated into the ground was continuously measured. Testing was continued until a steady infiltration rate was achieved (ASTM, 1997). The outside cylinder's water level was kept at the same height as the measuring infiltrometer to minimize the leakage between cylinders (Bouwer, 1986).

## CHAPTER 4: RESULTS AND DISCUSSION

### Soil Properties

#### *Sieve Analysis*

The soils at SO are uniformly graded soils as their particle-size distributions are without discontinuities and appear to be smoothly distributed. The particle-size distribution (PSD) at the 1-ft depth indicates 91.5% sand content and 8.5% silt and clay content using USDA classification system where sand is 0.05 – 2.0mm, silt is 0.002 – 0.05 mm, and clay is <0.002 mm (Figure 14). As for the 1.5-ft depth, the PSD indicates approximately 92% sand content and 8% silt and clay content (Figure 15). The South Oak soil at 2-ft depth has a sand content of 87.5% and a silt/clay content of 12.5% (Figure 16). The soil at 3-ft depth has a sand content of 90% and a silt/clay content of 10% (Figure 17). The soil at the 4.5-ft depth has a sand content of 87.7% and a silt/clay content of 12.3% (Figure 18). Therefore, all the soil samples have a textural class of “sand” on the textural triangle. The samples at the 2-ft and 4.5-ft depths are closer to “loamy sand” than the other soil samples because of their higher silt and clay content.



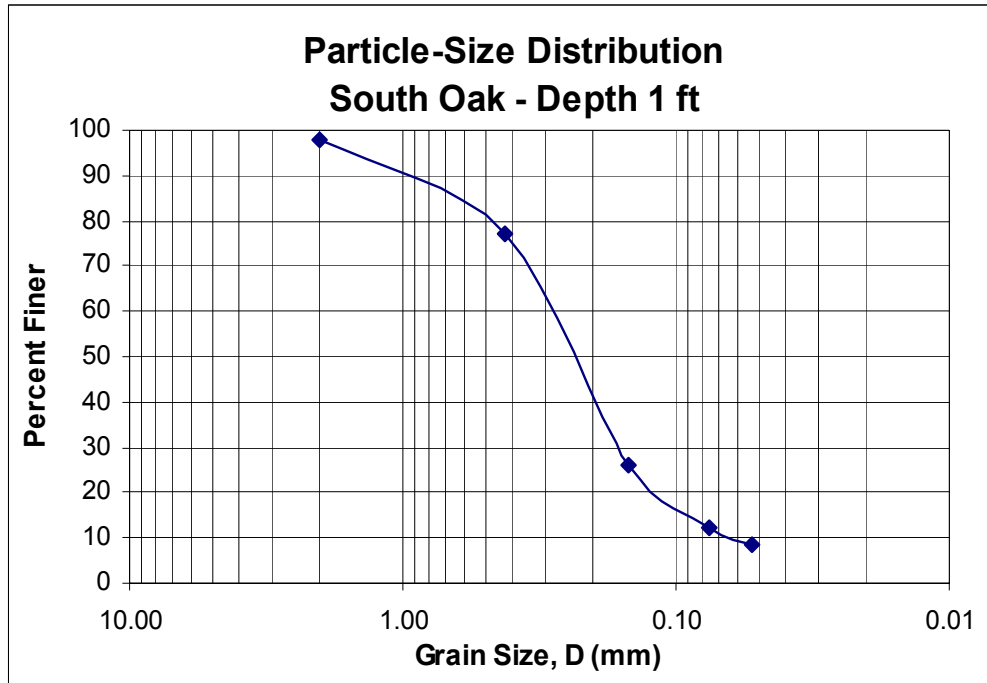


**Figure 14: South Oak Particle-Size Distribution (1-ft depth)**

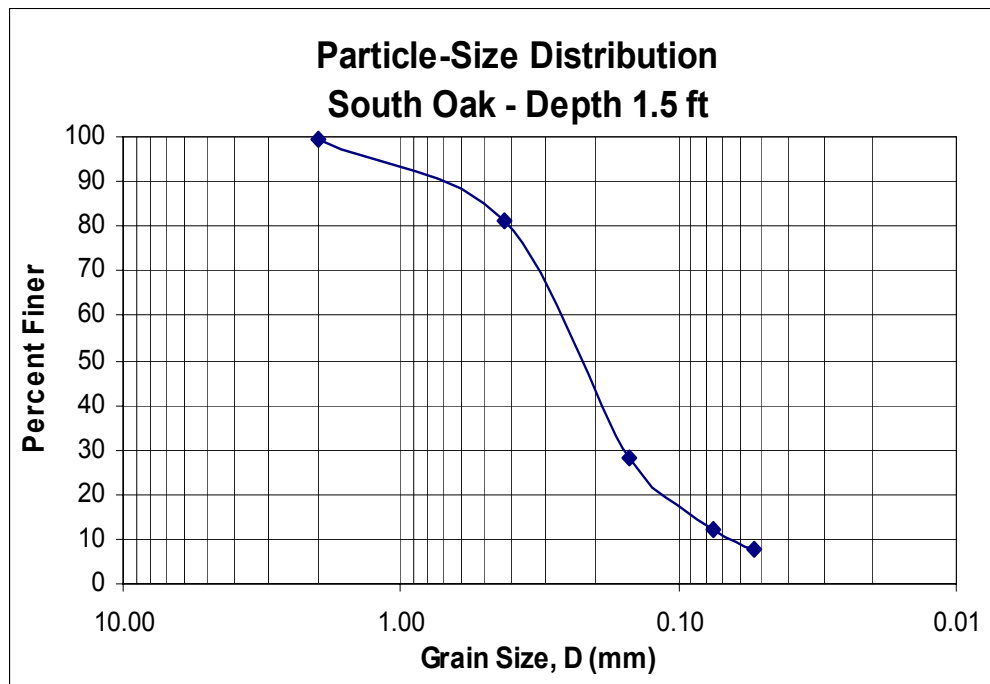


**Figure 15: South Oak Particle-Size Distribution (1.5-ft depth)**

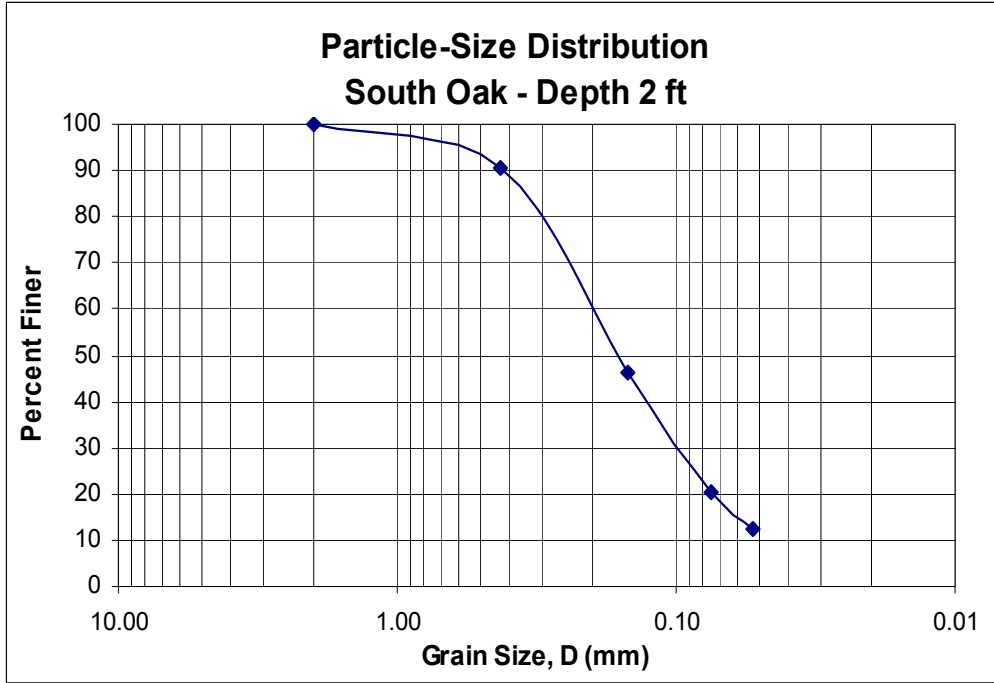


**Figure 16: South Oak Particle-Size Distribution (2-ft depth)**

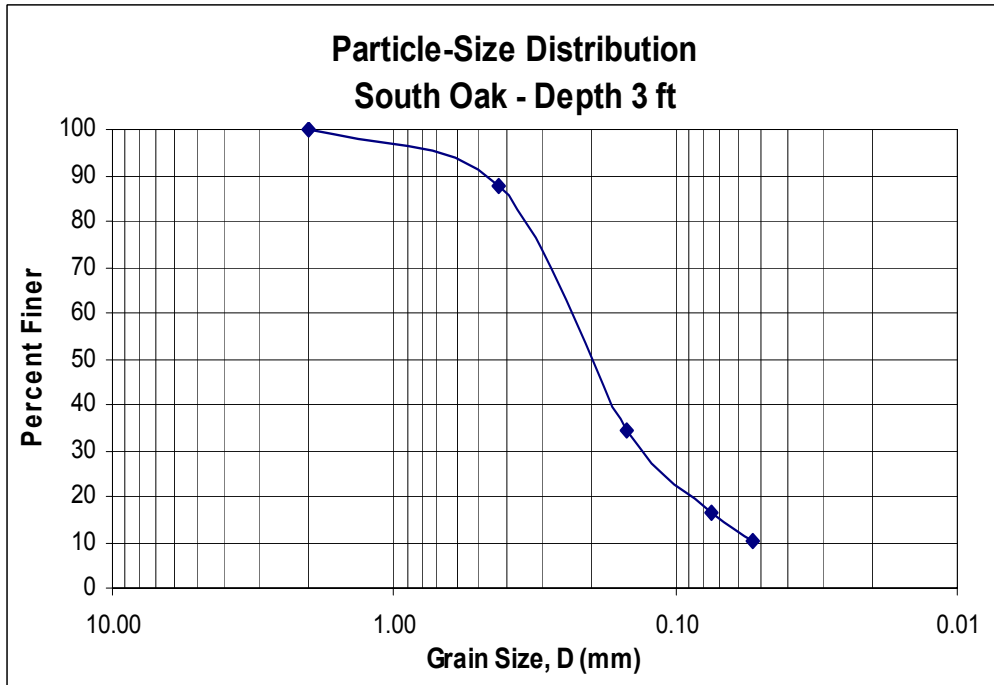


**Figure 17: South Oak Particle-Size Distribution (3-ft depth)**

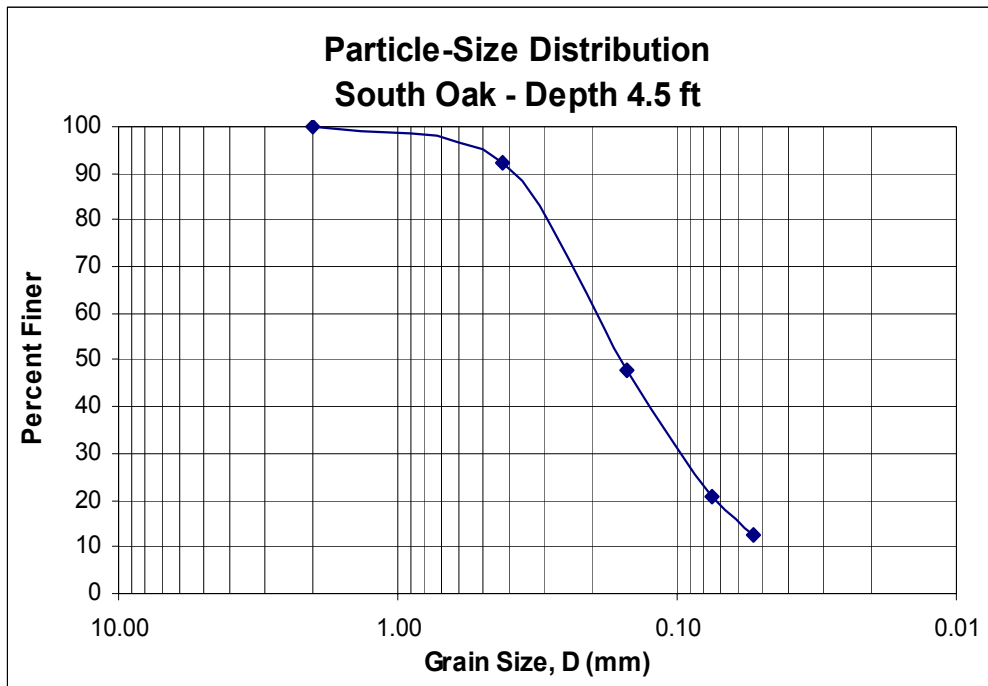


**Figure 18: South Oak Particle-Size Distribution (4.5-ft depth)**

The particle-size distributions for soils at HT are without discontinuities and appear to be smoothly distributed, so the soil is uniformly graded. The PSD at the 1-ft depth indicates approximately 99% sand content and 1% silt/clay content as seen in Figure 19. The composition of the 2-ft depth soil sample is 96.8% sand and the remaining is silt/clay (Figure 20). The 3-ft depth sample is composed of 98.7% sand and 1.3% silt/clay as seen in Figure 21. Therefore, the textural class for HT soils is “sand.”

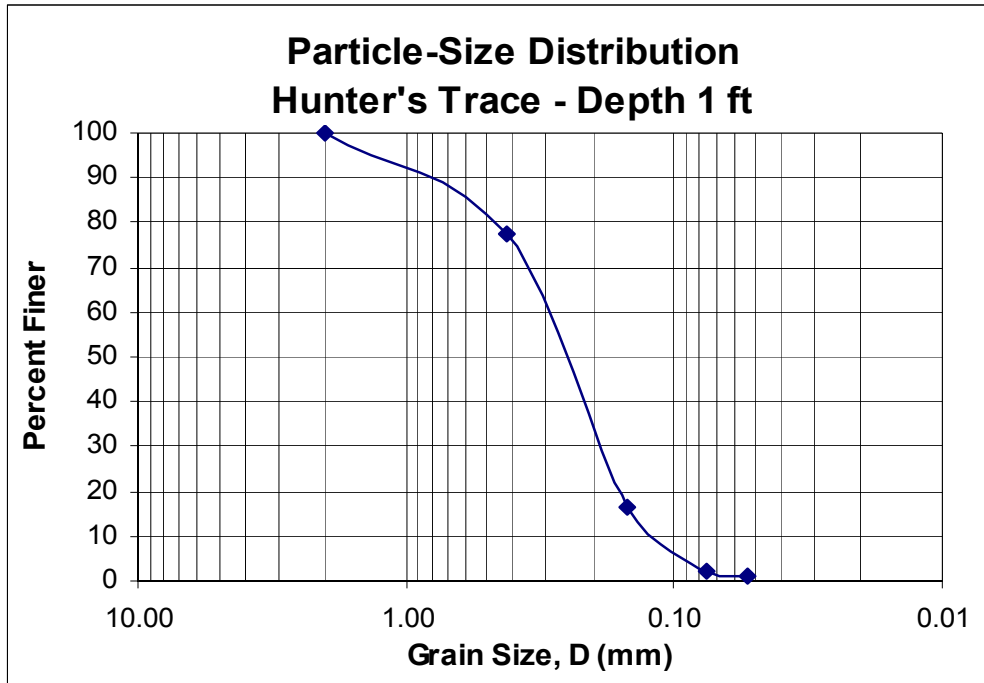


Figure 19: Hunter's Trace Particle-Size Distribution (1-ft depth)

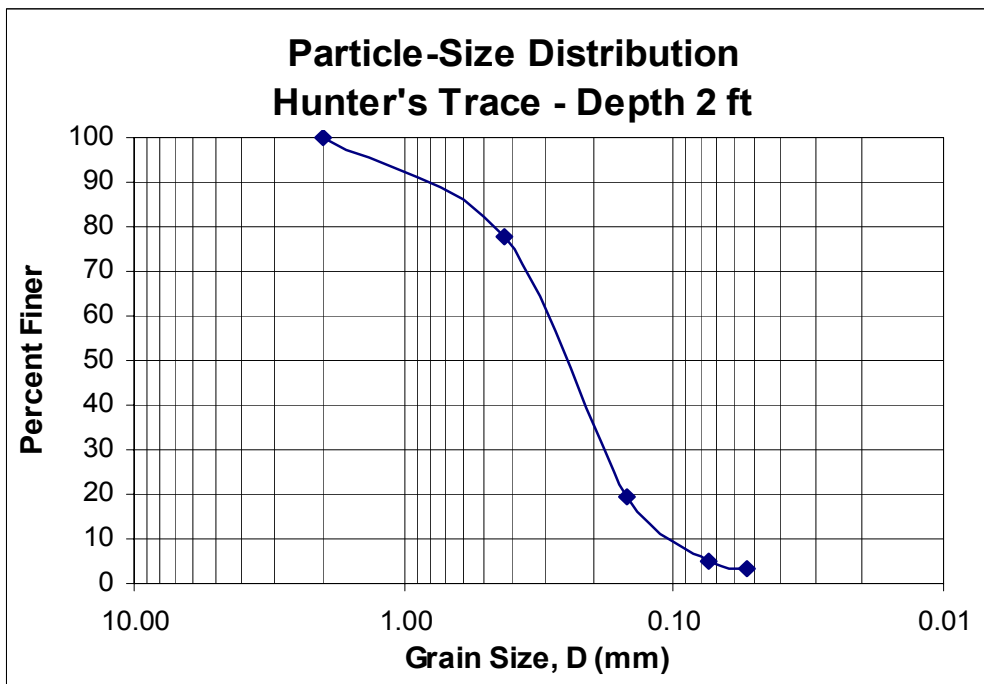
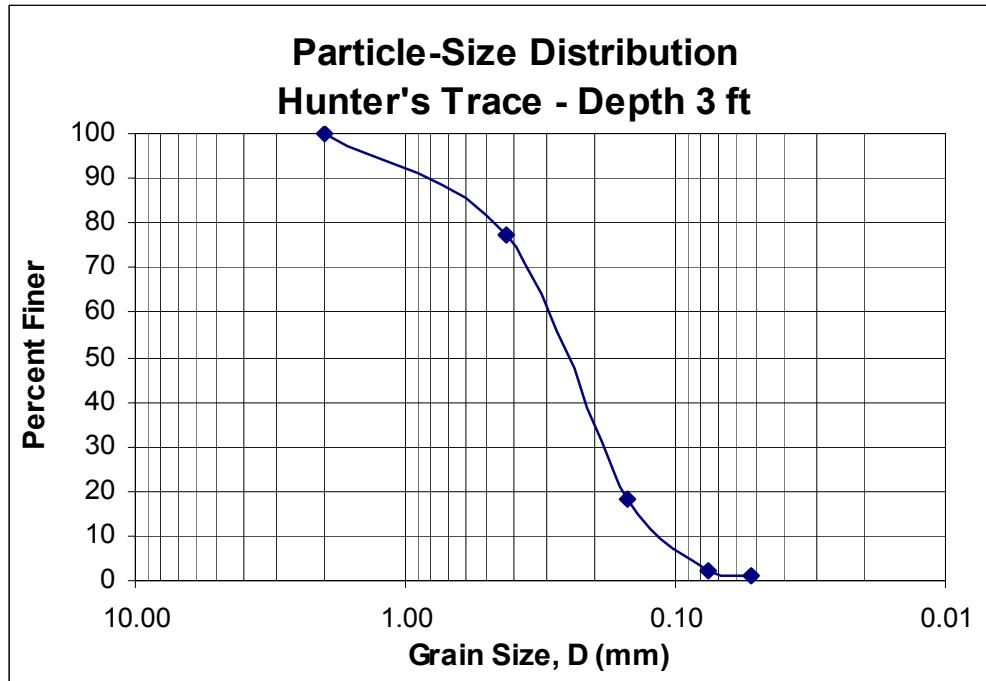


Figure 20: Hunter's Trace Particle-Size Distribution (2-ft depth)



**Figure 21: Hunter's Trace Particle-Size Distribution (3-ft depth)**

The combined sieve analysis for SO and HT can be seen in Figure 22. When the PSD for SO and HT are compared, SO soils have a higher content of silt/clay than HT soils.

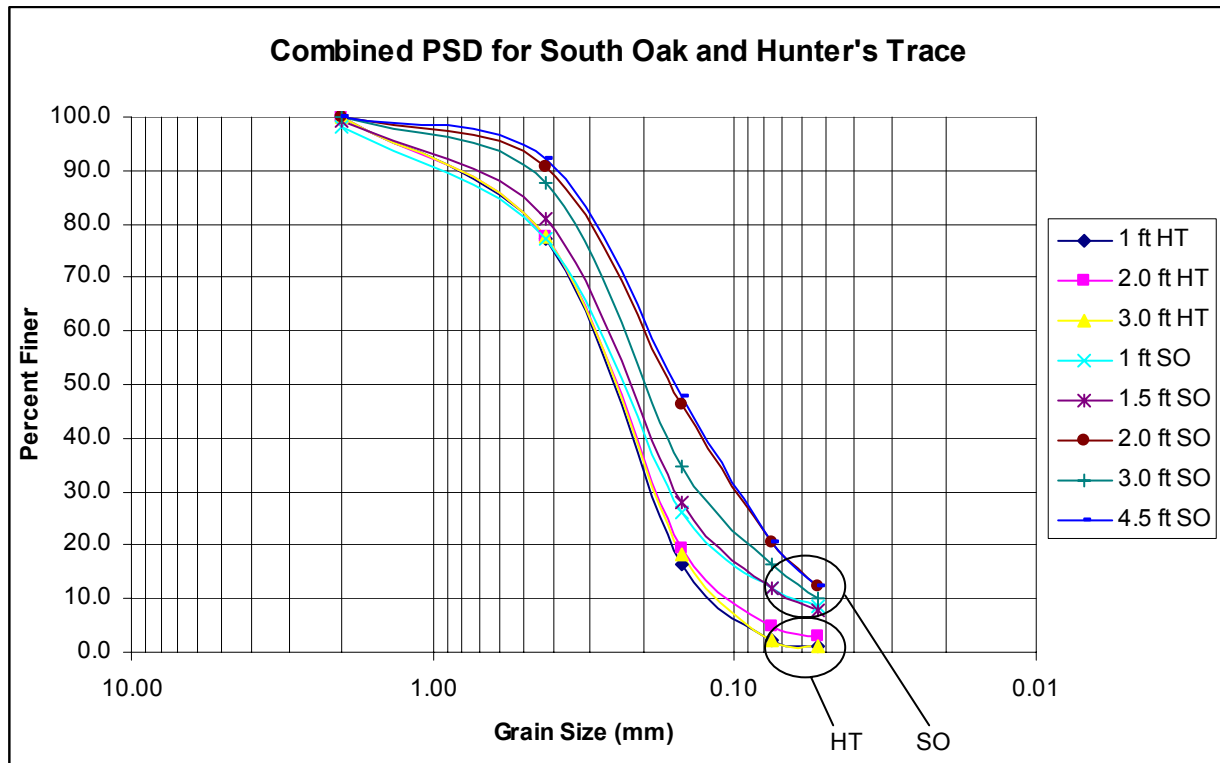


Figure 22: Combined PSD for South Oak and Hunter's Trace

Media 1 and media 2 have a gap graded distribution as can be seen in Figure 23 and Figure 24, respectively. The discontinuity in the particle distribution is more prominent in media 1 than in media 2 due to the additional limestone in media 2 and lower percent of tire crumb and sawdust. Media 1 has 10% more tire crumb and sawdust than media 2, therefore 24.4% for media 1 is retained on the Number 40 sieve whereas only 21.9% for media 2 was retained. After passing the Number 40 sieve, the cumulative percent retained on each sieve is comparable for both amendments.

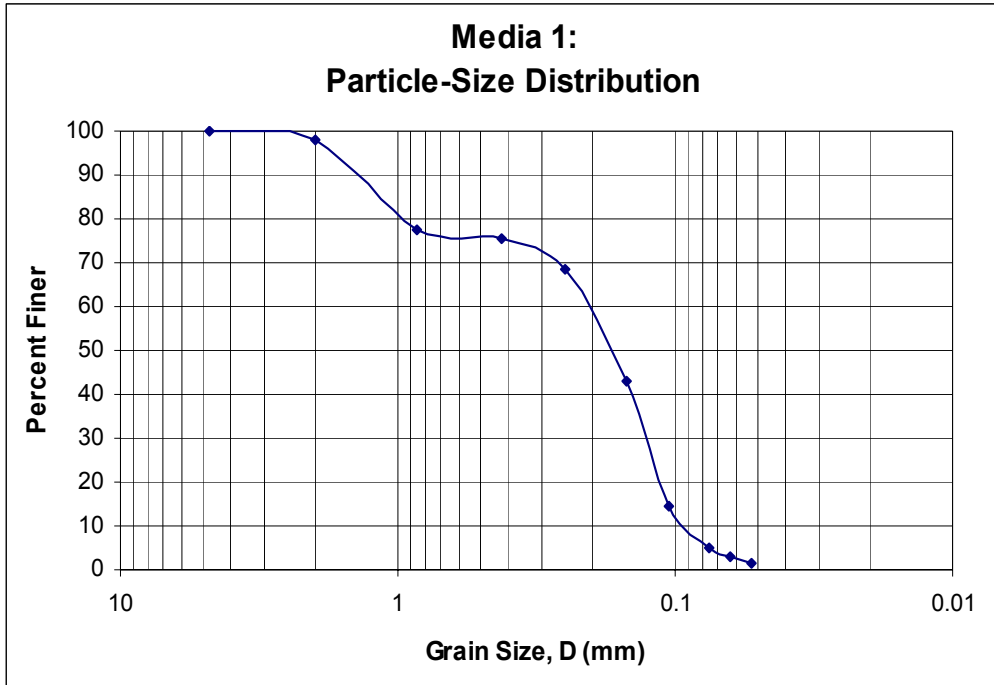


Figure 23: Media 1 Particle-Size Distribution

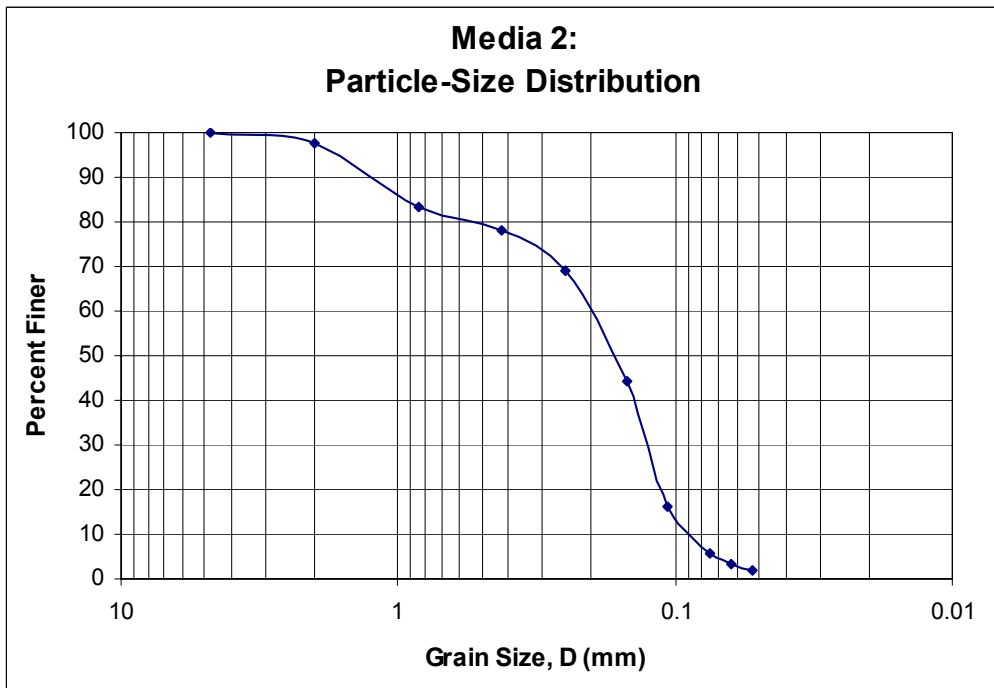


Figure 24: Media 2 Particle-Size Distribution

### *Specific Gravity, Bulk Density, and Porosity*

The SO soils have a specific gravity,  $G_s$ , range between 2.5 and 2.6 whereas the range at HT is 2.6 to 2.7 (Table 1). Media 1 has a  $G_s$  of 2.19 and 2.33 for media 2. The lower values of  $G_s$  at SO and in the soil amendments indicate a higher content of organic material than HT.

Bulk density is affected by the degree of compaction as it includes the volume of pores between the particles. The bulk density is considerably lower for the soils at SO than the soils at HT (Table 1). They range from 1.44 to 1.70 with an average of 1.57. The bulk densities for the soils at HT range from 1.61 to 1.69 with an average of 1.65. Therefore, the overall bulk density is higher at HT than the SO. The soil amendments have a considerably lower bulk density than the native soils when conducting the falling head permeability test. Media 1 has a value of 1.41 while media 2 has a value of 1.44 in the permeameter. However, the packing was different in the Tempe cells for the soil amendments. Therefore the bulk density was different. Media 1 had a bulk density of 1.32 and 1.29, respectively

The porosity for the silty sand soils at SO varies with depth (Table 1). The porosity at 1-ft, 1.5-ft, 2-ft, 3-ft, and 4.5-ft depths are 41%, 35%, 41%, 45%, and 39%, respectively. The sand soil at HT has a porosity of 36%, 38%, and 40% at the 1-ft, 2-ft, and 3-ft depths, respectively. The porosity of media 1 and media 2 are 36% and 38%, respectively, in the permeameter. Whereas the porosity of media 1 and media 2 are calculated to be 40% and 44%, respectively in the Tempe cell apparatus. The difference in the porosity for the soil amendments is due to the different packing techniques used. Therefore, packing plays an enormous role in the porosity of the soil amendment.



**Table 1: Specific gravity, bulk density, and porosity for the soil amendments and native soils**

<b>Sample</b>	<b>Specific Gravity, <math>G_s</math></b>	<b>Dry Bulk Density, <math>\rho_b</math> (<math>\text{g/cm}^3</math>)</b>	<b>Porosity, <math>n</math> (%)</b>
<b>SO 1 ft</b>	2.56	1.50	41
<b>SO 1.5 ft</b>	2.6	1.70	35
<b>SO 2 ft</b>	2.53	1.49	41
<b>SO 3 ft</b>	2.62	1.44	45
<b>SO 4.5</b>	2.57	1.57	39
<b>HT 1 ft</b>	2.66	1.69	36
<b>HT 2 ft</b>	2.61	1.61	38
<b>HT 3 ft</b>	2.72	1.62	40
<b>Media 1</b>	2.19	1.41 <sup>a</sup> , 1.32 <sup>b</sup>	36 <sup>a</sup> , 40 <sup>b</sup>
<b>Media 2</b>	2.33	1.44 <sup>a</sup> , 1.29 <sup>b</sup>	38 <sup>a</sup> , 44 <sup>b</sup>

<sup>a</sup> Measured from the falling head test; <sup>b</sup> Measured from the Tempe cell

## Hydraulic Properties

### *Hydraulic Conductivity*

The saturated hydraulic conductivity,  $K_s$ , for the silty sand at SO samples decreases as the depth below the surface increases until the last sample at 4.5-ft which increases slightly, most likely due to the heterogeneity of the soil (Table 2). Saturated hydraulic conductivity has no trend with depth for the sand at HT. This irregular change is due to the spatial heterogeneity of the soil from natural processes. The  $K_s$  is considerably lower at SO than HT most likely due to the lower average porosity and higher percentage of larger particles at HT than at SO.

**Table 2: Hydraulic conductivity for the native soils**

Depth (ft)	Hydraulic Conductivity, $K_s$ (ft/day)	
	South Oak	Hunter's Trace
1	1.113	7.054
1.5	0.498	--
2	0.065	7.317
3	1.20E-04	3.973
4.5	0.003	--

The  $K_s$  for media 1 and media 2 are more comparable to the permeability for the sand soils at HT (Table 3). Media 1 has a higher  $K_s$  value than media 2. Presumably, the higher permeability of media 1 is due to a lower porosity and a higher percentage of particles retained on the Number 20 and Number 40 sieve. In addition, media 2 has additional limestone particles of smaller particle size. Also, media 2 has a higher percentage of sawdust, 25% versus the 20% is media 1 which could create a more tortuous path for the flow because of the flaky shape.

**Table 3: Hydraulic conductivity for soil amendments**

Medias	Hydraulic Conductivity, $K_s$ (ft/d)
1	8.76
2	7.24

## *Soil Moisture Retention Curve*

### *Laboratory Measurement*

#### *South Oak*

A total of 5 soil cores were extracted from the SO retention pond at depths of 1-ft, 1.5-ft, 2-ft, 3-ft, and 4.5-ft. The SMRC obtained in the lab for the silty sand soils at SO with the Tempe Pressure Cells for the depths of 1-ft, 1.5-ft, 2-ft, 3-ft, and 4.5-ft are shown in Figure 25, Figure 26, Figure 27, Figure 28, and Figure 29, respectively. There is a change in volumetric water content,  $\theta_w$ , of  $0.13 \text{ cm}^3/\text{cm}^3$  at a depth of 1-ft (Figure 25). However, the largest drop in  $\theta_w$  was  $0.19 \text{ cm}^3/\text{cm}^3$  at the 1.5-ft depth (Figure 26). The soil sample taken at 2-ft depth lost  $0.08 \text{ cm}^3/\text{cm}^3$  in  $\theta_w$  (Figure 27). These three samples, 1-ft, 1.5-ft, and 2-ft, appear to lose the majority of their water content before  $-2.0 \text{ m H}_2\text{O}$  matric potential. The samples taken at depths of 3-ft and 4.5-ft only lost  $0.006 \text{ cm}^3/\text{cm}^3$  and  $0.007 \text{ cm}^3/\text{cm}^3$  in  $\theta_w$ , respectively (Figure 28 and Figure 29). These two samples continue to have a downward trend in their SMRC. Therefore, they could potentially lose more water at a higher matric potential. The air-entry value is clearly seen in the 3-ft and 4.5-ft depth samples at  $-1.0 \text{ m H}_2\text{O}$  matric head.

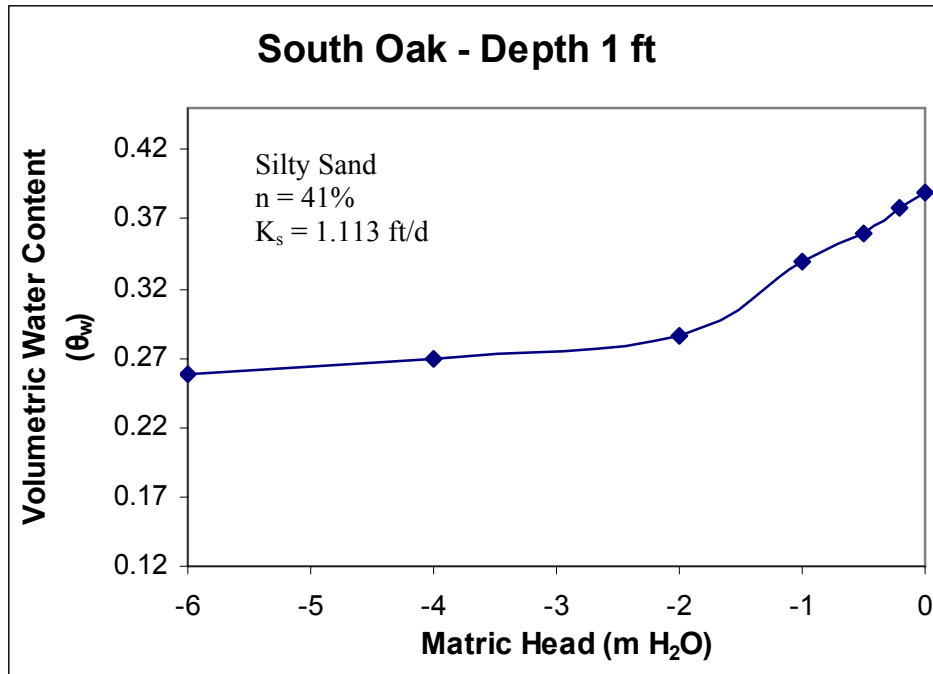


Figure 25: Laboratory SMRC for South Oak soils at a depth of 1-ft

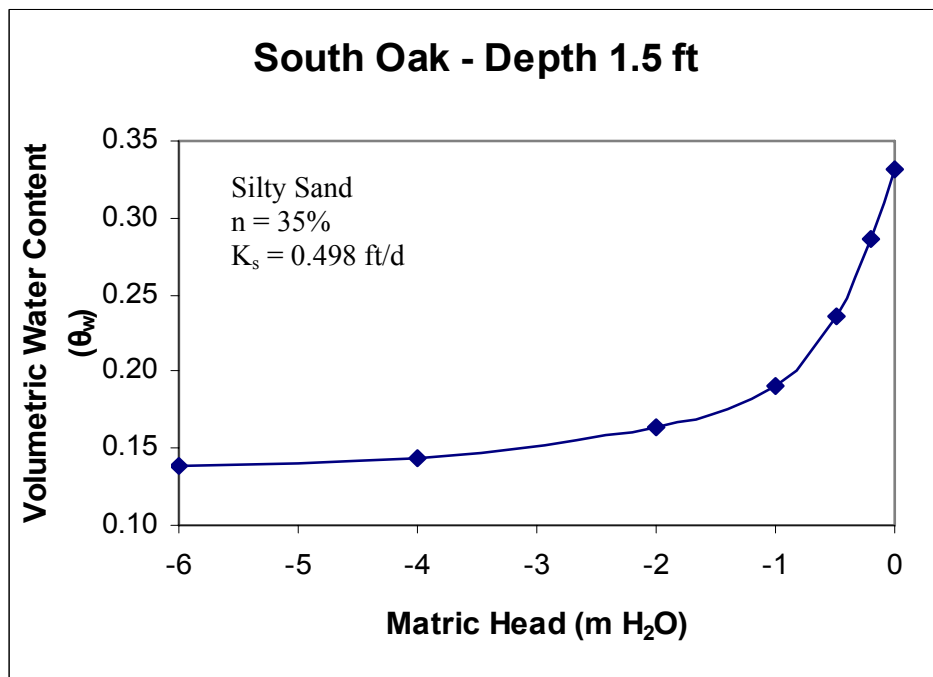


Figure 26: Laboratory SMRC for South Oak soils at a depth of 1.5-ft

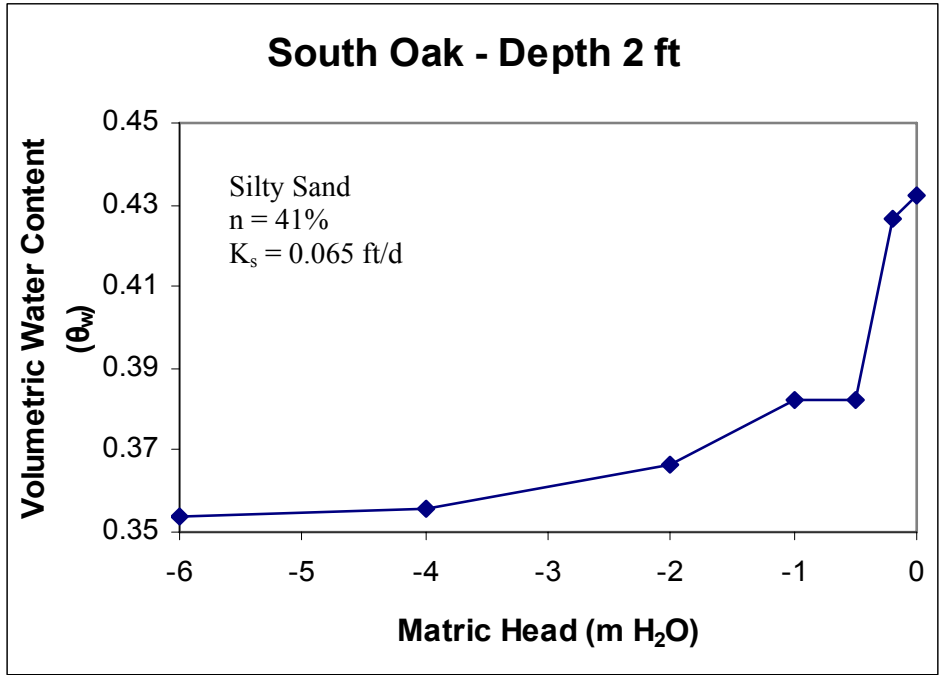


Figure 27: Laboratory SMRC for South Oak soils at a depth of 2-ft

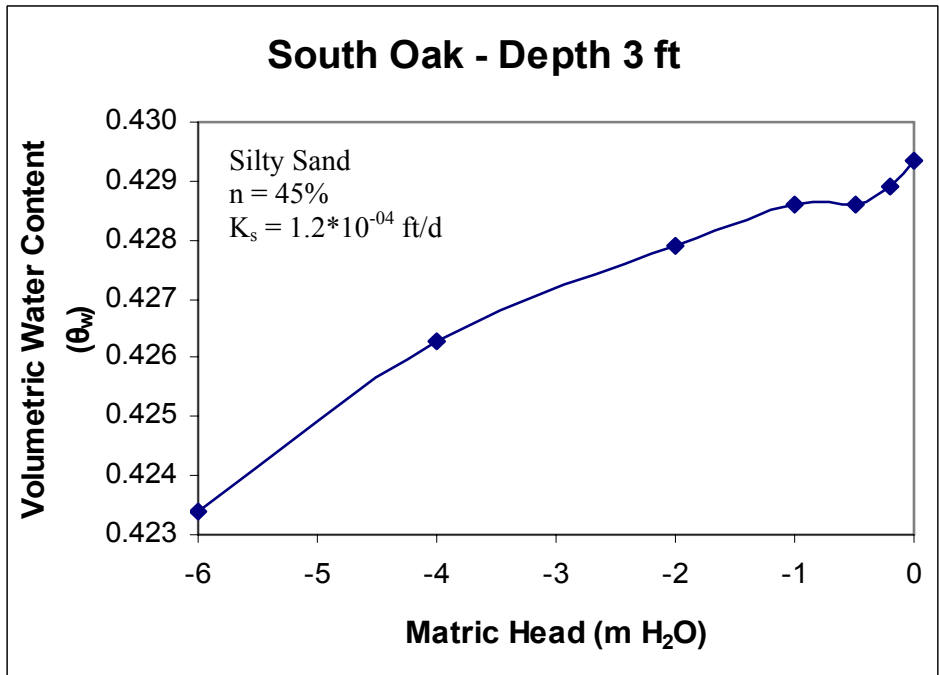


Figure 28: Laboratory SMRC for South Oak soils at a depth of 3-ft

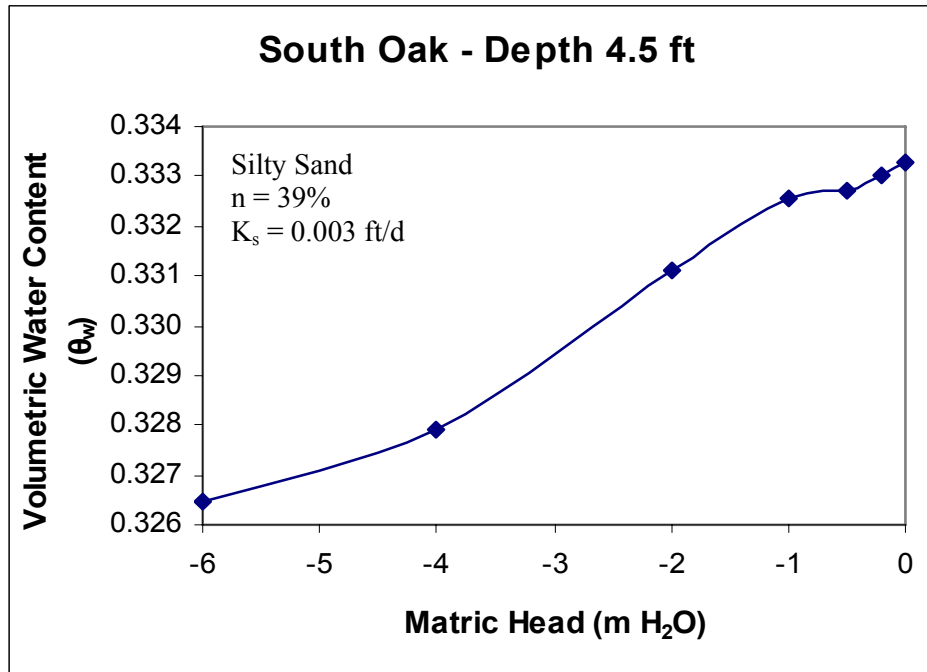


Figure 29: Laboratory SMRC for South Oak soils at a depth of 4.5-ft

### *Hunter's Trace*

A total of 3 soil cores were extracted from the HT retention pond at depths of 1-ft, 2-ft, and 3-ft. The SMRC was obtained in the lab for sand soils at HT with the Tempe Pressure Cells. The SMRC for the 1-ft, 2-ft, and 3-ft depths are shown in Figure 30, Figure 31, and Figure 32, respectively. The change in water content,  $\theta_w$ , for the 1-ft depth is  $0.23 \text{ cm}^3/\text{cm}^3$  (Figure 30). There is a change in  $\theta_w$  of  $0.21 \text{ cm}^3/\text{cm}^3$  at a depth of 2-ft (Figure 31). However, the largest drop in  $\theta_w$  is  $0.24 \text{ cm}^3/\text{cm}^3$  at the 3-ft depth (Figure 32). The 2-ft and 3-ft depth sample has an air-entry pressure head of  $-0.2 \text{ m H}_2\text{O}$  whereas the 1-ft depth is not clearly shown in the curve and  $\Psi_b$  appears to be  $-0.2 \text{ m H}_2\text{O}$ . However, the bulk of the water content lost for the 2-ft depth is at

-0.6 m H<sub>2</sub>O, whereas the 1-ft and 3-ft depth sample lost the majority of the water content at -0.4 m H<sub>2</sub>O. The 1-ft, 2-ft, and 3-ft samples appear to be at their residual water content.

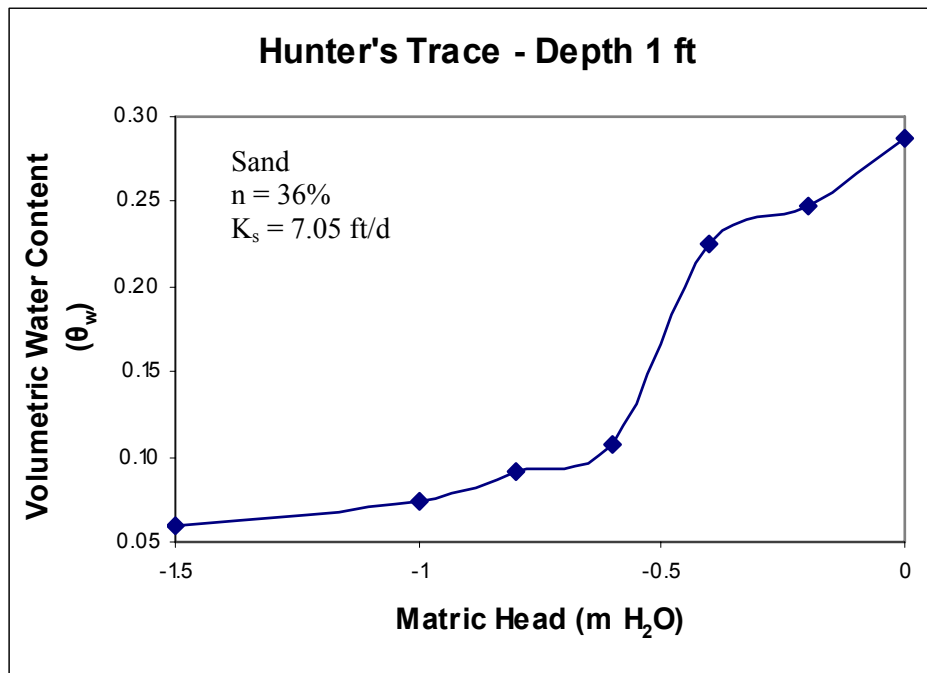


Figure 30: Laboratory SMRC for Hunter's Trace soils at a depth of 1-ft

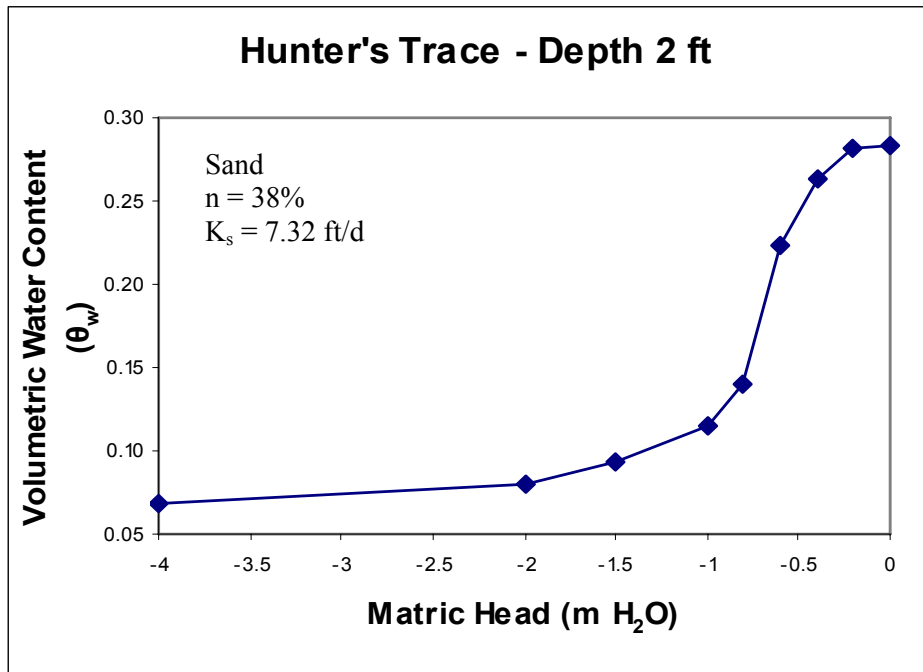


Figure 31: Laboratory SMRC for Hunter's Trace soils at a depth of 2-ft

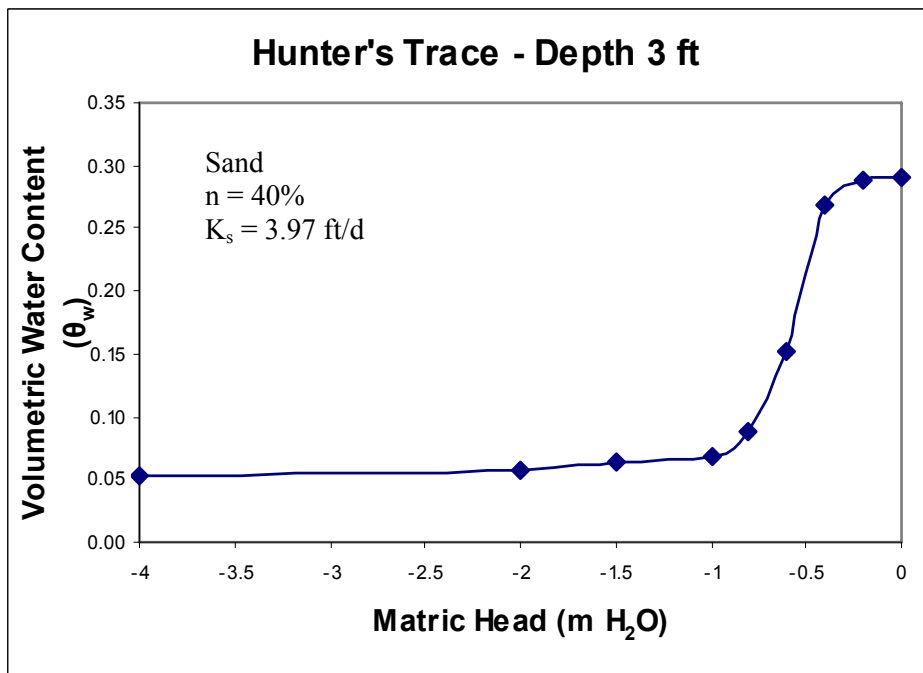


Figure 32: Laboratory SMRC for Hunter's Trace soils at a depth of 3-ft



### Soil Amendments

The SMRC for the two soil amendments were developed using Tempe Pressure Cells (Figure 33 and Figure 34). The saturated water content for media 1 and media 2 is  $0.39 \text{ cm}^3/\text{cm}^3$ . The residual water content,  $\theta_r$ , for both soil amendments is  $0.08 \text{ cm}^3/\text{cm}^3$ . The soil amendments follow the same curve except for one slight difference. The  $\theta_w$  at the matric head of  $-0.6 \text{ m H}_2\text{O}$  is  $0.30 \text{ cm}^3/\text{cm}^3$  for media 1 whereas it is  $0.25 \text{ cm}^3/\text{cm}^3$  for media 2. Therefore, there was a higher water content lost in media 2 which could be attributed to the addition of limestone or the flow paths created by the additional sawdust.

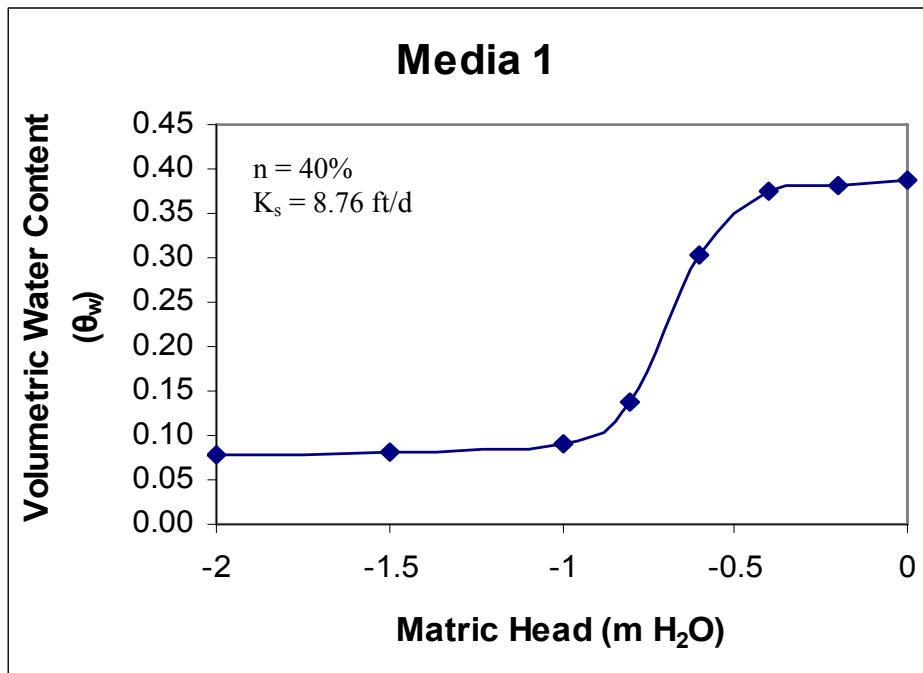


Figure 33: Laboratory SMRC for media 1

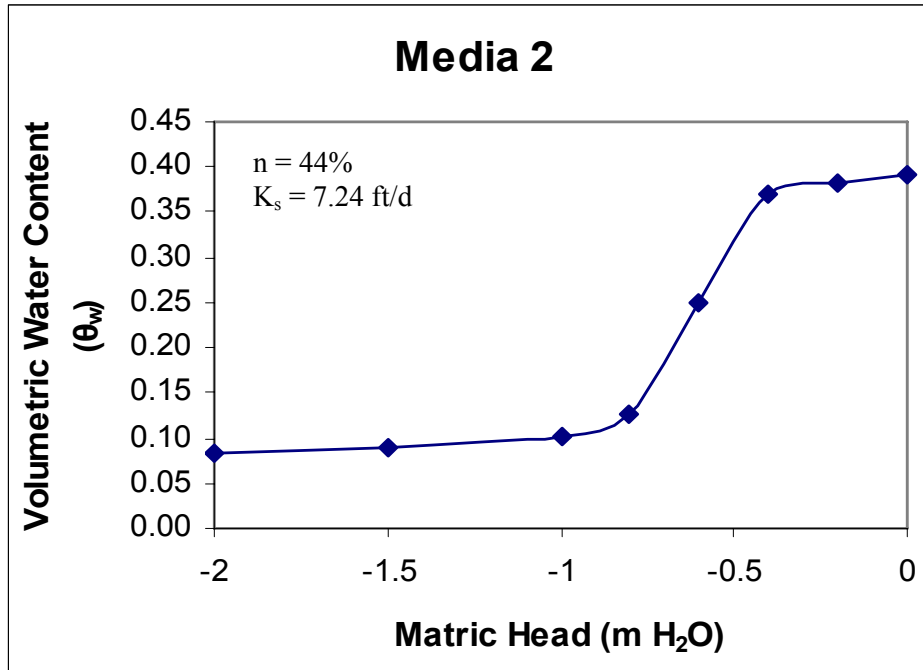


Figure 34: Laboratory SMRC for media 2

#### *Brooks and Corey and van Genuchten Models*

The fitted parameters from the Brooks and Corey model and the van Genuchten model are a good representation of the SMRC developed in the laboratory for the silty sand soils at SO and the sand soils at HT, in addition to the soil amendments as indicated by the low value of the Root Mean Square Error (RMSE). RMSE is the square root of the Mean Square Error (MSE). The MSE measures the average of the square of the errors which are the differences between the estimated and the measured volumetric water contents at each matric head. The closer the RMSE value is to zero, the better the estimator.

The fitted parameters to the Brooks and Corey model from the measured laboratory data are presented in Table 4. The fitted parameters to the van Genuchten model from the measured

data are in Table 5. The fitted parameters to both models were acquired using the tool Solver from Microsoft Excel. The graphical representation of the SO measured data with the Brooks and Corey and van Genuchten models can be seen in Figure 39, Figure 36, Figure 37, Figure 38, and Figure 39, whereas for Hunter's Trace, the visual comparison is in Figure 40, Figure 41, and Figure 42. The comparison of the measured data to the analytical models for the soil amendments are shown in Figure 43 and Figure 44.

**Table 4: Brooks and Corey Model Fitted Parameters**

<b>Location &amp; Depth</b>	<b>Porosity, n</b>	<b>Residual Water Content, <math>\theta_r</math></b>	<b>Air Entry Pressure Head, <math>\Psi_b</math> (m)</b>	<b>Pore Size Distribution Index, <math>\lambda</math></b>	<b>Root Mean Square Error</b>	<b>Hydraulic Conductivity, K (m/d)</b>
<b>SO 1 ft</b>	0.38	0.09	-0.36	0.20	0.019	0.34
<b>SO 1.5 ft</b>	0.33	0.07	-0.12	0.35	0.010	0.15
<b>SO 2 ft</b>	0.43	0.35	-0.18	0.63	0.011	0.02
<b>SO 3 ft</b>	0.43	0.34	-1.72	0.05	0.001	3.7E-05
<b>SO 4.5</b>	0.33	0.32	-1.46	0.34	0.001	9.1E-04
<b>HT 1 ft</b>	0.27	0.06	-0.37	2.74	0.030	2.15
<b>HT 2 ft</b>	0.28	0.07	-0.53	2.50	0.018	2.23
<b>HT 3 ft</b>	0.28	0.06	-0.48	3.71	0.019	1.21
<b>Media 1</b>	0.38	0.08	-0.56	4.69	0.013	2.67
<b>Media 2</b>	0.38	0.09	-0.53	4.61	0.017	2.21

**Table 5: van Genuchten Model Fitted Parameters**

Location & Depth	Porosity, n	Residual Water Content, $\theta_r$	$\alpha$	$\beta$	Root Mean Square Error	Hydraulic Conductivity, K (m/d)
SO 1 ft	0.38	0.24	1.16	2.08	0.014	0.34
SO 1.5 ft	0.33	0.12	3.92	1.72	0.004	0.15
SO 2 ft	0.43	0.35	3.40	2.04	0.015	0.02
SO 3 ft	0.43	0.31	0.05	1.48	0.001	3.7E-05
SO 4.5	0.33	-0.03*	0.08	1.06	0.001	9.1E-04
HT 1 ft	0.27	0.07	2.14	6.13	0.032	2.15
HT 2 ft	0.28	0.08	1.52	4.98	0.018	2.23
HT 3 ft	0.29	0.06	1.84	6.21	0.009	1.21
Media 1	0.38	0.08	1.51	8.81	0.009	2.67
Media 2	0.39	0.09	1.69	7.07	0.009	2.21

\*  $\theta_r$  value is extrapolated and cannot be negative

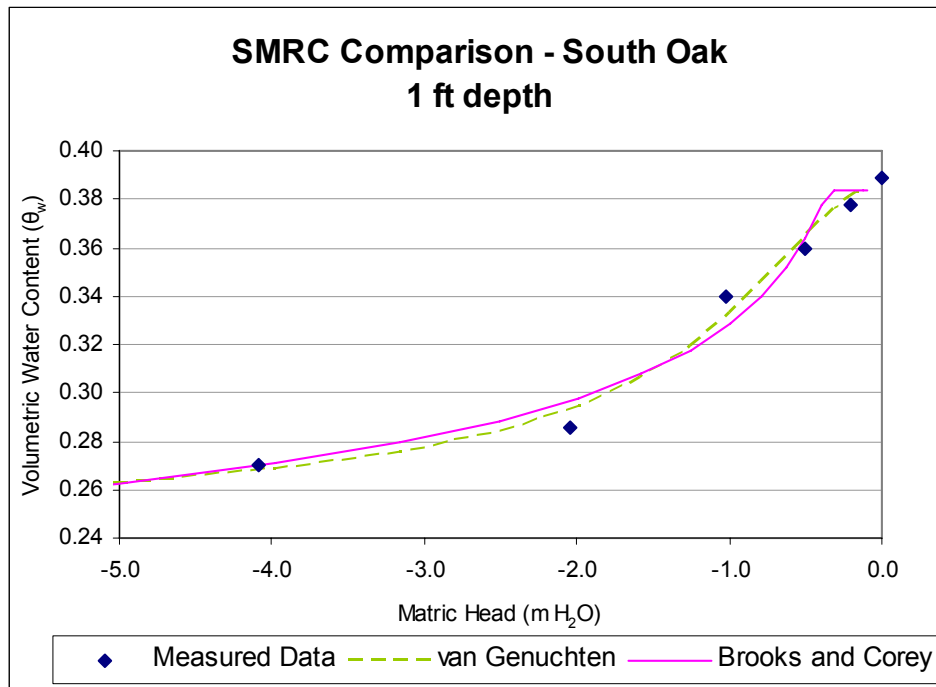


**Figure 35: Comparison of measured SMRC to analytical models for South Oak (1-ft depth)**

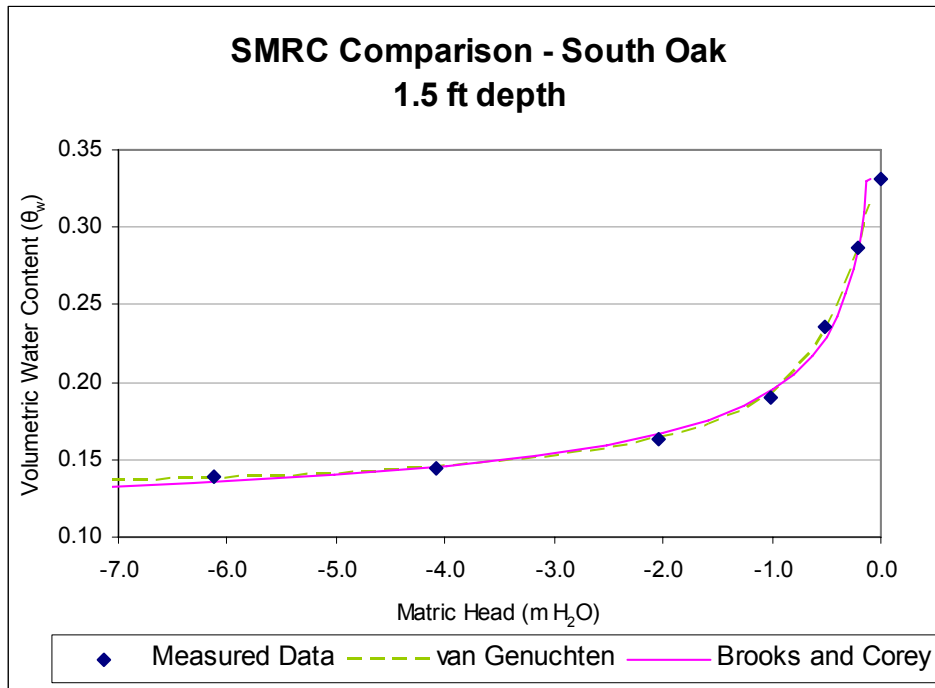


Figure 36: Comparison of measured SMRC to analytical models for South Oak (1.5-ft depth)

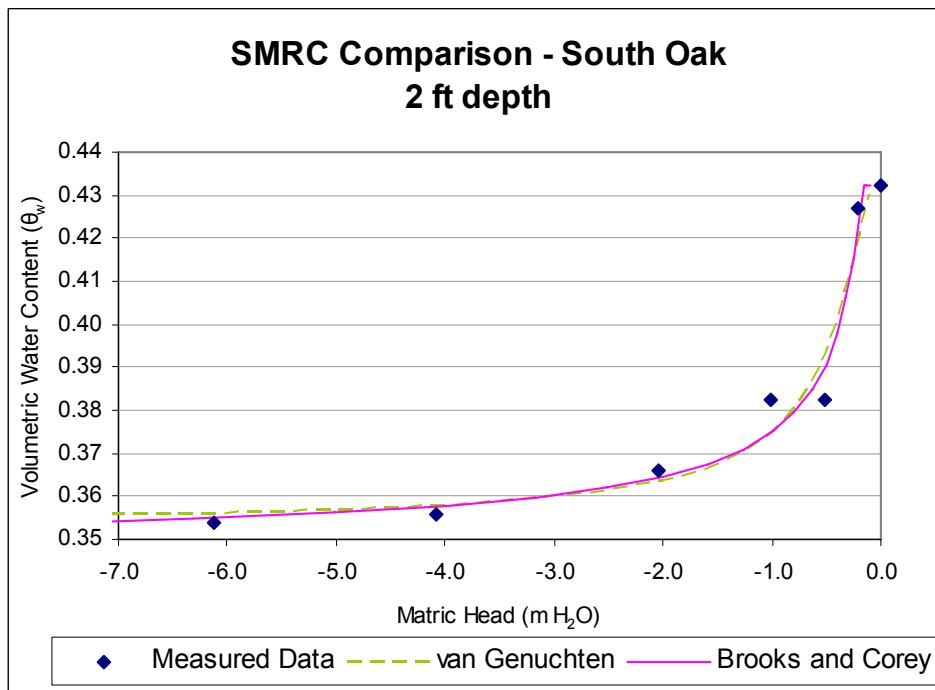


Figure 37: Comparison of measured SMRC to analytical models for South Oak (2-ft depth)

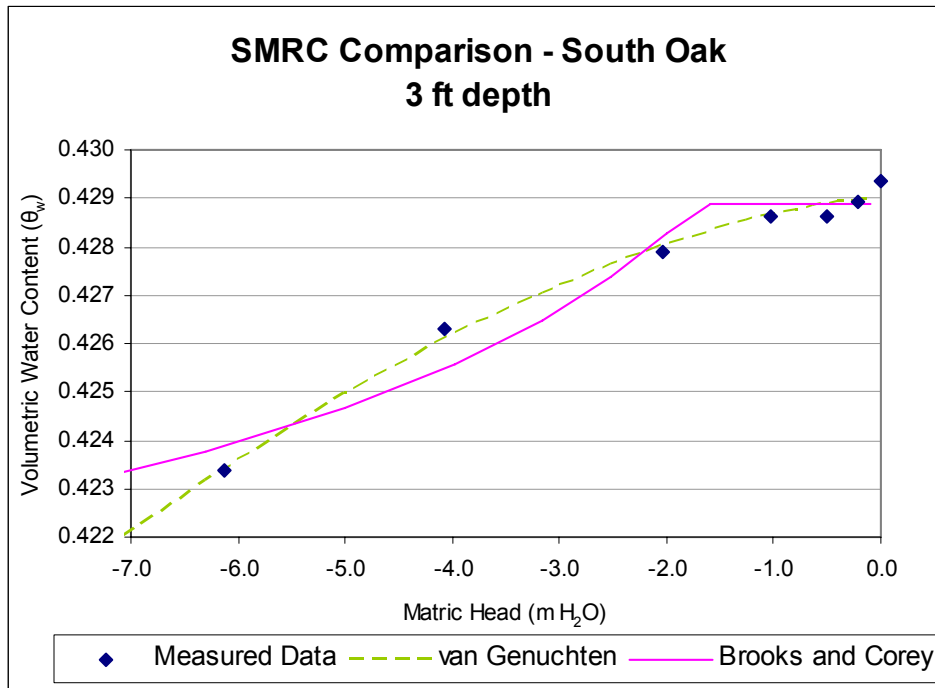


Figure 38: Comparison of measured SMRC to analytical models for South Oak (3-ft depth)

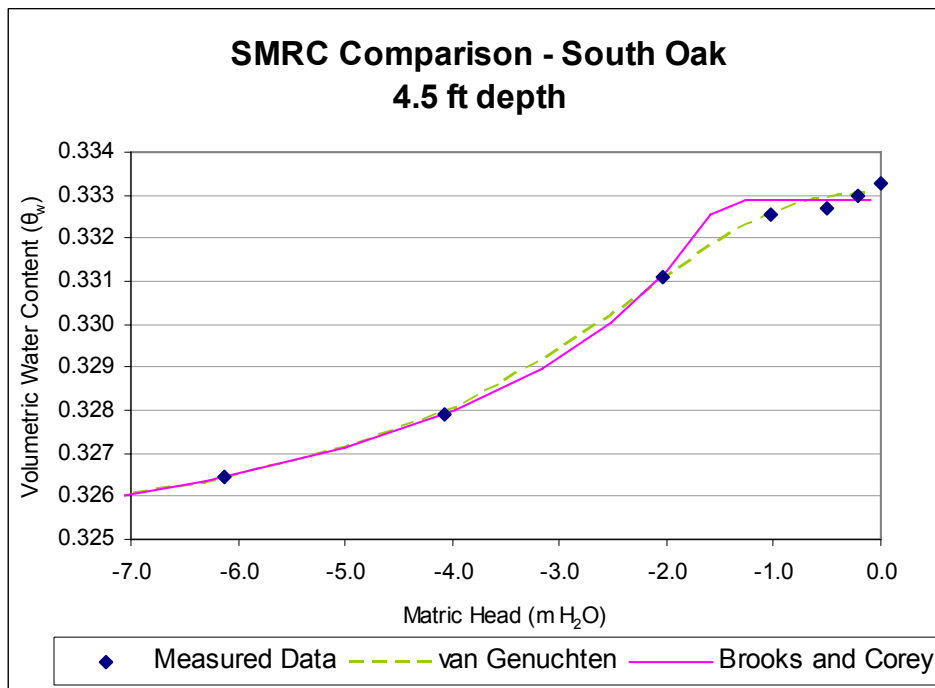


Figure 39: Comparison of measured SMRC to analytical models for South Oak (4.5-ft depth)

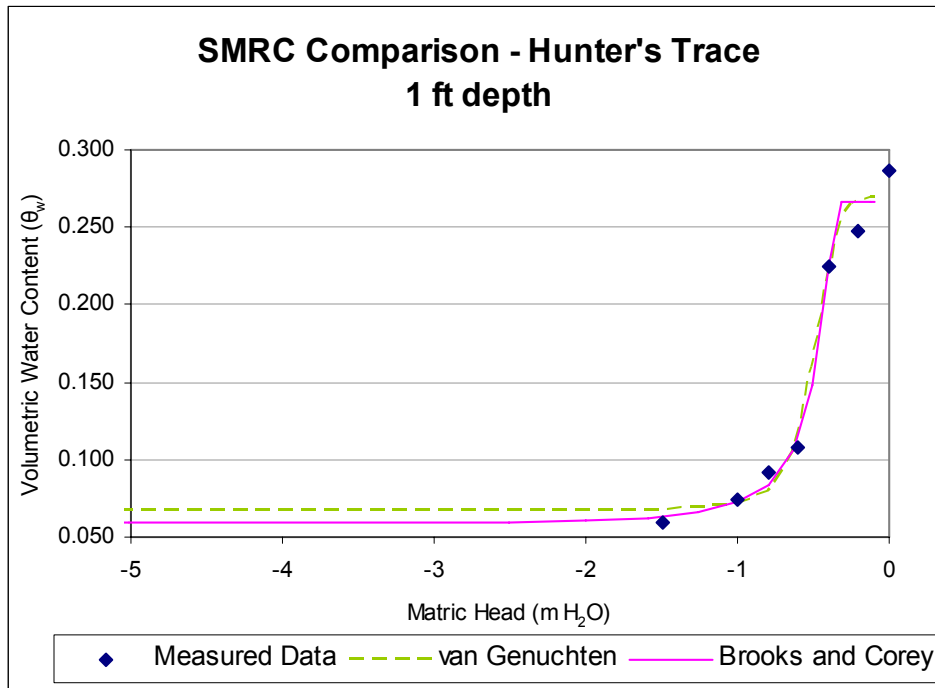


Figure 40: Comparison of measured SMRC to analytical models for Hunter's Trace (1-ft depth)

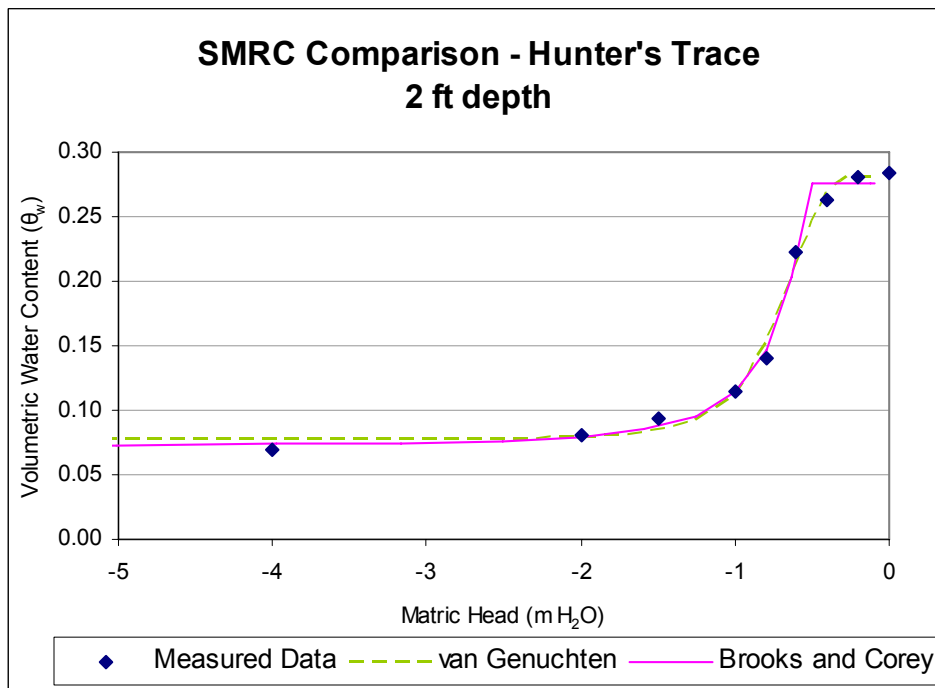


Figure 41: Comparison of measured SMRC to analytical models for Hunter's Trace (2-ft depth)

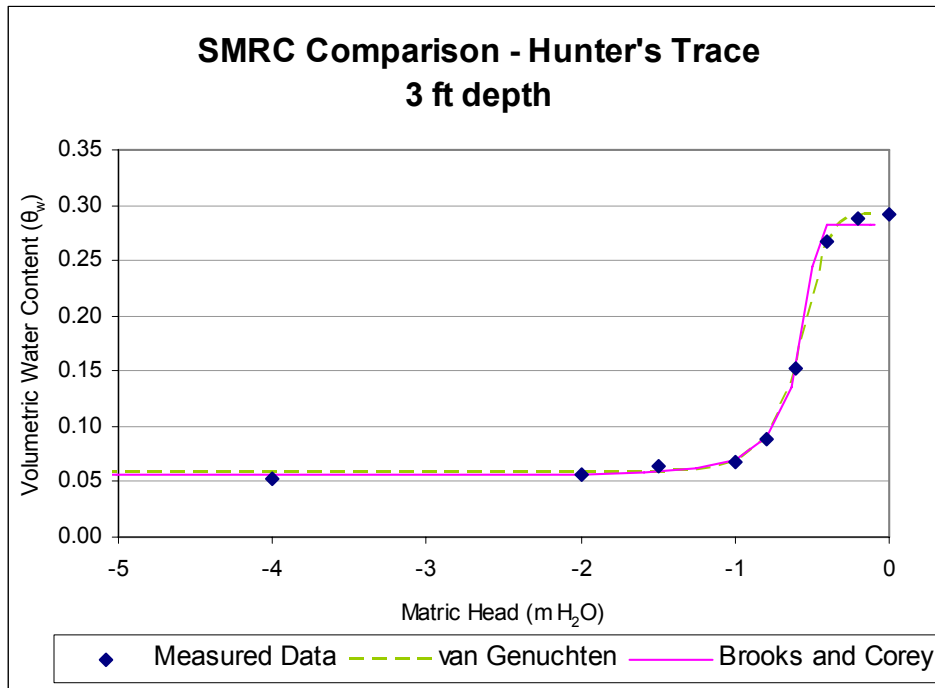


Figure 42: Comparison of measured SMRC to analytical models for Hunter's Trace (3-ft depth)

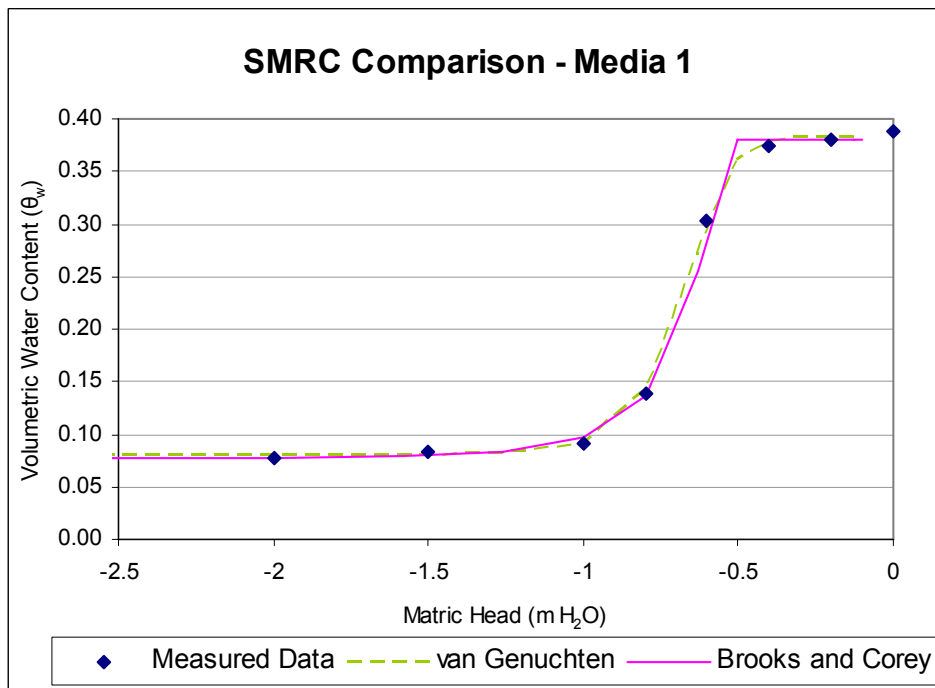
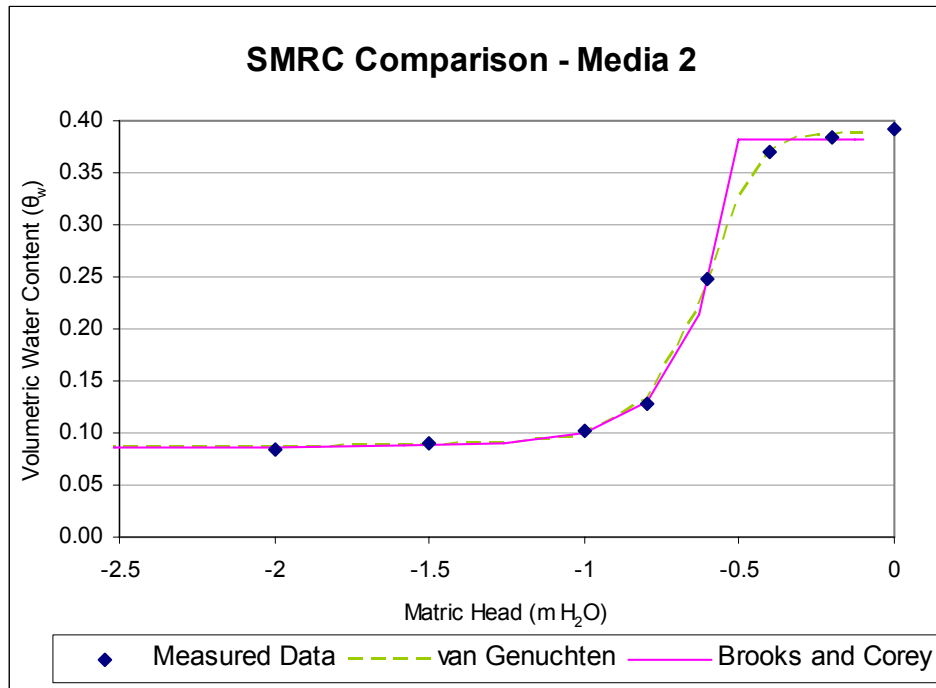


Figure 43: Comparison of measured SMRC to analytical models for media 1





**Figure 44: Comparison of measured SMRC to analytical models for media 2**

### *Field Measurements*

Tensiometers and TDR's were installed at only the HT location. The equipment could not be installed at SO because the water table was above the ground level at the time of attempted installation. Figure 45 displays the moisture content over an approximate 2 month period at HT (sample size, n, is 17,323).

The data at the 1-ft depth decreases to a lower  $\theta_w$  at a faster rate due to drainage at a higher matric potential (further from the water table). However at the same depth, it also increases to a higher  $\theta_w$  than the other depth measurements because of infiltration into the soil prior to evapotranspiration from plant roots and adhesive forces with the plant roots and organic material. The TDR data at the 2-ft depth lies in the intermediate vadose zone. It is a transitional

point between the 1-ft and 3-ft depths in the figure. The TDR data at the 3-ft depth is slower to drain than the 1-ft or 2-ft depths as it may be in the capillary fringe zone. The 3-ft depth TDR also is slower to drain than the 1-ft and 2-ft data points because it is at a lower matric potential as it is closer to the water table.

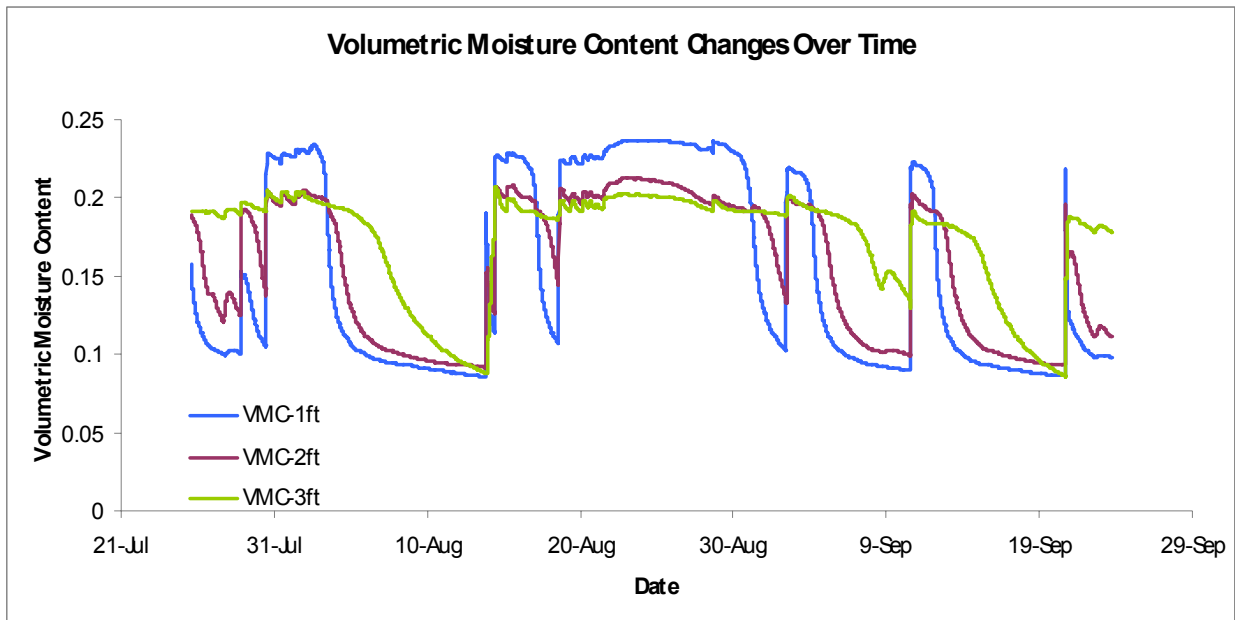


Figure 45: Hunter's Trace volumetric moisture content over time

The Hunter's Trace SMRC for 1-ft depth is shown in Figure 46. The air-entry pressure head is approximately  $-0.5 \text{ m H}_2\text{O}$ . The residual water content is approximately  $0.086 \text{ cm}^3/\text{cm}^3$ . The residual water content is noticeable because the lower end of the SMRC begins to level off. This is due to the water draining further down the soil column to the water table. The soil had a  $\theta_w$  loss of approximately  $0.15 \text{ cm}^3/\text{cm}^3$ . Possible scanning curves that connect the drainage and wetting curve can also be seen below the SMRC.

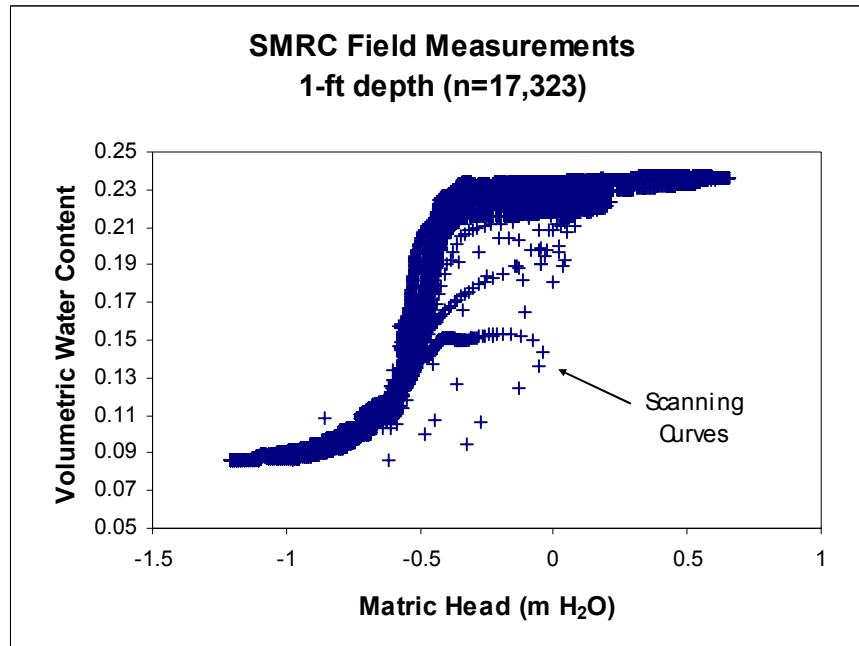


Figure 46: SMRC field measurements (1-ft depth)

The Hunter's Trace SMRC for 2-ft depth is shown in Figure 47. The air-entry pressure head is approximately -0.22 m H<sub>2</sub>O which is lower than the 1-ft depth as it is closer to the water table. The residual water content cannot be seen in the SMRC as the data are measured in the wet season; therefore there is still a downward trend in the SMRC. The soil had a  $\theta_w$  loss of approximately 0.11 cm<sup>3</sup>/cm<sup>3</sup>. The scanning curves that connect the drainage and wetting retention curve cannot be seen as readily as at the 1-ft depth.

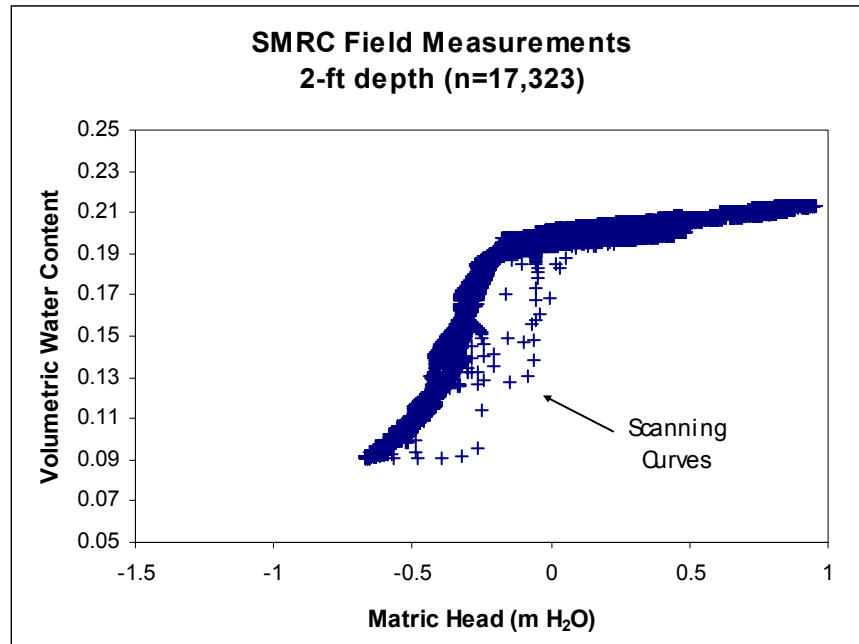


Figure 47: SMRC field measurements (2-ft depth)

The Hunter's Trace SMRC for 3-ft depth is shown in Figure 48. The air-entry pressure head is approximately -0.18 m H<sub>2</sub>O which is lower than the 1-ft and 2-ft measurement as it is closer to the water table. Since the measurements were taken in the wet season, the SMRC never reach the residual water content which can be seen in the sustained downward trend. The soil had a  $\theta_w$  loss of approximately 0.10 cm<sup>3</sup>/cm<sup>3</sup>. The moisture content at a given matric potential in the 1-ft depth is very similar to the 2-ft and 3ft depths because organic matter could possibly be holding more moisture within the soil. The scanning curves that connect the drainage and wetting retention curve cannot be seen as readily as at the 1-ft depth.

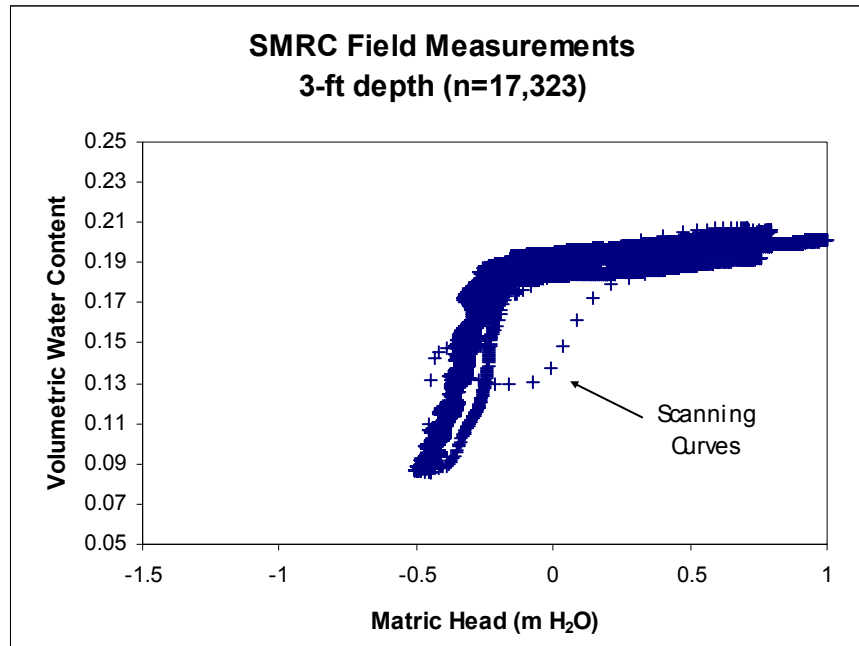


Figure 48: SMRC field measurements (3-ft depth)

#### *Double-Ring Infiltrometer*

HT has consistent sediment across a flat terrain whereas SO has an irregular substrate at the surface with small fluctuation in the topography. Therefore, only one test was performed at HT and two were conducted at SO. The infiltration at HT was measured at 1.1 ft/hr. The SO infiltration at the first location was measured at 0.3 ft/hr whereas the second location was 2.2 ft/hr. The first location appeared to be finer sediment with more vegetation and roots. The second location was slightly coarser than the first location with less vegetation.

Source of error includes disturbance of the soil when the equipment was installed, short circuit flow along the walls of the cylinders, and siltation. Error within the system was minimized by careful insertion of the measuring cylinder. The soil in contact with the inside of

the cylinders was lightly tamped to prevent short circuit flow whereas larger gaps were backfilled with bentonite. To minimize siltation, the force of the incoming water was reduced by spraying the side of the cylinder or the pink styrofoam suspended from the buffer cylinder. (Reynolds et al, 2002)

### Pedotransfer Function (Arya and Paris Model)

#### *South Oak*

A comparison for AP model to the laboratory SMRC for the SO silty sand soils at 1-ft, 1.5-ft, 2-ft, 3-ft, and 4.5-ft depths can be seen in Figure 49, Figure 50, Figure 51, Figure 52, and Figure 53, respectively. From the graphs, it can be seen that the AP model is not the best fit for the soils at the SO location. The scaling factor varies significantly between the five depths in order to maximize the fit of the AP model to the measured SMRC. At SO, the 1-ft, 1.5-ft, 2-ft, 3-ft, and 4.5-ft depths have a scaling of 1.350, 1.200, 1.400, 1.500, and 1.450, respectively (Table 6).

**Table 6: Summary of AP scaling factor for soils at South Oak**

Sample Depth (ft)	South Oak Scaling Factor, $\alpha$
1	1.350
1.5	1.200
2	1.400
3	1.500
4.5	1.450

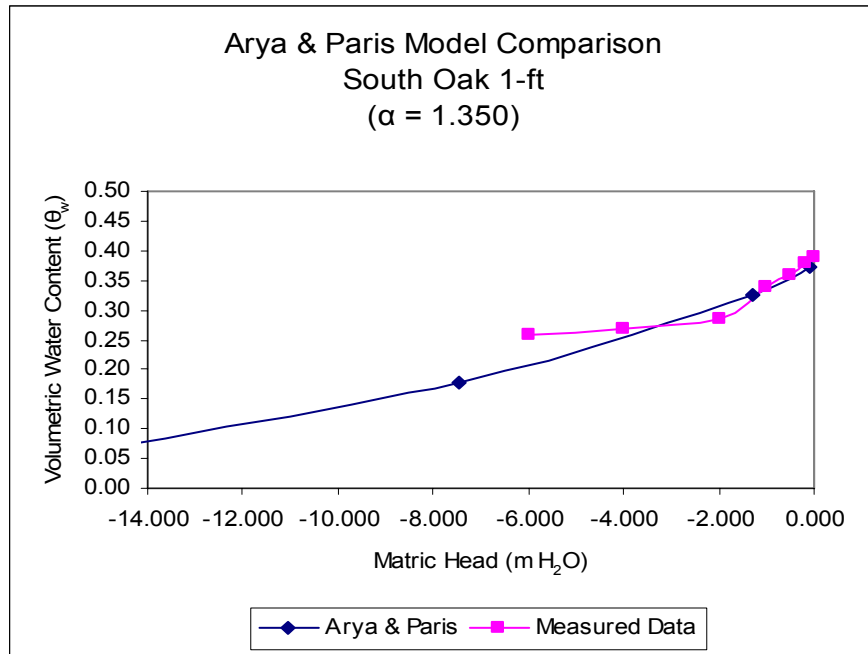


Figure 49: Comparison of AP model to measured SMRC for South Oak at 1-ft depth

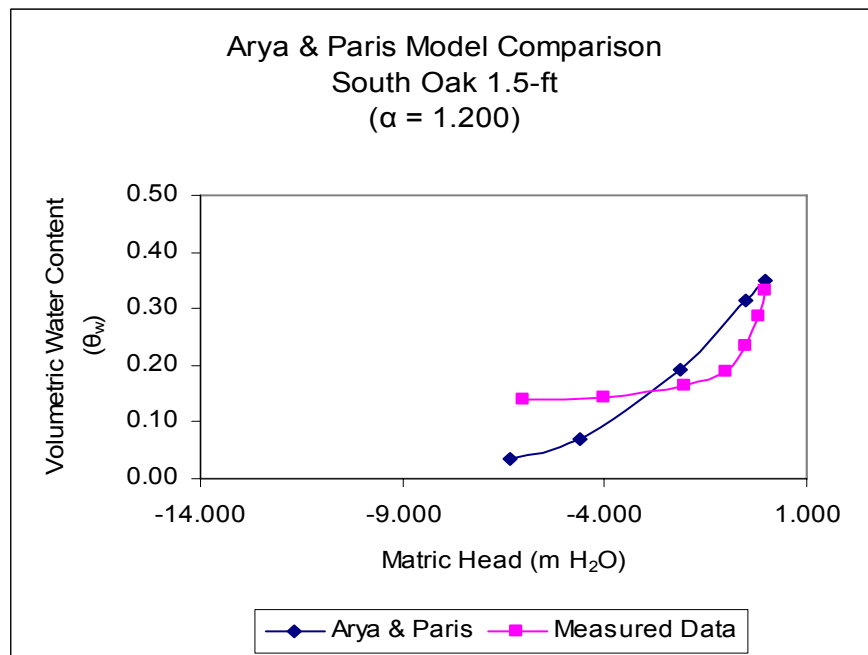


Figure 50: Comparison of AP model to measured SMRC for South Oak at 1.5-ft depth

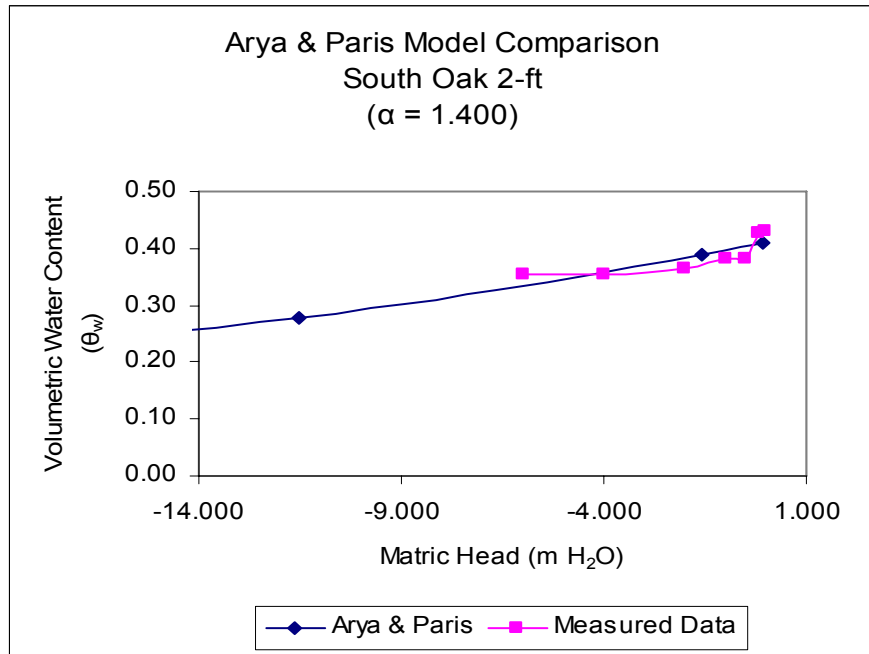


Figure 51: Comparison of AP model to measured SMRC for South Oak at 2-ft depth

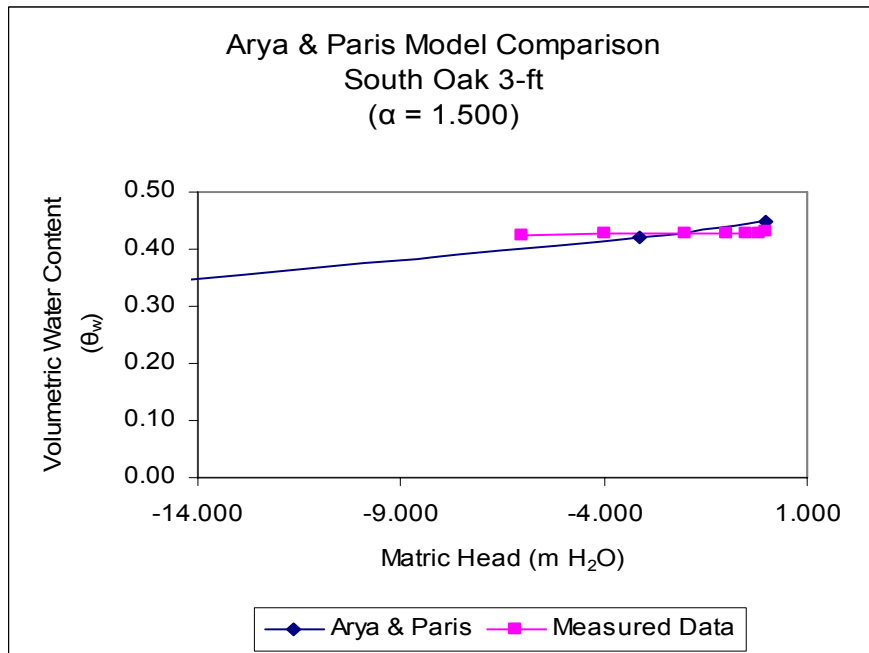
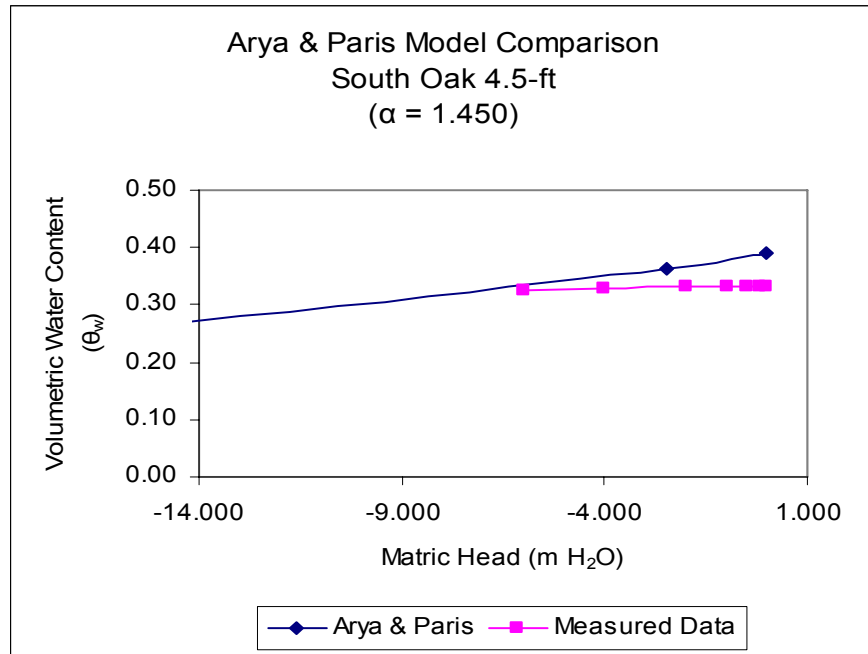


Figure 52: Comparison of AP model to measured SMRC for South Oak at 3-ft depth





**Figure 53: Comparison of AP model to measured SMRC for South Oak at 4.5-ft depth**

### *Hunter's Trace*

The measured SMRCs are compared to the AP model for the sand soils at HT for the depths of 1-ft, 2-ft, and 3-ft. These can be seen in Figure 54, Figure 55, and Figure 56, respectively. The AP model is a better fit for the soils at the HT than the soils at SO. In addition, there is no variation in the scaling factor,  $\alpha$ , within the model. A scaling factor of 1.070 provides the best fit of the AP model to the measured SMRC for the HT soils.

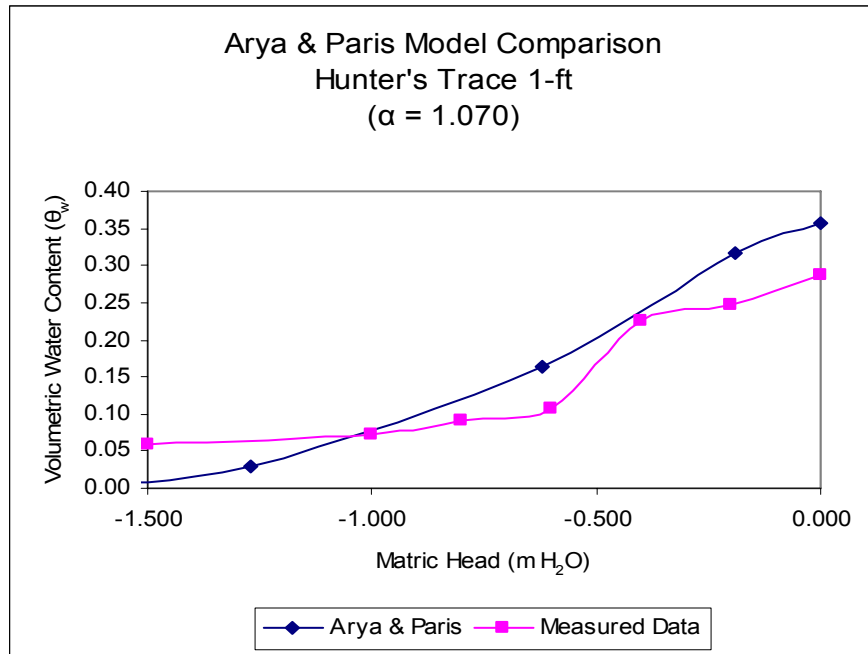


Figure 54: Comparison of AP model to measured SMRC for Hunter's Trace at 1-ft depth

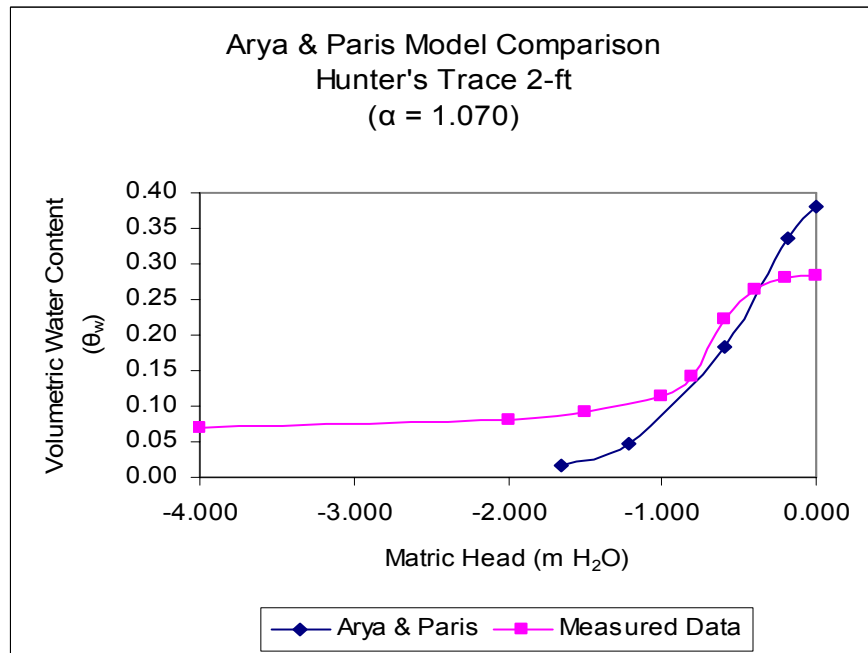
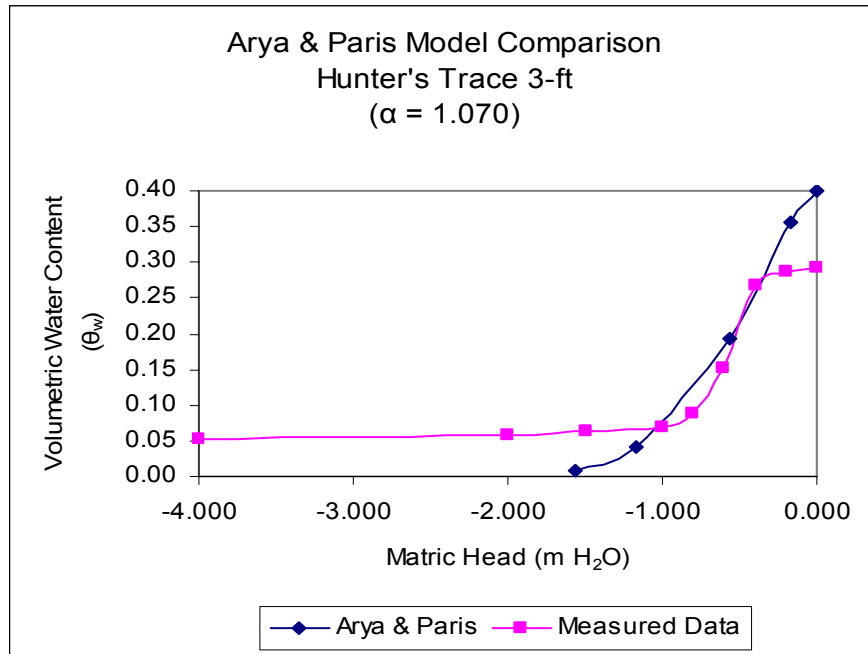


Figure 55: Comparison of AP model to measured SMRC for Hunter's Trace at 2-ft depth



**Figure 56: Comparison of AP model to measured SMRC for Hunter's Trace at 3-ft depth**

### *Soil Amendments*

The AP model was used to create a SMRC for the soil amendments, media 1 and media 2. The visual comparison can be seen in Figure 57 and Figure 58. The AP model does work for the soil amendments. The same scaling factor as the HT soils of 1.070 provides the best fit to the measured SMRC for the soil amendments.

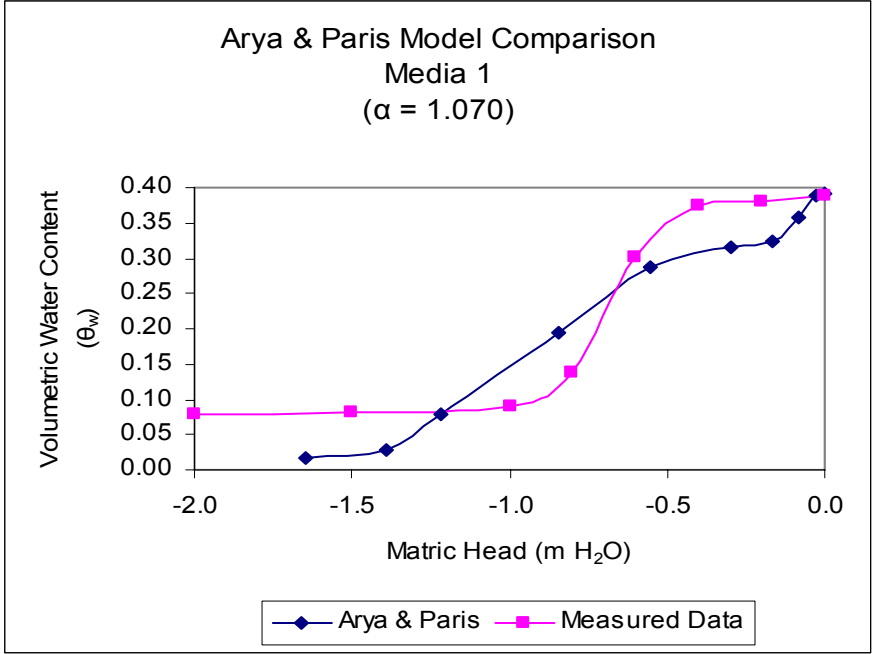


Figure 57: Comparison of AP model to measured SMRC for the Media 1

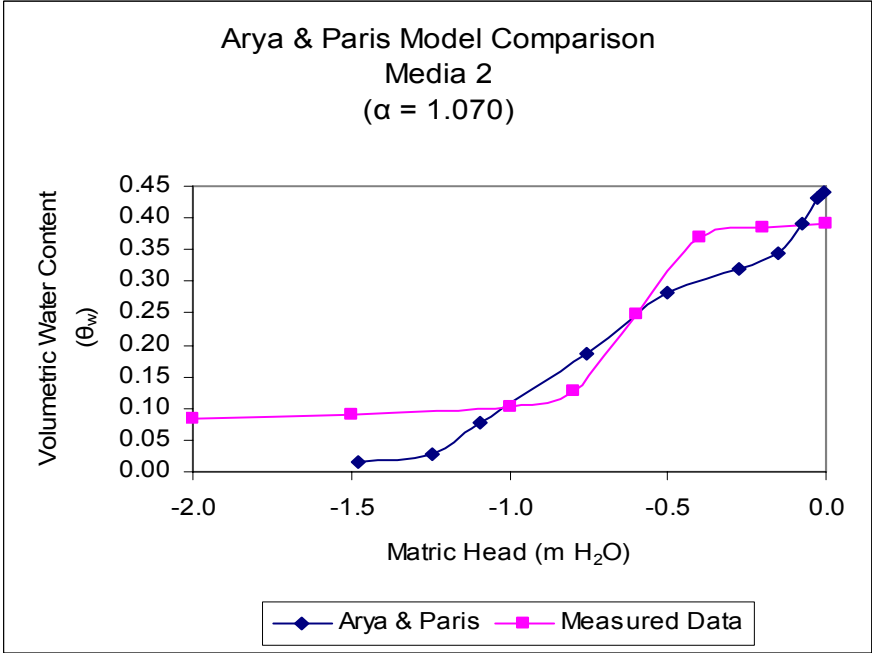


Figure 58: Comparison of AP model to measured SMRC for the Media 2

### Comparing Different Scaling Factors for South Oak

Different scaling factors,  $\alpha$ , are compared to the measured laboratory data for SO silty sand samples (Figure 59, Figure 60, Figure 61, Figure 62, and Figure 63). The scaling factor used for the sand at HT and the soil amendments of 1.07 is used, in addition to an average value of 1.35 from the scaling factors used for SO soils (Table 6). A scaling factor of 1.07 is the worst fit presented out of the various  $\alpha$  values used for the five SO soil samples. The scaling factor of 1.35 was a better fit than the value of 1.07, however, still not as good as the individually fitted scaling factor.

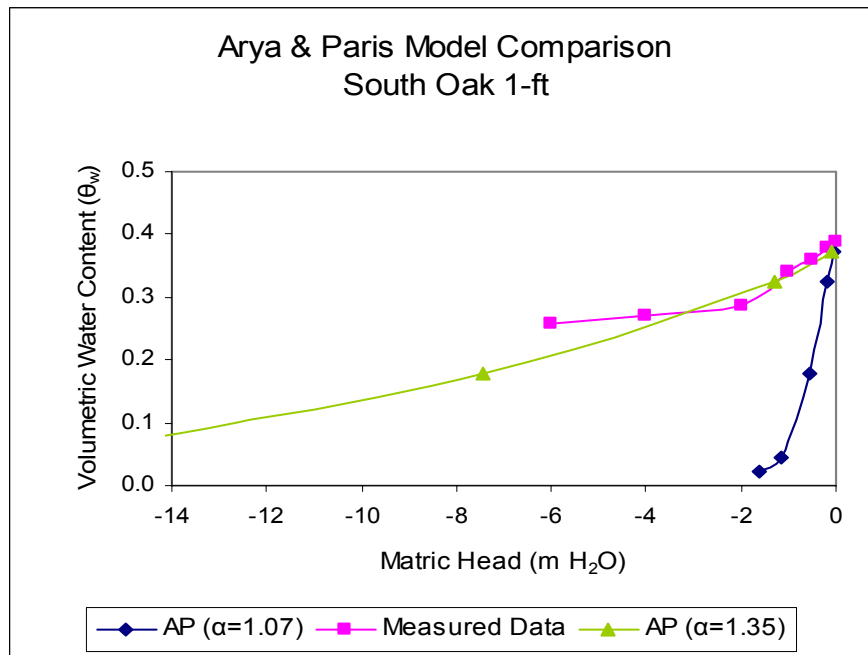


Figure 59: Comparing SMRC with different AP scaling factors for South Oak at 1-ft depth

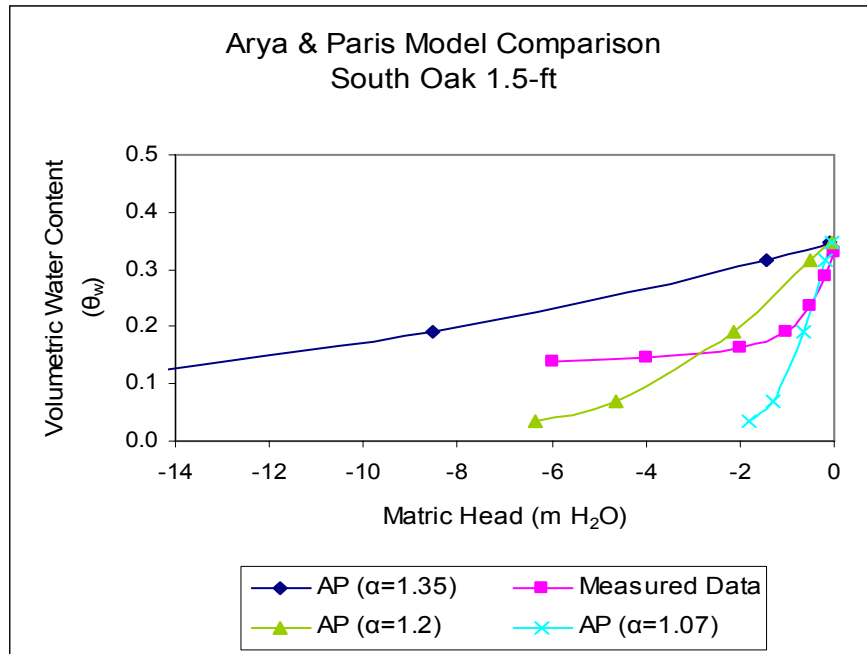


Figure 60: Comparing SMRC with different AP scaling factors for South Oak at 1.5-ft depth

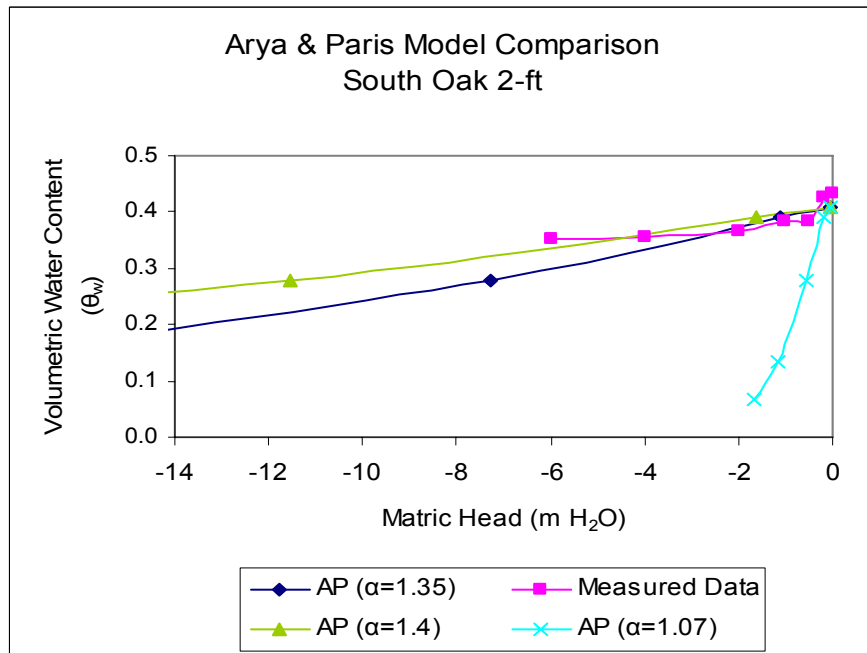
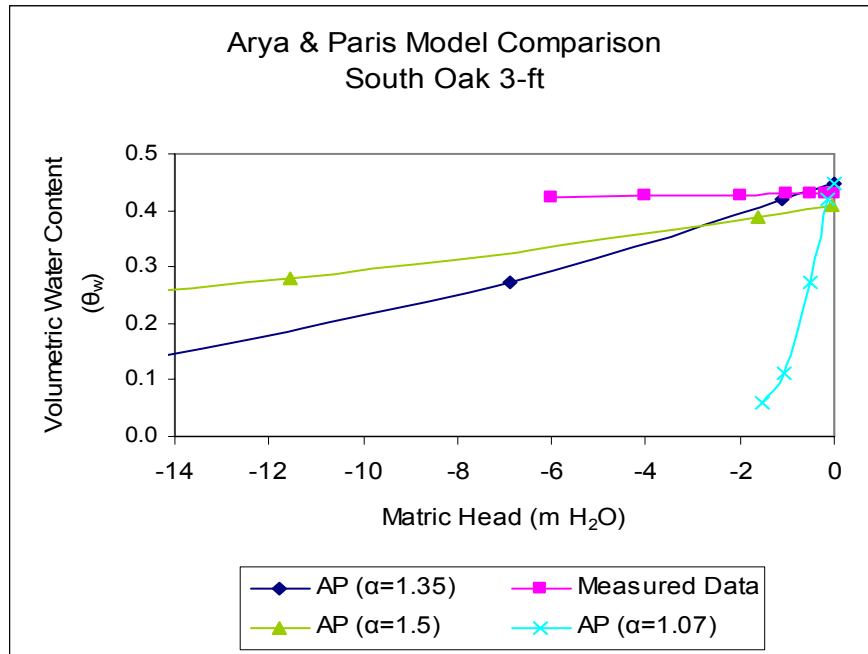
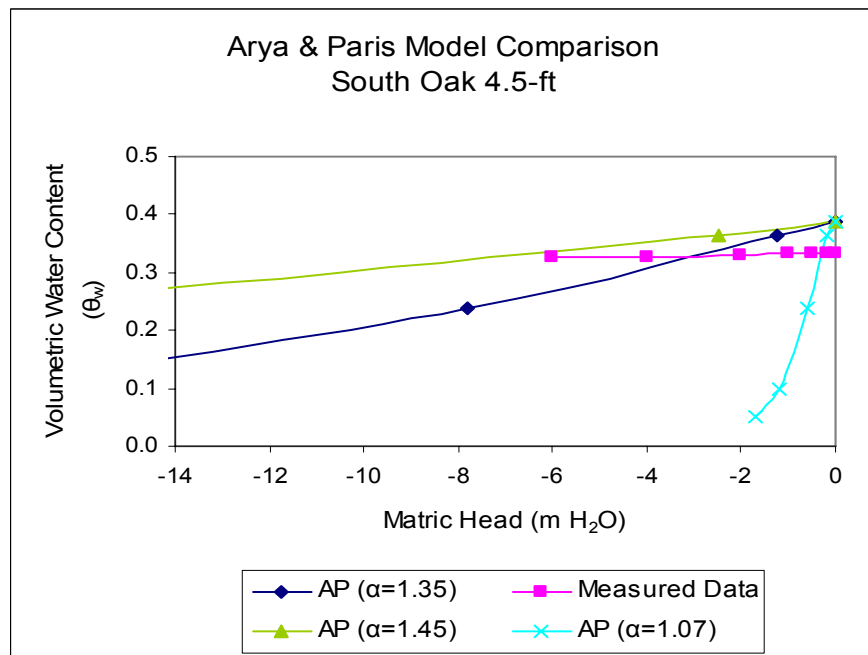


Figure 61: Comparing SMRC with different AP scaling factors for South Oak at 2-ft depth



**Figure 62: Comparing SMRC with different AP scaling factors for South Oak at 3-ft depth**



**Figure 63: Comparing SMRC with different AP scaling factors for South Oak at 4.5-ft depth**

## CHAPTER 5: SUMMARY

### Summary

Ground water is vulnerable to contamination from nitrogen species due to the impacts of land-use activities. If soil-borne nitrogen migrates to water bodies or accumulates in the ground water, the water may be rendered an unsuitable source of fresh water. The analysis of water movement within the vadose zone to reduce contaminant transport begins with accurately predicting the water balance and rates and patterns of flow. This is crucial in ground water remediation. The soil moisture retention curve (SMRC) facilitates an understanding of the soils ability to transmit water and to store water.

With the SMRC for the soil amendments and native soils, the accuracy in modeling the unsaturated zone is increased. The SMRC is developed for a total of two soil amendments, media 1 and media 2, and for the soils in Marion County, Florida, at the South Oak (SO) and Hunter's Trace (HT) locations. The SMRC is dependent on the soil structure and soil texture. This information characterizes the soil at these locations in Marion County, Florida, and for the soil amendments from which the pore-size distribution and water holding capacities can be derived.

The SMRC for the soil amendments and native soils is developed in the laboratory using a Tempe cell apparatus. In addition, the SMRC is measured in the field at the HT location with TDR and tensiometer equipment at three depths of 1-ft, 2-ft, and 3-ft over approximately a two month period. The laboratory data are then compared to two analytical models, Brooks and Corey and van Genuchten.



The Arya and Paris (AP) model, a pedotransfer function, is used to test the accuracy of predicting the SMRC for the soil amendments and native soils from textural and structural soil properties. Measuring the SMRC in the lab is a time consuming process; therefore, inferring the SMRC from easier measured characteristics, such as the particle-size distribution and bulk density, would be advantageous.

### Conclusions

The soils at South Oak (SO) and Hunter's Trace (HT) are uniformly graded and have a textural classification of "sand." However, SO has a slightly lower percentage of sand ranging from 87.5% to 92%, whereas HT has a slightly higher percentage of sand ranging from 96.8% to 99%. Therefore, SO has a higher content of silt and clay which is conducive to a longer retention time.

The silty sand soils at SO and the amendments have a lower specific gravity ( $G_s$ ) and bulk density than the sand soils at HT. A low  $G_s$  indicates a higher content of organic matter which is clearly true for the amendments as they contain sawdust. Bulk density is affected by the degree of compaction within the soil or media. Therefore, the sand soils at HT have more mass within a given volume which could be an indication of a lower porosity. However, the soil amendments have a low bulk density and a low porosity. This could be due to the addition of sawdust and tire crumb. The porosity is lower in the soil amendments and the sand at HT than the silty sand at SO which is related to the higher silt/clay content found in the soils at SO.

The hydraulic properties of the soils and soil amendments are directly related to the soil properties. Overall, the saturated hydraulic conductivity ( $K_s$ ) is considerably lower for the silty

sand at SO than sand at HT, most likely due to the lower porosity and higher percentage of larger particles at HT. SO soils have a lower sand content and a higher silt/clay content. There are some irregular changes with depth in the  $K_s$  due to the spatial heterogeneity of the soil from natural processes at SO. Therefore, the SO location is layered with different soil types.

The  $K_s$  for media 1 and media 2 are more comparable to the permeability for the sand at HT. Media 1 has a higher  $K_s$  value than media 2. Presumably, the higher permeability of media 1 is due to a lower porosity and a higher percentage of particles retained on the Number 20 and Number 40 sieve. In addition, media 2 has additional limestone with smaller particle size. Media 2 has a higher percentage of sawdust, 25% versus the 20% in media 1, which could create a more tortuous path for the flow because of the flaky shape.

The double-ring infiltrometer measurements made in the field at HT coincide with the hydraulic conductivity measurements in the laboratory at the 1-ft and 2-ft depths. The double-ring infiltrometer measurements at SO varied greatly between the two sample sites. The soil heterogeneity was very prominent even at the surface at SO. The lower infiltration of 0.03 ft/d is expected based on the low  $K_s$  values obtained in the laboratory.

The laboratory measurements of the SMRC for the silty sand soils at SO and the sand at HT follow a trend with the measured soil properties. The largest water content for all samples is slightly lower than the porosity values. However, there is a larger gap in the saturated water content and the porosity for the sand at HT. Entrapped air or incomplete wetting could account for incomplete saturation of the pores (Bruce, 1986). The smaller the silt/clay content, such as in all the HT samples and the 1-ft, 1.5-ft and 2-ft depth at SO, the more abrupt the loss in water

content in the SMRC. In addition, the coarser the texture, the closer the SMRC gets to the residual moisture content.

The analytical models are a good representation of the SMRC obtained in the laboratory as indicated by the low root mean square error value. The porosity parameter for the Brooks and Corey and van Genuchten models fit exceedingly well to the porosity for the SO silty sand samples and the soil amendments whereas the porosity for the sand at HT is underestimated by both models. In addition, the residual moisture content parameter for both models fits well with the measured data for most of the samples at SO, all the samples at HT, and both soil amendments. The van Genuchten model extrapolated the residual moisture content at the SO 4.5-ft depth sample to be a negative  $0.03 \text{ cm}^3/\text{cm}^3$ . The particle-size distribution (PSD) for this sample indicated the highest fraction of smaller size particles; therefore, it could potentially have a higher water holding capacity.

The field measurements are aggravated by the soil heterogeneity and by uncertainties over the hysteresis phenomena. In addition, the inability to wet the voids completely and entrapped air plays a major role in the measurements (Bruce, 1986). It can be seen from the field measurements that the moisture content at HT decreases with depth. The residual water content between the three depths is comparable at  $0.09 \text{ cm}^3/\text{cm}^3$ , most likely because rain events are continually introducing water into the system. However, the water content at saturation is progressively lower with depth. This is possibly due to the compressibility or increased pressure from overburden or due to spatial heterogeneity. The air-entry pressure increases with increasing depth between the three locations which is expected; as the water table is approached the matric suction increases.

The AP model may be used for a generalization of the SMRC at the HT location and for the soil amendments. It is not a good prediction of the SMRC at the SO location due to the variation in the scaling factor,  $\alpha$ . The scaling factor varied significantly for the silty sand at SO, whereas for sand at HT and the soil amendments, the scaling factor was consistently a value of 1.070. A more segmented particle-distribution curve is suggested, to better fit the AP model to the measured data for all soils samples.

### Recommendations

Retention ponds should be located at sites similar to the SO site due to the ability of the soils to store and transmit water with a high retention time. This allows for natural remediation of the excess nutrients through denitrifying bacteria. The soil structure, texture, and water holding capacity of the silty sand soils creates an anaerobic environment for denitrifiers.

If the native soils at the site of an existing pond do not have similar soil and hydraulic properties as the SO location, a soil amendment should be used to aid remediation. For implementation of a new retention pond, a location should be found that has soil and hydraulic characteristics similar to SO.

The soil amendment should be designed with the ability to store and transmit water with a high retention time. The soil properties and hydraulic properties need to resemble the silty sand soils found at SO. Instead of using fine sand in the soil amendment, use soil from the SO location in addition to the tire crumb, limestone, and sawdust to increase the volumetric water content and retention time at HT. This will create the anaerobic environment needed for denitrification to occur.

## Future Work

Research should be conducted to model the transitions between the native soil and the soil amendments through the vadose zone. The information gained from either the field or laboratory measurements of the SMRC could be used to model the transitions between the soils and amendment. Otherwise, the parameters acquired from the Brooks and Corey model or the van Genuchten model could be used to simulate the water movement through the vadose zone to obtain the retention time.

The implementation of the soil amendment should be to excavate the bottom of the retention pond to a depth that will allow the soil amendment to be installed and then a layer of native soil installed on top of the amendment so that the amendment stays in place. Modeling the water movement within these horizontal layers will provide an overall perception to the ability of the system to transmit and store water. In addition, modeling the flow within these layers will aid in the understanding of the performance of the media to remove nutrients, establish the life span of the soil amendment, and determine how the flows changes from the natural conditions of the retention pond.

## **APPENDIX A: SIEVE ANALYSIS DATA**

South Oak

**Table 7: South Oak sieve analysis (1-ft depth)**

**Sample Depth:** 1 ft  
**Sample ID:** E-1  
**Mass of oven dry sample, W (g):** 104.0  
 **$\Sigma W_n$  (g):** 103.6

Sieve Number	Sieve Opening (mm)	Mass retained on each sieve, $W_n$ (g)	Percent of mass retained of each sieve, $R_n$	Cumulative percent retained, $\Sigma R_n$	Percent finer, $100 - \Sigma R_n$
10	2.0	2.1	2.0	2.0	98.0
40	0.425	21.7	20.9	22.9	77.1
100	0.15	53.1	51.1	73.9	26.1
200	0.075	14.6	14.0	88.0	12.0
270	0.053	3.7	3.6	91.5	8.5
Pan	□	8.4	8.1	99.6	

**Table 8: South Oak sieve analysis (1.5-ft depth)**

**Sample Depth:** 1.5 ft  
**Sample ID:** C-1  
**Mass of oven dry sample, W (g):** 117.8  
 **$\Sigma W_n$  (g):** 117.7

Sieve Number	Sieve Opening (mm)	Mass retained on each sieve, $W_n$ (g)	Percent of mass retained of each sieve, $R_n$	Cumulative percent retained, $\Sigma R_n$	Percent finer, $100 - \Sigma R_n$
10	2.0	0.9	0.8	0.8	99.2
40	0.425	21.3	18.1	18.8	81.2
100	0.15	62.6	53.1	72.0	28.0
200	0.075	18.9	16.0	88.0	12.0
270	0.053	4.8	4.1	92.1	7.9
Pan	□	9.2	7.8	99.9	

**Table 9: South Oak sieve analysis (2-ft depth)**

**Sample Depth:** 2.0 ft

**Sample ID:** E-2

**Mass of oven dry sample, W (g):** 105.8

**$\Sigma W_n$  (g):** 105.5

Sieve Number	Sieve Opening (mm)	Mass retained on each sieve, $W_n$ (g)	Percent of mass retained of each sieve, $R_n$	Cumulative percent retained, $\square R_n$	Percent finer, $100 - \square R_n$
10	2.0	0.1	0.1	0.1	99.9
40	0.425	9.9	9.4	9.5	90.5
100	0.15	46.9	44.3	53.8	46.2
200	0.075	27.3	25.8	79.6	20.4
270	0.053	8.4	7.9	87.5	12.5
Pan	$\square$	12.9	12.2	99.7	

**Table 10: South Oak sieve analysis (3-ft depth)**

**Sample Depth:** 3.0 ft

**Sample ID:** D-1

**Mass of oven dry sample, W (g):** 109.5

**$\Sigma W_n$  (g):** 109.1

Sieve Number	Sieve Opening (mm)	Mass retained on each sieve, $W_n$ (g)	Percent of mass retained of each sieve, $R_n$	Cumulative percent retained, $\square R_n$	Percent finer, $100 - \square R_n$
10	2.0	0	0.0	0.0	100.0
40	0.425	13.6	12.4	12.4	87.6
100	0.15	58.1	53.1	65.5	34.5
200	0.075	19.8	18.1	83.6	16.4
270	0.053	6.8	6.2	89.8	10.2
Pan	$\square$	10.8	9.9	99.6	



**Table 11: South Oak sieve analysis (4.5-ft depth)**

**Sample Depth:** 4.5 ft

**Sample ID:** E-3

**Mass of oven dry sample, W (g):** 101.4

**$\Sigma, W_n$  (g):** 101.4

Sieve Number	Sieve Opening (mm)	Mass retained on each sieve, $W_n$ (g)	Percent of mass retained of each sieve, $R_n$	Cumulative percent retained, $\square R_n$	Percent finer, $100 - \square R_n$
10	2.0	0.1	0.1	0.1	99.9
40	0.425	7.8	7.7	7.8	92.2
100	0.15	45	44.4	52.2	47.8
200	0.075	27.6	27.2	79.4	20.6
270	0.053	8.4	8.3	87.7	12.3
Pan	$\square$	12.5	12.3	100.0	

Hunter's Trace

**Table 12: Hunter's Trace sieve analysis (1-ft depth)**

**Sample Depth:** 1.0 ft

**Sample ID:** D-2

**Mass of oven dry sample, W (g):** 116.3

**$\Sigma, W_n$  (g):** 116.3

Sieve Number	Sieve Opening (mm)	Mass retained on each sieve, $W_n$ (g)	Percent of mass retained of each sieve, $R_n$	Cumulative percent retained, $\square R_n$	Percent finer, $100 - \square R_n$
10	2.0	0	0.0	0.0	100.0
40	0.425	26.3	22.6	22.6	77.4
100	0.15	71.1	61.1	83.7	16.3
200	0.075	16.5	14.2	97.9	2.1
270	0.053	1.3	1.1	99.1	0.9
Pan	$\square$	1.1	0.9	100.0	

**Table 13: Hunter's Trace sieve analysis (2-ft depth)**

**Sample Depth:** 2.0 ft

**Sample ID:** C-1

**Mass of oven dry sample, W (g):** 110.6

**$\Sigma, W_n$  (g):** 110.6

Sieve Number	Sieve Opening (mm)	Mass retained on each sieve, $W_n$ (g)	Percent of mass retained of each sieve, $R_n$	Cumulative percent retained, $\square R_n$	Percent finer, $100 - \square R_n$
10	2.0	0	0.0	0.0	100.0
40	0.425	24.8	22.4	22.4	77.6
100	0.15	64.4	58.2	80.7	19.3
200	0.075	16	14.5	95.1	4.9
270	0.053	1.9	1.7	96.8	3.2
Pan	$\square$	3.5	3.2	100.0	

**Table 14: Hunter's Trace sieve analysis (3-ft depth)**

**Sample Depth:** 3.0 ft

**Sample ID:** D-3

**Mass of oven dry sample, W (g):** 111.6

**$\Sigma, W_n$  (g):** 111.5

Sieve Number	Sieve Opening (mm)	Mass retained on each sieve, $W_n$ (g)	Percent of mass retained of each sieve, $R_n$	Cumulative percent retained, $\square R_n$	Percent finer, $100 - \square R_n$
10	2.0	0	0.0	0.0	100.0
40	0.425	25.1	22.5	22.5	77.5
100	0.15	65.9	59.1	81.5	18.5
200	0.075	17.9	16.0	97.6	2.4
270	0.053	1.3	1.2	98.7	1.3
Pan	$\square$	1.3	1.2	99.9	

## Soil Amendments

**Table 15: Media 1 sieve analysis**

**Sample:** Media 1  
**Mass of oven dry sample, W (g):** 258.6  
 **$\Sigma, W_n$  (g):** 258.6

Sieve Number	Sieve Opening (mm)	Mass retained on each sieve, $W_n$ (g)	Percent of mass retained of each sieve, $R_n$	Cumulative percent retained, $\square R_n$	Percent finer, $100 - \square R_n$
4	4.75	0.1	0.04	0.04	99.96
10	2.00	4.7	1.82	1.86	98.14
20	0.85	53.9	20.84	22.70	77.30
40	0.425	4.5	1.74	24.44	75.56
60	0.250	17.7	6.84	31.28	68.72
100	0.150	67	25.91	57.19	42.81
140	0.106	73.6	28.46	85.65	14.35
200	0.075	24	9.28	94.93	5.07
230	0.063	5.5	2.13	97.06	2.94
270	0.053	3.3	1.28	98.34	1.66
Pan	$\square$	4.3	1.66	100.00	

**Table 16: Media 2 sieve analysis**

**Sample:** Media 2  
**Mass of oven dry sample, W (g):** 311.7  
 **$\Sigma, W_n$  (g):** 311.8

Sieve Number	Sieve Opening (mm)	Mass retained on each sieve, $W_n$ (g)	Percent of mass retained of each sieve, $R_n$	Cumulative percent retained, $\square R_n$	Percent finer, $100 - \square R_n$
4	4.75	0.4	0.13	0.13	99.87
10	2.00	7.3	2.34	2.47	97.53
20	0.85	43.8	14.05	16.52	83.48
40	0.425	16.9	5.42	21.94	78.06
60	0.250	28.6	9.18	31.12	68.88
100	0.150	76.7	24.61	55.73	44.27
140	0.106	88	28.23	83.96	16.04
200	0.075	32.1	10.30	94.26	5.74
230	0.063	7.2	2.31	96.57	3.43
270	0.053	4.5	1.44	98.01	1.99
Pan	$\square$	6.3	2.02	100.03	

**Table 17: Limestone screening sieve analysis**

**Sample** Limestone Screenings  
**Mass of oven dry sample, W (g):** 1000

Sieve Number	Sieve Opening (mm)	Mass retained on each sieve, $W_n$ (g)	Percent of mass retained of each sieve, $R_n$	Cumulative percent retained, $\sum R_n$	Percent finer, $100 - \sum R_n$
4	4.75	1.5	0.15	0.15	99.85
10	2.00	134.3	13.43	13.58	86.42
20	0.85	290.2	29.02	42.6	57.4
40	0.425	231.4	23.14	65.74	34.26
60	0.250	190.3	19.03	84.77	15.23
100	0.150	101.9	10.19	94.96	5.04
140	0.106	27.8	2.78	97.74	2.26
200	0.075	14.1	1.41	99.15	0.85
230	0.063	3.1	0.31	99.46	0.54
270	0.053	1.5	0.15	99.61	0.39
Pan	—	3.5	0.35	99.96	0.04

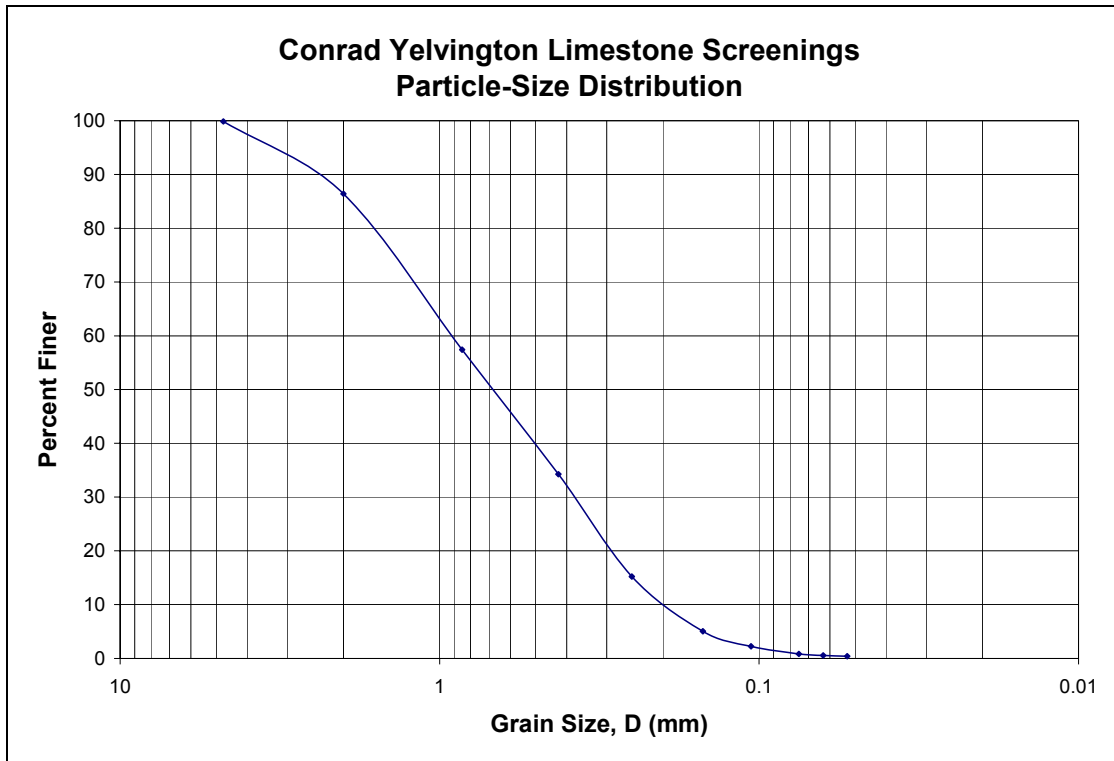


**Figure 64: Limestone screening particle-size distribution**

## **APPENDIX B: SPECIFIC GRAVITY DATA**

South Oak

**Table 18: Specific gravity for South Oak soil samples**

Description of soil:	E-1 (depth 1')	C-1 (depth 1.5')	E-2 (depth 2')	D-1 (depth 3')	E-3 (depth 4.5')
Temperature of test (°C):	20	21	21	22	22
A:	1	0.9998	0.9998	0.9996	0.9996
Date:	8/4/2008	8/4/2008	8/4/2008	10/13/2008	10/13/2008
<b>Item</b>					
Mass of flask + water filled to mark, $W_1$ (g):	674.8	683.2	674	676.2	682.9
Mass of flask + soil + water filled to mark, $W_2$ (g):	738.4	755.7	737.7	743	743.8
Mass of dry soil, $W_s$ (g):	104.3	117.7	105.4	108.1	99.7
Mass of equal volume of water as the soil solids, $W_w$ (g) = $(W_1 + W_s) - W_2$ :	40.7	45.2	41.7	41.3	38.8
$G_{s(T1°C)} = W_s / W_w$ :	2.56	2.60	2.53	2.62	2.57
$G_{s(20°C)} = G_{s(T1°C)} \times A$ :	2.56	2.60	2.53	2.62	2.57

## Hunter's Trace

**Table 19: Specific gravity for Hunter's Trace soil samples**

Description of soil:	D-2 (depth 1')	C-1 (depth 2')	D-3 (depth 3')
Temperature of test (°C):	21	22	22
A:	0.9998	0.9996	0.9996
Date:	10/16/2008	10/3/2008	10/3/2008
<b>Item</b>			
Mass of flask + water filled to mark, $W_1$ (g):	682.9	676.1	682.7
Mass of flask + soil + water filled to mark, $W_2$ (g):	755.3	745	752.7
Mass of dry soil, $W_s$ (g):	116	111.6	110.6
Mass of equal volume of water as the soil solids, $W_w$ (g) = $(W_1 + W_s) - W_2$ :	43.6	42.7	40.6
$G_{s(T1^\circ C)} = W_s / W_w$ :	2.66	2.61	2.72
$G_{s(20^\circ C)} = G_{s(T1^\circ C)} \times A$ :	2.66	2.61	2.72

## Soil Amendments

**Table 20: Specific gravity for Medias**

Temperature of tests (°C)	21	
A	0.9998	
Date	11/27/2007	
<b>Item</b>	<b>Media 1</b>	<b>Media 2</b>
Mass of flask + water filled to mark, $W_1$ (g):	701.1	690.1
Mass of flask + soil + water filled to mark, $W_2$ (g):	755	746.8
Mass of dry soil, $W_s$ (g):	99.3	99.2
Mass of equal volume of water as the soil solids, $W_w$ (g) = $(W_1 + W_s) - W_2$ :	45.4	42.5
$G_{s(T1^\circ C)} = W_s / W_w$ :	2.19	2.33
$G_{s(20^\circ C)} = G_{s(T1^\circ C)} \times A$ :	2.19	2.33

## **APPENDIX C: HYDRAULIC CONDUCTIVITY DATA**



South Oak

**Table 21: Hydraulic conductivity at South Oak (1-ft depth)**

**Depth:** 1 ft  
**Sample ID:** E-1  
**Date:** 5/27/2008  
**Temp (°C):** 22

Test	4	5	6
Diameter of specimen, $D$ (cm)	5.3	5.3	5.3
Length of specimen, $L$ (cm)	3	3	3
Area of specimen, $A$ (cm <sup>2</sup> )	22.06	22.06	22.06
Beginning head difference, $h_1$ (cm)	36.5	36.5	36.5
Ending head difference, $h_2$ (cm)	18.8	18.8	18.8
Cross sectional area of burette, $a$ (cm <sup>2</sup> )	1.767	1.767	1.767
Test duration, $t$ (s)	386.4	387.6	387
Volume of water flow through the specimen, $V_w$ (cm <sup>3</sup> )	31.2759	31.2759	31.2759
Hydraulic conductivity, $k$ (cm/s)	0.0004126	0.0004114	0.0004120
Avg $k$ =	0.0004120	cm/s	
$k_{20^\circ\text{C}}$ =	0.0003926	cm/s	
	0.5564903	in/hr	
	1.1129805	ft/day	
	0.339236	m/day	

**Table 22: Hydraulic conductivity at South Oak (1.5-ft depth)**

**Depth:** 1.5 ft  
**Sample ID:** C - 1  
**Date:** 6/2/2008  
**Temp (°C):** 21.7

<b>Test</b>	<b>1</b>	<b>2</b>	<b>3</b>
Diameter of specimen, $D$ (cm)	5.3	5.3	5.3
Length of specimen, $L$ (cm)	3	3	3
Area of specimen, $A$ (cm <sup>2</sup> )	22.06	22.06	22.06
Beginning head difference, $h_1$ (cm)	53.9	45.5	38.5
Ending head difference, $h_2$ (cm)	47.9	39.7	33.7
Cross sectional area of burette, $a$ (cm <sup>2</sup> )	1.767	1.767	1.767
Test duration, $t$ (s)	142.2	189	186.6
Volume of water flow through the specimen, $V_w$ (cm <sup>3</sup> )	10.602	10.2486	8.4816
Hydraulic conductivity, $k$ (cm/s)	0.0001994	0.0001734	0.0001715
Avg $k$ = 0.0001814 cm/s			
$k_{20^\circ\text{C}}$ = 0.000176 cm/s			
0.24922 in/hr			
0.498441 ft/day			
0.151925 m/day			

**Table 23: Hydraulic conductivity at South Oak (2-ft depth)**

**Depth:** 2.0 ft  
**Sample ID:** E-2  
**Date:** 6/2/2008  
**Temp (°C):** 20.4

<b>Test</b>	<b>1</b>	<b>2</b>	<b>3</b>
Diameter of specimen, $D$ (cm)	5.3	5.3	5.3
Length of specimen, $L$ (cm)	3	3	3
Area of specimen, $A$ (cm <sup>2</sup> )	22.06	22.06	22.06
Beginning head difference, $h_1$ (cm)	66.6	59.6	55
Ending head difference, $h_2$ (cm)	60.6	56.1	51.4
Cross sectional area of burette, $a$ (cm <sup>2</sup> )	1.767	1.767	1.767
Test duration, $t$ (s)	1710.6	1104.6	381.6
Volume of water flow through the specimen, $V_w$ (cm <sup>3</sup> )	10.602	6.1845	6.3612
Hydraulic conductivity, $k$ (cm/s)	0.0000133	0.0000132	0.0000426
Avg $k$ = 0.0000230 cm/s			
$k_{20^\circ\text{C}}$ = 2.28E-05 cm/s			
0.032315 in/hr			
0.06463 ft/day			
0.019699 m/day			

**Table 24: Hydraulic conductivity at South Oak (depth 3 ft)**

**Depth:** 3.0 ft  
**Sample ID:** D-1  
**Date:** 6/5/2008  
**Temp (°C):** 21

<b>Test</b>	<b>1</b>	<b>2</b>	<b>3</b>
Diameter of specimen, $D$ (cm)	5.3	5.3	5.3
Length of specimen, $L$ (cm)	3	3	3
Area of specimen, $A$ (cm <sup>2</sup> )	22.06	22.06	22.06
Beginning head difference, $h_1$ (cm)	76.7	75.5	74.3
Ending head difference, $h_2$ (cm)	75.6	74.3	71.2
Cross sectional area of burette, $a$ (cm <sup>2</sup> )	1.767	1.767	1.767
Test duration, $t$ (s)	74760	85800	263400
Volume of water flow through the specimen, $V_w$ (cm <sup>3</sup> )	1.9437	2.1204	5.4777
Hydraulic conductivity, $k$ (cm/s)	4.64E-08	4.49E-08	3.89E-08
Avg $k$ = 4.34E-08 cm/s			
$k_{20^\circ\text{C}}$ = 4.236E-08 cm/s			
6.003E-05 in/hr			
0.0001201 ft/day			
3.66E-05 m/day			

**Table 25: Hydraulic conductivity at South Oak (4.5-ft depth)**

**Depth:** 4.5 ft  
**Sample ID:** E-3  
**Date:** 6/5/2008  
**Temp (°C):** 22

<b>Test</b>	<b>1</b>	<b>2</b>	<b>3</b>
Diameter of specimen, $D$ (cm)	5.3	5.3	5.3
Length of specimen, $L$ (cm)	3	3	3
Area of specimen, $A$ (cm <sup>2</sup> )	22.06	22.06	22.06
Beginning head difference, $h_1$ (cm)	68.3	64.8	63.8
Ending head difference, $h_2$ (cm)	65.3	64.3	62.4
Cross sectional area of burette, $a$ (cm <sup>2</sup> )	1.767	1.767	1.767
Test duration, $t$ (s)	9600	2100	4080
Volume of water flow through the specimen, $V_w$ (cm <sup>3</sup> )	5.301	0.8835	2.4738
Hydraulic conductivity, $k$ (cm/s)	0.0000011	0.0000009	0.0000013
Avg $k$ = 0.0000011 cm/s			
$k_{20^\circ\text{C}}$ = 1.05E-06 cm/s			
0.001494 in/hr			
0.002988 ft/day			
0.000911 m/day			

## Hunter's Trace

**Table 26: Hydraulic conductivity at Hunter's Trace (1-ft depth)**

**Depth:** 1 ft  
**Sample ID:** D-2  
**Date:** 7/9/2008  
**Temp (°C):** 20.6

Test	1	2	3
Diameter of specimen, $D$ (cm)	5.3	5.3	5.3
Length of specimen, $L$ (cm)	3	3	3
Area of specimen, $A$ (cm <sup>2</sup> )	22.06	22.06	22.06
Beginning head difference, $h_1$ (cm)	73	55.3	35.2
Ending head difference, $h_2$ (cm)	61.2	43.3	23.3
Cross sectional area of burette, $a$ (cm <sup>2</sup> )	1.767	1.767	1.767
Test duration, $t$ (s)	17.1	23.35	38.44
Volume of water flow through the specimen, $V_w$ (cm <sup>3</sup> )	20.8506	21.204	21.0273
Hydraulic conductivity, $k$ (cm/s)	0.0024779	0.0025177	0.0025795
Avg $k$ =	0.0025250	cm/s	
$k_{20^\circ\text{C}}$ =	0.002489	cm/s	
	3.527226	in/hr	
	7.054452	ft/day	
	2.150197	m/day	

**Table 27: Hydraulic conductivity at Hunter's Trace (2-ft depth)**

**Depth:** 2.0 ft  
**Sample ID:** C-1  
**Date:** 7/10/2008  
**Temp (°C):** 24.5

<b>Test</b>	<b>1</b>	<b>2</b>	<b>3</b>
Diameter of specimen, $D$ (cm)	5.3	5.3	5.3
Length of specimen, $L$ (cm)	3	3	3
Area of specimen, $A$ (cm <sup>2</sup> )	22.06	22.06	22.06
Beginning head difference, $h_1$ (cm)	69.1	51.3	31.2
Ending head difference, $h_2$ (cm)	57.2	39.4	19.3
Cross sectional area of burette, $a$ (cm <sup>2</sup> )	1.767	1.767	1.767
Test duration, $t$ (s)	16.47	21.94	39
Volume of water flow through the specimen, $V_w$ (cm <sup>3</sup> )	21.0273	21.0273	21.0273
Hydraulic conductivity, $k$ (cm/s)	0.0027578	0.0028909	0.0029597
Avg $k$ = 0.0028695 cm/s			
$k_{20^\circ\text{C}}$ = 0.002581 cm/s 3.658269 in/hr 7.316539 ft/day 2.230081 m/day			

**Table 28: Hydraulic conductivity at Hunter's Trace (3-ft depth)**

**Depth:** 3  
**Sample ID:** D-3  
**Date:** 7/15/2008  
**Temp (°C):** 21.2

<b>Test</b>	<b>1</b>	<b>2</b>	<b>3</b>
Diameter of specimen, $D$ (cm)	5.3	5.3	5.3
Length of specimen, $L$ (cm)	3	3	3
Area of specimen, $A$ (cm <sup>2</sup> )	22.06	22.06	22.06
Beginning head difference, $h_1$ (cm)	72.3	54.5	34.4
Ending head difference, $h_2$ (cm)	60.5	42.7	22.5
Cross sectional area of burette, $a$ (cm <sup>2</sup> )	1.767	1.767	1.767
Test duration, $t$ (s)	30.63	40.65	68.59
Volume of water flow through the specimen, $V_w$ (cm <sup>3</sup> )	20.8506	20.8506	21.0273
Hydraulic conductivity, $k$ (cm/s)	0.0013980	0.0014425	0.0014875
Avg $k$ = 0.0014427 cm/s			
$k_{20^\circ\text{C}}$ = 0.0014014 cm/s 1.9862583 in/hr 3.9725167 ft/day 1.2108231 m/day			

## Soil Amendments

**Table 29: Hydraulic conductivity of Media 1**

**Description Of Media:** fine sand (50%), sawdust (20%),  
tire crumb (30%)

**Date:** 9/16/2007

Test	1	2	3
Diameter of specimen, $D$ (cm)	6.2	6.2	6.2
Length of specimen, $L$ (cm)	11.3	11.3	11.3
Area of specimen, $A$ (cm <sup>2</sup> )	30.19	30.19	30.19
Beginning head difference, $h_1$ (cm)	45.9	45.9	45.9
Ending head difference, $h_2$ (cm)	22.2	22.2	22.2
Cross sectional area of burette, $a$ (cm <sup>2</sup> )	1.767	1.767	1.767
Test duration, $t$ (s)	144.6	144.6	145.2
Volume of water flow through the specimen, $V_w$ (cm <sup>3</sup> )	41.8779	41.8779	41.8779
Hydraulic conductivity, $k$ (cm/s)	0.0033229	0.0033229	0.0033091
Avg $k$ = 0.0033183 cm/s			
$k_{20^\circ\text{C}}$ = 0.003089 cm/s			
4.378558 in/hr			
8.757116 ft/day			
2.669169 m/day			

**Table 30: Hydraulic conductivity of Media 2**

**Description Of Media:** fine sand (50%), sawdust (25%),  
tire crumb (15%), limestone (10%)

**Date:** 9/14/2007

<b>Test</b>	<b>1</b>	<b>2</b>	<b>3</b>
Diameter of specimen, $D$ (cm)	6.2	6.2	6.2
Length of specimen, $L$ (cm)	12.4	12.4	12.4
Area of specimen, $A$ (cm <sup>2</sup> )	30.19	30.19	30.19
Beginning head difference, $h_1$ (cm)	45.9	45.9	45.9
Ending head difference, $h_2$ (cm)	22.2	22.2	22.2
Cross sectional area of burette, $a$ (cm <sup>2</sup> )	1.767	1.767	1.767
Test duration, $t$ (s)	191.4	192.6	192.6
Volume of water flow through the specimen, $V_w$ (cm <sup>3</sup> )	41.8779	41.8779	41.8779
Hydraulic conductivity, $k$ (cm/s)	0.0027547	0.0027376	0.0027376
	Avg $k =$	0.0027433	cm/s
	$k_{20^\circ\text{C}} =$	0.002554	cm/s
		3.619859	in/hr
		7.239718	ft/day
		2.206666	m/day

## **APPENDIX D: SOIL MOISTURE RETENTION CURVES**



South Oak

**Table 31: SMRC for South Oak (1-ft depth)**

<p style="text-align: right;"><b>Sample Depth:</b> 1 ft</p> <p style="text-align: right;"><b>Sample ID:</b> E-1</p> <p><b>Mass of core w/ brass cylinder &amp; caps (g):</b> 204.48</p> <p style="text-align: right;"><b>Caps (g):</b> 8.88</p> <p style="text-align: right;"><b>Cylinder (g):</b> 73.56</p> <p style="text-align: right;"><b>Initial mass of moist soil core (g)</b> 122.04</p> <p><b>Mass of equip &amp; saturated soil (g):</b> 538.42</p> <p style="text-align: right;"><b>Mass of equipment (g):</b> 408.58</p> <p style="text-align: right;"><b>Moist soil (g):</b> 120.88</p> <p style="text-align: right;"><b>Dry Bulk Density (g/cm<sup>3</sup>):</b> 1.50</p> <p style="text-align: right;"><b>Oven Dry Weight (g):</b> 103.11</p> <p style="text-align: right;"><b>Total water lost (g):</b> 8.96</p>			
Pressure (m H <sub>2</sub> O)	Tempe Cell, Water, & Soil Mass (g)	Gravimetric Water Content, w <sub>g</sub>	Volumetric Water Content, θ <sub>w</sub>
0.0	538.42	0.26	0.39
-0.2	537.66	0.25	0.38
-0.5	536.38	0.24	0.36
-1.0	535.04	0.23	0.34
-2.0	531.33	0.19	0.29
-4.0	530.24	0.18	0.27
-6.0	529.46	0.17	0.26

**Table 32: SMRC for South Oak (1.5-ft depth)**

<b>Sample Depth:</b> 1.5 ft <b>Sample ID:</b> C-1 <b>Mass of core w/ brass cylinder &amp; caps (g):</b> 210.57 <b>Caps (g):</b> 8.8 <b>Cylinder (g):</b> 74.65 <b>Initial mass of moist soil core (g)</b> 127.12 <b>Mass of equip &amp; saturated soil (g):</b> 539.81 <b>Mass of equipment (g):</b> 400.16  <b>Moist soil (g):</b> 126.4 <b>Dry Bulk Density (g/cm<sup>3</sup>):</b> 1.70 <b>Oven Dry Weight (g):</b> 116.88 <b>Total water lost (g):</b> 13.25			
Pressure (m H <sub>2</sub> O)	Tempe Cell, Water, & Soil Mass (g)	Gravimetric Water Content, w <sub>g</sub>	Volumetric Water Content, θ <sub>w</sub>
0.0	539.81	0.19	0.33
-0.2	536.76	0.17	0.29
-0.5	533.25	0.14	0.24
-1.0	530.10	0.11	0.19
-2.0	528.25	0.10	0.16
-4.0	526.95	0.08	0.14
-6.0	526.56	0.08	0.14

**Table 33: SMRC for South Oak (2-ft depth)**

<p style="text-align: right;"><b>Sample Depth:</b> 2.0 ft</p> <p style="text-align: right;"><b>Sample ID:</b> E-2</p> <p style="text-align: right;"><b>Mass of core w/ brass cylinder &amp; caps (g):</b> 210.22</p> <p style="text-align: right;"><b>Caps (g):</b> 8.94</p> <p style="text-align: right;"><b>Cylinder (g):</b> 74.71</p> <p style="text-align: right;"><b>Initial mass of moist soil core (g)</b> 126.57</p> <p style="text-align: right;"><b>Mass of equip &amp; saturated soil (g):</b> 531.3</p> <p style="text-align: right;"><b>Mass of equipment (g):</b> 399.19</p> <p style="text-align: right;"><b>Moist soil (g):</b> 126.71</p> <p style="text-align: right;"><b>Dry Bulk Density (g/cm<sup>3</sup>):</b> 1.49</p> <p style="text-align: right;"><b>Oven Dry Weight (g):</b> 102.41</p> <p style="text-align: right;"><b>Total water lost (g):</b> 5.40</p>			
Pressure (m H <sub>2</sub> O)	Tempe Cell, Water, & Soil Mass (g)	Gravimetric Water Content, w <sub>g</sub>	Volumetric Water Content, θ <sub>w</sub>
0.0	531.3	0.29	0.43
-0.2	530.92	0.29	0.43
-0.5	527.88	0.26	0.38
-1.0	527.86	0.26	0.38
-2.0	526.76	0.25	0.37
-4.0	526.05	0.24	0.36
-6.0	525.90	0.24	0.35

**Table 34: SMRC for South Oak (3-ft depth)**

<p style="text-align: right;"><b>Sample Depth:</b> 3.0 ft</p> <p style="text-align: right;"><b>Sample ID:</b> D-1</p> <p style="text-align: right;"><b>Mass of core w/ brass cylinder &amp; caps (g):</b> 212.69</p> <p style="text-align: right;"><b>Caps (g):</b> 8.78</p> <p style="text-align: right;"><b>Cylinder (g):</b> 74.7</p> <p style="text-align: right;"><b>Initial mass of moist soil core (g)</b> 129.21</p> <p style="text-align: right;"><b>Mass of equip &amp; saturated soil (g):</b> 527.87</p> <p style="text-align: right;"><b>Mass of equipment (g):</b> 399.41</p> <p style="text-align: right;"><b>Moist soil (g):</b> 128.05</p> <p style="text-align: right;"><b>Dry Bulk Density (g/cm<sup>3</sup>):</b> 1.44</p> <p style="text-align: right;"><b>Oven Dry Weight (g):</b> 98.96</p> <p style="text-align: right;"><b>Total water lost (g):</b> 0.41</p>			
<b>Pressure (m H<sub>2</sub>O)</b>	<b>Tempe Cell, Water, &amp; Soil Mass (g)</b>	<b>Gravimetric Water Content, w<sub>g</sub></b>	<b>Volumetric Water Content, θ<sub>w</sub></b>
0.0	527.87	0.298	0.429
-0.2	527.84	0.298	0.429
-0.5	527.82	0.298	0.429
-1.0	527.82	0.298	0.429
-2.0	527.77	0.297	0.428
-4.0	527.66	0.296	0.426
-6.0	527.46	0.294	0.423

**Table 35: SMRC for South Oak (4.5-ft depth)**

<b>Sample Depth:</b> 4.5 ft			
<b>Sample ID:</b> E-3			
<b>Mass of core w/ brass cylinder &amp; caps (g):</b> 217.51			
<b>Caps (g):</b> 8.76			
<b>Cylinder (g):</b> 77.11			
<b>Initial mass of moist soil core (g)</b> 131.64			
<b>Mass of equip &amp; saturated soil (g):</b> 533.9			
<b>Mass of equipment (g):</b> 402.97			
<b>Moist soil (g):</b> 130.46			
<b>Dry Bulk Density (g/cm<sup>3</sup>):</b> 1.57			
<b>Oven Dry Weight (g):</b> 108.03			
<b>Total water lost (g):</b> 0.47			
<b>Pressure (m H<sub>2</sub>O)</b>	<b>Tempe Cell, Water, &amp; Soil Mass (g)</b>	<b>Gravimetric Water Content, w<sub>g</sub></b>	<b>Volumetric Water Content, θ<sub>w</sub></b>
0.0	533.9	0.212	0.333
-0.2	533.88	0.212	0.333
-0.5	533.86	0.212	0.333
-1.0	533.85	0.212	0.333
-2.0	533.75	0.211	0.331
-4.0	533.53	0.209	0.328
-6.0	533.43	0.208	0.326

## Hunter's Trace

**Table 36: SMRC for Hunter's Trace (1-ft depth)**

<b>Sample Depth:</b> 1 ft <b>Sample ID:</b> D-2 <b>Mass of core w/ brass cylinder &amp; caps (g):</b> 205.29 <b>Caps (g):</b> 8.98 <b>Cylinder (g):</b> 73.03 <b>Initial mass of moist soil core (g)</b> 196.31 <b>Mass of equip &amp; saturated soil (g):</b> 534.39 <b>Mass of equipment (g):</b> 398.39  <b>Moist soil (g):</b> 120.37 <b>Dry Bulk Density (g/cm<sup>3</sup>):</b> 1.69 <b>Oven Dry Weight (g):</b> 116.30 <b>Total water lost (g):</b> 15.63			
Pressure (m H <sub>2</sub> O)	Tempe Cell, Water, & Soil Mass (g)	Gravimetric Water Content, w <sub>g</sub>	Volumetric Water Content, θ <sub>w</sub>
0	534.39	0.169	0.287
-0.2	531.68	0.146	0.247
-0.4	530.14	0.133	0.225
-0.6	522.09	0.064	0.108
-0.8	520.97	0.054	0.091
-1	519.76	0.044	0.074
-1.5	518.76	0.035	0.059

**Table 37: SMRC for Hunter's Trace (2-ft depth)**

<b>Sample Depth:</b> 2.0 ft <b>Sample ID:</b> C-1 <b>Mass of core w/ brass cylinder &amp; caps (g):</b> 204.84 <b>Caps (g):</b> 8.68 <b>Cylinder (g):</b> 73.30 <b>Initial mass of moist soil core (g)</b> 122.86 <b>Mass of equip &amp; saturated soil (g):</b> 529.02 <b>Mass of equipment (g):</b> 398.99  <b>Moist soil (g):</b> 115.30 <b>Dry Bulk Density (g/cm<sup>3</sup>):</b> 1.61 <b>Oven Dry Weight (g):</b> 110.55 <b>Total water lost (g):</b> 14.73			
Pressure (m H <sub>2</sub> O)	Tempe Cell, Water, & Soil Mass (g)	Gravimetric Water Content, w <sub>g</sub>	Volumetric Water Content, θ <sub>w</sub>
0	529.02	0.18	0.28
-0.2	528.86	0.17	0.28
-0.4	527.59	0.16	0.26
-0.6	524.83	0.14	0.22
-0.8	519.20	0.09	0.14
-1	517.39	0.07	0.11
-1.5	515.92	0.06	0.09
-2	515.09	0.05	0.08
-4	514.29	0.04	0.07

**Table 38: SMRC for Hunter's Trace (3-ft depth)**

<b>Sample Depth:</b> 3 ft <b>Sample ID:</b> D-3 <b>Mass of core w/ brass cylinder &amp; caps (g):</b> 212.6 <b>Caps (g):</b> 8.71 <b>Cylinder (g):</b> 74.68 <b>Initial mass of moist soil core (g)</b> 129.21 <b>Mass of equip &amp; saturated soil (g):</b> 532.51 <b>Mass of equipment (g):</b> 400.86  <b>Moist soil (g):</b> 115.21 <b>Dry Bulk Density (g/cm<sup>3</sup>):</b> 1.62 <b>Oven Dry Weight (g):</b> 111.61 <b>Total water lost (g):</b> 16.44			
Pressure (m H <sub>2</sub> O)	Tempe Cell, Water, & Soil Mass (g)	Gravimetric Water Content, w <sub>g</sub>	Volumetric Water Content, θ <sub>w</sub>
0	532.51	0.18	0.29
-0.2	532.27	0.18	0.29
-0.4	530.88	0.16	0.27
-0.6	522.96	0.09	0.15
-0.8	518.58	0.05	0.09
-1	517.18	0.04	0.07
-1.5	516.85	0.04	0.06
-2	516.41	0.04	0.06
-4	516.07	0.03	0.05



## Soil Amendments

**Table 39: SMRC for Media 1**

<b>Sample:</b> Media 1 <b>Mass of equip &amp; saturated soil (g):</b> 711.38 <b>Mass of equipment (g):</b> 476.46 <b>Moist soil (g):</b> 192.23 <b>Dry Bulk Density (g/cm<sup>3</sup>):</b> 1.32 <b>Oven Dry Weight (g):</b> 181.54 <b>Total water lost (g):</b> 42.06			
Pressure (m H <sub>2</sub> O)	Tempe Cell, Water, & Soil Mass (g)	Gravimetric Water Content, w <sub>g</sub>	Volumetric Water Content, θ <sub>w</sub>
0	711.38	0.29	0.39
-0.2	710.33	0.29	0.38
-0.4	709.32	0.28	0.37
-0.6	699.52	0.23	0.30
-0.8	677.04	0.10	0.14
-1	670.47	0.07	0.09
-1.5	669.32	0.06	0.08
-2	668.69	0.06	0.08

**Table 40: SMRC for Media 2**

<b>Sample:</b> Media 2 <b>Mass of equip &amp; saturated soil (g):</b> 709.52 <b>Mass of equipment (g):</b> 477.80 <b>Moist soil (g):</b> 189.32 <b>Dry Bulk Density (g/cm<sup>3</sup>):</b> 1.29 <b>Oven Dry Weight (g):</b> 177.81 <b>Total water lost (g):</b> 709.52			
Pressure (m H <sub>2</sub> O)	Tempe Cell, Water, & Soil Mass (g)	Gravimetric Water Content, w <sub>g</sub>	Volumetric Water Content, θ <sub>w</sub>
0	709.52	0.303	0.39
-0.2	708.32	0.296	0.38
-0.4	706.40	0.286	0.37
-0.6	689.71	0.192	0.25
-0.8	673.17	0.099	0.13
-1	669.59	0.079	0.10
-1.5	667.97	0.070	0.09
-2	667.12	0.065	0.08

## **APPENDIX E: ARYA AND PARIS MODEL**

South Oak

Table 41: AP model for South Oak 1-ft depth

South Oak (1-ft depth)									
Particle Density, $\rho_p$ (kg/cm <sup>3</sup> ): 2.56E-03									
Bulk Density, $\rho_b$ (kg/cm <sup>3</sup> ): 1.50E-03									
scaling factor, $\alpha$ : 1.350									
Porosity, $\Phi$ : 0.41									
Void ratio, $e$ : 0.69									
Particle diameter (cm)	Particle diameter (m)	$W_i$ (kg)	$\Sigma w_i$	Volumetric water content, $\theta_w$ (m <sup>3</sup> /m <sup>3</sup> )	Avg. Vol. water content, $\theta_w$ (m <sup>3</sup> /m <sup>3</sup> )	Number of particles, $n_i$	Pore radius, $r_i$ (m)	Matric Potential, $\Psi$ (m H <sub>2</sub> O)	Matric Potential, $\Psi$ (cbar or kPa)
pan		0.081	0.08	0.03					
0.0053	5.30E-05	0.036	0.04	0.01	0.02	1.78E+08	6.49E-07	-22.870	-228.70
0.0075	7.50E-05	0.140	0.18	0.07	0.04	2.48E+08	8.67E-07	-17.126	-171.26
0.0150	1.50E-04	0.511	0.69	0.28	0.18	1.13E+08	1.99E-06	-7.459	-74.59
0.0425	4.25E-04	0.209	0.90	0.37	0.32	2.03E+06	1.14E-05	-1.303	-13.03
0.2000	2.00E-03	0.020	0.92	0.38	0.37	1.88E+03	1.82E-04	-0.082	-0.82

**Table 42: AP model for South Oak 1.5-ft depth**

<b>South Oak (1.5-ft depth)</b>									
Particle Density, $\rho_p$ (kg/cm <sup>3</sup> ): 2.60E-03									
Bulk Density, $\rho_b$ (kg/cm <sup>3</sup> ): 1.70E-03									
scaling factor, $\alpha$ : 1.200									
Porosity, $\Phi$ : 0.35									
Void ratio, $e$ : 0.54									
Particle diameter (cm)	Particle diameter (m)	$W_i$ (kg)	$\Sigma w_i$	Volumetric water content, $\theta_w$ (m <sup>3</sup> /m <sup>3</sup> )	Avg. Vol. water content, $\theta_w$ (m <sup>3</sup> /m <sup>3</sup> )	Number of particles, $n_i$	Pore radius, $r_i$ (m)	Matric Potential, $\Psi$ (m H <sub>2</sub> O)	Matric Potential, $\Psi$ (cbar or kPa)
pan		0.078	0.08	0.03					
0.0053	5.30E-05	0.041	0.12	0.04	0.03	2.02E+08	2.35E-06	-6.329	-63.29
0.0075	7.50E-05	0.160	0.28	0.10	0.07	2.79E+08	3.21E-06	-4.618	-46.18
0.0150	1.50E-04	0.531	0.81	0.28	0.19	1.16E+08	7.02E-06	-2.114	-21.14
0.0425	4.25E-04	0.181	0.99	0.35	0.32	1.73E+06	3.03E-05	-0.490	-4.90
0.2000	2.00E-03	0.008	1.00	0.35	0.35	7.35E+02	3.10E-04	-0.048	-0.48

**Table 43: AP model for South Oak 2-ft depth**

<b>South Oak (2-ft depth)</b>									
Particle Density, $\rho_p$ ( $\text{kg}/\text{cm}^3$ ): 2.53E-03									
Bulk Density, $\rho_b$ ( $\text{kg}/\text{cm}^3$ ): 1.49E-03									
scaling factor, $\alpha$ : 1.400									
Porosity, $\Phi$ : 0.41									
Void ratio, $e$ : 0.69									
Particle diameter (cm)	Particle diameter (m)	$W_i$ (kg)	$\Sigma w_i$	Volumetric water content, $\theta_w$ ( $\text{m}^3/\text{m}^3$ )	Avg. Vol. water content, $\theta_w$ ( $\text{m}^3/\text{m}^3$ )	Number of particles, $n_i$	Pore radius, $r_i$ (m)	Matric Potential, $\Psi$ (m $\text{H}_2\text{O}$ )	Matric Potential, $\Psi$ (cbar or kPa)
pan		0.122	0.12	0.05					
0.0053	5.30E-05	0.079	0.20	0.08	0.07	4.01E+08	3.43E-07	-43.238	-432.38
0.0075	7.50E-05	0.258	0.46	0.19	0.14	4.62E+08	4.72E-07	-31.434	-314.34
0.0150	1.50E-04	0.443	0.90	0.37	0.28	9.91E+07	1.28E-06	-11.553	-115.53
0.0425	4.25E-04	0.094	1.00	0.41	0.39	9.24E+05	9.27E-06	-1.601	-16.01
0.2000	2.00E-03	0.001	1.00	0.41	0.41	9.44E+01	2.74E-04	-0.054	-0.54

**Table 44: AP model for South Oak 3-ft depth**

<b>South Oak (3-ft depth)</b>									
Particle Density, $\rho_p$ (kg/cm <sup>3</sup> ): 2.62E-03									
Bulk Density, $\rho_b$ (kg/cm <sup>3</sup> ): 1.44E-03									
scaling factor, $\alpha$ : 1.500									
Porosity, $\Phi$ : 0.45									
Void ratio, $e$ : 0.82									
Particle diameter (cm)	Particle diameter (m)	$W_i$ (kg)	$\Sigma w_i$	Volumetric water content, $\theta_w$ (m <sup>3</sup> /m <sup>3</sup> )	Avg. Vol. water content, $\theta_w$ (m <sup>3</sup> /m <sup>3</sup> )	Number of particles, $n_i$	Pore radius, $r_i$ (m)	Matric Potential, $\Psi$ (m H <sub>2</sub> O)	Matric Potential, $\Psi$ (cbar or kPa)
pan		0.099	0.10	0.04					
0.0053	5.30E-05	0.062	0.16	0.07	0.06	3.04E+08	1.48E-07	-100.100	-1001.00
0.0075	7.50E-05	0.181	0.34	0.15	0.11	3.13E+08	2.08E-07	-71.266	-712.66
0.0150	1.50E-04	0.531	0.87	0.39	0.27	1.15E+08	5.35E-07	-27.729	-277.29
0.0425	4.25E-04	0.124	1.00	0.45	0.42	1.18E+06	4.76E-06	-3.115	-31.15
0.2000	2.00E-03	0.000	1.00	0.45	0.45	0.00E+00			

**Table 45: AP model for South Oak 4.5-ft depth**

<b>South Oak (4.5-ft depth)</b>									
Particle Density, $\rho_p$ (kg/cm <sup>3</sup> ): 2.57E-03									
Bulk Density, $\rho_b$ (kg/cm <sup>3</sup> ): 1.57E-03									
scaling factor, $\alpha$ : 1.450									
Porosity, $\Phi$ : 0.39									
Void ratio, $e$ : 0.64									
Particle diameter (cm)	Particle diameter (m)	$W_i$ (kg)	$\Sigma w_i$	Volumetric water content, $\theta_w$ (m <sup>3</sup> /m <sup>3</sup> )	Avg. Vol. water content, $\theta_w$ (m <sup>3</sup> /m <sup>3</sup> )	Number of particles, $n_i$	Pore radius, $r_i$ (m)	Matric Potential, $\Psi$ (m H <sub>2</sub> O)	Matric Potential, $\Psi$ (cbar or kPa)
pan		0.099	0.10	0.04					
0.0053	5.30E-05	0.062	0.16	0.06	0.05	3.09E+08	2.13E-07	-69.794	-697.94
0.0075	7.50E-05	0.181	0.34	0.13	0.10	3.19E+08	2.99E-07	-49.652	-496.52
0.0150	1.50E-04	0.531	0.87	0.34	0.24	1.17E+08	7.49E-07	-19.810	-198.10
0.0425	4.25E-04	0.124	1.00	0.39	0.36	1.20E+06	5.95E-06	-2.496	-24.96
0.2000	2.00E-03	0.000	1.00	0.39	0.39	0.00E+00			

## Hunter's Trace

**Table 46: AP model for Hunter's Trace 1-ft depth**

<b>Hunter's Trace (1-ft depth)</b>									
Particle Density, $\rho_p$ (kg/cm <sup>3</sup> ): 2.66E-03									
Bulk Density, $\rho_b$ (kg/cm <sup>3</sup> ): 1.69E-03									
scaling factor, $\alpha$ : 1.070									
Porosity, $\Phi$ : 0.36									
Void ratio, $e$ : 0.56									
Particle diameter (cm)	Particle diameter (m)	$W_i$ (kg)	$\Sigma w_i$	Volumetric water content, $\theta_w$ (m <sup>3</sup> /m <sup>3</sup> )	Avg. Vol. water content, $\theta_w$ (m <sup>3</sup> /m <sup>3</sup> )	Number of particles, $n_i$	Pore radius, $r_i$ (m)	Matric Potential, $\Psi$ (m H <sub>2</sub> O)	Matric Potential, $\Psi$ (cbar or kPa)
pan		0.009	0.01	0.00					
0.0053	5.30E-05	0.011	0.01	0.00	0.00	5.30E+07	8.71E-06	-1.704	-17.04
0.0075	7.50E-05	0.142	0.15	0.06	0.03	2.42E+08	1.17E-05	-1.270	-12.70
0.0150	1.50E-04	0.611	0.76	0.28	0.17	1.30E+08	2.39E-05	-0.621	-6.21
0.0425	4.25E-04	0.226	0.99	0.36	0.32	2.11E+06	7.82E-05	-0.190	-1.90
0.2000	2.00E-03	0.000	0.99	0.36	0.36	0.00E+00			



**Table 47: AP model for Hunter's Trace 2-ft depth**

<b>Hunter's Trace (2-ft depth)</b>									
Particle Density, $\rho_p$ (kg/cm <sup>3</sup> ): 2.61E-03									
Bulk Density, $\rho_b$ (kg/cm <sup>3</sup> ): 1.61E-03									
scaling factor, $\alpha$ : 1.070									
Porosity, $\Phi$ : 0.38									
Void ratio, $e$ : 0.61									
Particle diameter (cm)	Particle diameter (m)	$W_i$ (kg)	$\Sigma w_i$	Volumetric water content, $\theta_w$ (m <sup>3</sup> /m <sup>3</sup> )	Avg. Vol. water content, $\theta_w$ (m <sup>3</sup> /m <sup>3</sup> )	Number of particles, $n_i$	Pore radius, $r_i$ (m)	Matric Potential, $\Psi$ (m H <sub>2</sub> O)	Matric Potential, $\Psi$ (cbar or kPa)
pan		0.032	0.03	0.01					
0.0053	5.30E-05	0.017	0.05	0.02	0.02	8.36E+07	8.95E-06	-1.659	-16.59
0.0075	7.50E-05	0.145	0.19	0.07	0.05	2.52E+08	1.22E-05	-1.219	-12.19
0.0150	1.50E-04	0.582	0.78	0.29	0.18	1.26E+08	2.50E-05	-0.595	-5.95
0.0425	4.25E-04	0.224	1.00	0.38	0.34	2.14E+06	8.16E-05	-0.182	-1.82
0.2000	2.00E-03	0.000	1.00	0.38	0.38	0.00E+00			

**Table 48: AP model for Hunter's Trace 3-ft depth**

<b>Hunter's Trace (3-ft depth)</b>									
Particle Density, $\rho_p$ (kg/cm <sup>3</sup> ): 2.72E-03									
Bulk Density, $\rho_b$ (kg/cm <sup>3</sup> ): 1.62E-03									
scaling factor, $\alpha$ : 1.070									
Porosity, $\Phi$ : 0.40									
Void ratio, $e$ : 0.67									
Particle diameter (cm)	Particle diameter (m)	$W_i$ (kg)	$\Sigma w_i$	Volumetric water content, $\theta_w$ (m <sup>3</sup> /m <sup>3</sup> )	Avg. Vol. water content, $\theta_w$ (m <sup>3</sup> /m <sup>3</sup> )	Number of particles, $n_i$	Pore radius, $r_i$ (m)	Matric Potential, $\Psi$ (m H <sub>2</sub> O)	Matric Potential, $\Psi$ (cbar or kPa)
pan		0.012	0.01	0.00					
0.0053	5.30E-05	0.012	0.02	0.01	0.01	5.66E+07	9.46E-06	-1.569	-15.69
0.0075	7.50E-05	0.160	0.18	0.07	0.04	2.66E+08	1.27E-05	-1.171	-11.71
0.0150	1.50E-04	0.591	0.78	0.31	0.19	1.23E+08	2.61E-05	-0.570	-5.70
0.0425	4.25E-04	0.225	1.00	0.40	0.36	2.06E+06	8.52E-05	-0.174	-1.74
0.2000	2.00E-03	0.000	1.00	0.40	0.40	0.00E+00			

## Soil Amendments

**Table 49: AP model for Media 1**

<b>Media 1</b>									
Particle Density, $\rho_p$ (kg/cm <sup>3</sup> ): 2.190E-03									
Bulk Density, $\rho_b$ (kg/cm <sup>3</sup> ): 1.320E-03									
Scaling factor, $\alpha$ : 1.070									
Porosity, $\Phi$ : 0.390									
Void ratio, $e$ : 0.64									
Particle diameter (cm)	Particle diameter (m)	$W_i$ (kg)	$\Sigma w_i$	Volumetric water content, $\theta_w$ (m <sup>3</sup> /m <sup>3</sup> )	Avg. Vol. water content, $\theta_w$ (m <sup>3</sup> /m <sup>3</sup> )	Number of particles, $n_i$	Pore radius, $r_i$ (m)	Matric Potential, $\Psi$ (m H <sub>2</sub> O)	Matric Potential, $\Psi$ (cbar or kPa)
pan		0.033	0.033	0.01					
0.0053	5.30E-05	0.022	0.06	0.02	0.02	1.30E+08	9.00E-06	-1.649748	-16.497481
0.0063	6.30E-05	0.040	0.10	0.04	0.03	1.41E+08	1.07E-05	-1.391664	-13.916643
0.0075	7.50E-05	0.220	0.32	0.12	0.08	4.54E+08	1.22E-05	-1.217945	-12.179448
0.0106	1.06E-04	0.368	0.68	0.27	0.19	2.69E+08	1.75E-05	-0.846146	-8.461459
0.0150	1.50E-04	0.113	0.80	0.31	0.29	2.91E+07	2.68E-05	-0.553185	-5.531846
0.0250	2.50E-04	0.026	0.82	0.32	0.32	1.46E+06	4.97E-05	-0.298908	-2.989076
0.0425	4.25E-04	0.014	0.84	0.33	0.32	1.60E+05	9.12E-05	-0.162732	-1.627320
0.0850	8.50E-04	0.156	0.99	0.39	0.36	2.22E+05	1.80E-04	-0.082296	-0.822965
0.2000	2.00E-03	0.009	1.00	0.39	0.39	9.92E+02	5.13E-04	-0.028943	-0.289433
0.475	0.00475	0	1.00	0.39	0.39	0.00E+00			

**Table 50: AP model for Media 2**

<b>Media 2</b>									
Particle Density, $\rho_p$ ( $\text{kg}/\text{cm}^3$ ): 2.330E-03									
Bulk Density, $\rho_b$ ( $\text{kg}/\text{cm}^3$ ): 1.290E-03									
Scaling factor, $\alpha$ : 1.070									
Porosity, $\Phi$ : 0.440									
Void ratio, $e$ : 0.79									
Particle diameter (cm)	Particle diameter (m)	$W_i$ (kg)	$\Sigma w_i$	Volumetric water content, $\theta_w$ ( $\text{m}^3/\text{m}^3$ )	Avg. Vol. water content, $\theta_w$ ( $\text{m}^3/\text{m}^3$ )	Number of particles, $n_i$	Pore radius, $r_i$ (m)	Matric Potential, $\Psi$ (m H <sub>2</sub> O)	Matric Potential, $\Psi$ (cbar or kPa)
pan		0.029	0.029	0.01					
0.0053	5.30E-05	0.018	0.05	0.02	0.02	1.00E+08	1.01E-05	-1.474657	-14.746567
0.0063	6.30E-05	0.033	0.08	0.04	0.03	1.09E+08	1.19E-05	-1.244437	-12.444375
0.0075	7.50E-05	0.186	0.27	0.12	0.08	3.61E+08	1.36E-05	-1.089942	-10.899423
0.0106	1.06E-04	0.315	0.58	0.26	0.19	2.16E+08	1.96E-05	-0.757473	-7.574727
0.0150	1.50E-04	0.117	0.70	0.31	0.28	2.85E+07	2.98E-05	-0.498606	-4.986064
0.0250	2.50E-04	0.056	0.75	0.33	0.32	2.92E+06	5.37E-05	-0.276228	-2.762277
0.0425	4.25E-04	0.058	0.81	0.36	0.34	6.15E+05	9.65E-05	-0.153872	-1.538715
0.0850	8.50E-04	0.152	0.96	0.42	0.39	2.02E+05	2.01E-04	-0.074001	-0.740014
0.2000	2.00E-03	0.035	1.00	0.44	0.43	3.63E+03	5.43E-04	-0.027321	-0.273206
0.475	0.00475	0.001	1.00	0.44	0.44	7.65E+00	1.60E-03	-0.009272	-0.092719

## REFERENCES

- Arya, L.M. and Paris, J.F. (1981). A physicoempirical model to predict the soil moisture characteristic curve from particle-size distribution and bulk density data. *Soil Science Society of America Journal*, 44:1023-1030.
- ASTM Standard C 29/C29M-97, (1997), "Standard Test Method for Bulk Density and Voids in Aggregate," ASTM International, West Conshohocken, PA, [www.astm.org](http://www.astm.org).
- ASTM Standard D 421-85, (1993), "Standard Practice for Dry Preparation of Soil Samples for Particle-Size Analysis and Determination of Soil Constants," ASTM International, West Conshohocken, PA, [www.astm.org](http://www.astm.org).
- ASTM Standard D 854-92, 1993, "Standard Test Method for Specific Gravity of Soils," ASTM International, West Conshohocken, PA, [www.astm.org](http://www.astm.org).
- ASTM Standard D 2434, 1968 (1994), "Standard Test Method for Permeability of Granular Soils (Constant Head)," ASTM International, West Conshohocken, PA, [www.astm.org](http://www.astm.org).
- ASTM Standard D 6836 - 02, 2003, "Standard Test Method for Determination of the Soil Water Characteristic Curve for Desorption Using a Hanging Column, Pressure Extractor, Chiller Mirror Hygrometer, and/or Centrifuge," ASTM International, West Conshohocken, PA, [www.astm.org](http://www.astm.org).
- ASTM Standard D 5093 - 90, 1997, "Standard Test Method for Field Measurement of Infiltration Rate Using a Double-Ring Infiltrometer with Sealed-Inner Ring," ASTM International, West Conshohocken, PA, [www.astm.org](http://www.astm.org).

- Baver, L.D., Gardner, W.H., and Gardner, W.R (1972). *Soil Physics* (4<sup>th</sup> ed.). New York: John Wiley & Sons, Inc.
- Bouwer, H. (1986). “Intake Rate: Cylinder Infiltrometer” in *American Society of Agronomy – Soil Science Society of America – Method of Soil Analysis: Part 1 – Physical and Mineralogical Methods* (2<sup>nd</sup> ed.). Madison, Wisconsin: Soil Science Society of America, Inc.
- Brooks, R.H., and Corey, A.T. (1964). *Hydraulic properties of porous media*, Colorado State University Hydrology Paper No. 3, Fort Collins, Colorado.
- Bruce, R.R., and Luxmoore, R.J. (1986). “Water Retention: Field Methods” in *American Society of Agronomy – Soil Science Society of America – Methods of Soil Analysis: Part 1 – Physical and Mineralogical Methods* (2<sup>nd</sup> ed.). Madison, Wisconsin: Soil Science Society of America, Inc.
- Carsel, R.F. and R.S. Parrish (1988). *Developing Joint Probability Distributions of Soil Water Retention Characteristics*, *Water Resources Research*, 24 (5), 755-769.
- Cavazza, L., Patruno, A., and Cirillo, E. (2007). Effect of yearly oscillating water table on soil moisture retention curves. *Biosystems Engineering*, 98, 257-265.
- Charbeneau, R.J. (2000). *Groundwater Hydraulics and Pollutant Transport*. Long Grove, IL: Waveland Press, Inc.
- Dane, J.H. and Hopmans, J.W. (2002). “Water Retention and Storage” in *Soil Science Society of America Book Series: 5 – Method of Soil Analysis: Part 4 – Physical Methods*. Madison, Wisconsin: Soil Science Society of America, Inc.

- Das, B.M. (2006). *Principles of Geotechnical Engineering* (6<sup>th</sup> ed.). Toronto, ON: Thomson Canada Limited, Inc.
- Das, B.M. (2002). *Soil Mechanics Laboratory Manual* (6<sup>th</sup> ed.). New York : Oxford University Press.
- Fetter, C.W. (1988), *Applied Hydrogeology* (2<sup>nd</sup> ed.). Columbus, Ohio: Merrill Publishing Company.
- Flint, A.L., and Flint, L.E. (2002). “Particle Density” in *Soil Science Society of America Book Series: 5 – Method of Soil Analysis: Part 4 – Physical Methods*. Madison, Wisconsin: Soil Science Society of America, Inc.
- Hillel, D. (1980). *Fundamentals of Soil Physics*. San Diego, California: Academic Press, Inc.
- Hillel, D. (1982). *Introduction to Soil Physics*. San Diego, California: Academic Press, Inc.
- Grossman, R.B. and Reinsch, T.G. (2002). “The Solid Phase” in *Soil Science Society of America Book Series: 5 – Method of Soil Analysis: Part 4 – Physical Methods*. Madison, Wisconsin: Soil Science Society of America, Inc.
- Haverkamp, R. and Regginia, P. (2002). “Physically Based Water Retention Prediction Models” in *Soil Science Society of America Book Series: 5 – Method of Soil Analysis: Part 4 – Physical Methods*. Madison, Wisconsin: Soil Science Society of America, Inc.
- Henderson, E.D. (2008). *An Investigation of the Capabilities and Kinetics of Selected Filtration Media for Reduction of Nitrate and Orthophosphorus at Various Temperatures*. Master’s thesis, University of Central Florida, Orlando, Florida.
- Klute, A., and Dirksen, C. (1986). “Hydraulic Conductivity and Diffusivity: Laboratory Methods” in *American Society of Agronomy – Soil Science Society of America – Methods*

- of Soil Analysis: Part 1 – Physical and Mineralogical Methods* (2<sup>nd</sup> ed.). Madison, Wisconsin: Soil Science Society of America, Inc.
- Li, A.G., Tham, L.G., Yue, Z.Q., Lee, C.F., and Law, K.T. (2005). Comparison of field and laboratory soil-water characteristic curves. *Journal of Geotechnical and Geoenvironmental Engineering*, 131(9):1176-1180.
- Moberg, M. (2008), *The Effectiveness of Specifically Designed Filter Media to Reduce Nitrate and Orthophosphate in Stormwater Runoff*, Master's thesis, University of Central Florida, Orlando Florida.
- Mualem, Y. (1976). A new model for predicting the hydraulic conductivity of unsaturated porous media. *Water Resources Research*, 12:513-522.
- Pachepsky, Y., Rawls, W.J., and Giménez, D. (2001). Comparison of soil water retention at field and laboratory scales. *Soil Science Society of America Journal*, 65, 460-462.
- Rawls, W.J. and Brakensiek, D.L. (1985). Prediction of soil water properties for hydrologic modeling, in *Proceedings of Symposium on Watershed Management*, 293-299, American Society of Civil Engineers, New York.
- Rawls, W.J. and Pachepsky, Y.A. (2002). Soil consistence and structure as predictors of water retention. *Soil Science Society of America Journal*, 66, 1115-1126.
- Reddi, L.N. (2003). *Seepage in Soils: Principles and Applications*, Hoboken, New Jersey: John Wiley & Sons, Inc.
- Reynolds, W.D., Elrick, D.E. and Youngs, E.G. (2002). “Single-Ring and Double- or Concentric-Ring Infiltrimeters” in *Soil Science Society of America Book Series: 5 –*



- Method of Soil Analysis: Part 4 – Physical Methods*. Madison, Wisconsin: Soil Science Society of America, Inc.
- Reynolds, W.D., Elrick, D.E., Youngs, E.G., Amoozegar, A., Booltink, H.W.G., and Bouma, J., et al. (2002). “Saturated and Field-Saturated Water Flow Parameters” in *Soil Science Society of America Book Series: 5 – Method of Soil Analysis: Part 4 – Physical Methods*. Madison, Wisconsin: Soil Science Society of America, Inc.
- Satyavathi, P.L.A. (1996). Soil water characteristic curves as influenced by soil porosity. *Journal of the Indian Society of Soil Science*, 44(2): 317-317.
- Simms, P.H. and Yanful, E.K. (2004). Estimation of soil-water characteristic curve of clayey till using measured pore-size distributions. *Journal of Environmental Engineering*, 130(8):847-854.
- Tindall, J.A., and Kundel, J.R. (1999). *Unsaturated Zone Hydrology for Scientists and Engineers*. Upper Saddle River, New Jersey: Prentice Hall, Inc.
- van Genuchten, M.T. (1980). A closed-form equation for predicting the hydraulic conductivity of unsaturated soils. *Soil Science Society of America Journal*, 44(5): 892-898.
- Vaz, C.M.P., Iossi, M., Naime, J, Macedo, Á., Reichert, J.M., Reinert, D.J., and Cooper, M. (2005). *Validation of the Arya and Paris Water Retention Model for Brazilian Soils*, Soil Science Society of America Journal, 69 (3), 577-583.
- Walczak, R.T. et al. (2006). *Modeling of soil water retention curve using soil solid phase parameters*, Journal of Hydrology, 329, 527-533.
- Wanielista, M., Kersten, R. and Eaglin, R. (1997). *Hydrology: Water Quality and Quality Control*. New York: John Wiley & Sons, Inc.